Università degli Studi di Padova

Dipartimento di Fisica e Astronomia "Galileo Galilei"
Corso di Laurea Magistrale in Fisica

CAVITY QED IN A BOSONIC JOSEPHSON JUNCTION COUPLED TO PHOTONS

Laureando:
Paolo Rosson
Matricola:
1078973

Relatore:
Ch.mo Prof. Luca Salasnich
Correlatore:
Dott. Giovanni Mazzarella

Anno accademico 2014/2015

Contents

Chapter 1

Introduction

A system made of bosonic particles makes a Bose-Einstein condensate when, under a critical temperature T_C, a finite fraction of its particles occupies the lowest accessible energy state. Since these particles can be described by the same wave function, they show the same behaviour, which can lead to quantum effects on a macroscopic scale. Bose-Einstein condensation (BEC) was first theorized by A. Einstein in 1924 [1, 2], however, its experimental realization in atomic gases has come almost a century later. The main problem that needed to be solved in order to achieve the Bose-Einstein condensation was the extremely low temperature that needed to be reached for the condensation to take place, which is of the order of the nK. The development of laser cooling techniques has allowed to overcome this problem and BEC in atomic gases was first observed in 1995 [3]. The fact that the Nobel Prize was awarded in 2001 to E. A. Cornell, W. Ketterle and C. E. Wieman "for the achievement of Bose-Einstein condensation in dilute gases of alkali atoms, and for early fundamental studies of the properties of the condensates" and in 1997 to S. Chu, C. Cohen-Tannoudji and W. D. Phillips "for development of methods to cool and trap atoms with laser light" clearly shows how remarkable such achievements have been.

The development of techniques aimed at confining the atoms has allowed the creation of systems with easily tunable parameters. In particular, the combined use of laser beams and magnetic fields in the so called magneto-optic traps has given the possibility to study condensates in optical lattices and also in quasi one-dimensional systems.

A fundamental effect in quantum mechanics is the so called quantum tunneling. It consists in the fact that a particle that does not have enough energy to classically cross a barrier, can do so. In solid state physics this phenomenon happens in a Josephson junction, which is formed by two superconductors separated by a thin layer of insulating material. Using a BEC, a similar system can be realized by inserting a barrier in the potential trap that contains the atoms, thus making a double well potential, which

separates the condensate in two parts. In both systems particles can move from one side of the barrier to the other through quantum tunneling. This can occur because the wave functions that describe the particles in either side of the barrier are not completely localized, but have a non-zero overlap. The Josephson effect was first theorized in 1962 by B.D. Josephson [4], who predicted the tunneling of Cooper pairs between to superconductors, and was seen experimentally by P. Anderson a year later [5]. The first observation of Josephson oscillations in a single Bosonic Josephson junction was achieved in 2005 by M. Albiez et al. [6].

When ultracold atoms are inside of an optical cavity, the interaction between light and matter plays a crucial role, even in the dilute gas limit [14]. As a consequence the atomic and photon degrees of freedom influence each other. Therefore the description of the atomic motion dynamically depends on the photon field [15].

In this thesis we study a Bosonic Josephson junction (BJJ) that is inside of a optical cavity, following and expanding on the work carried out in [11]. While previous proposals of similar systems [17, 18, 19, 20, 21] considered the effect of the cavity photons on the on-site energies of the Bosonic Josephson junction, in our system, because of its geometry, we also consider the phenomena arising from cavity assisted boson tunneling.

We will start in the second chapter by describing the components of the system, i.e. the Bosonic Josephson junction and the cavity and we will derive a model that describes their interaction. Adopting the semiclassical approximation, that uses coherent states to describe both the cavity photons and the bosonic atoms, we will derive a set of equations that describes the dynamics of the system. In the third chapter we will study some features of the dynamics of the system, and we will show how the dynamics of the Josephson junction is influenced when the photon field is constant. In particular, using this last approximation, we will show how the cavity photons can be used to induce a crossover between the different regimes in which a Josephson junction can be found. This is one of the novelties presented in this thesis. In the fourth chapter, we will study the system in a different way, by treating the bosonic atoms in the junction in a purely quantum manner. This description of the system, which we will call "half-semiclassical", is an original contribution to the topic. We will study the ground state of the system and see how the presence of the cavity photons influences it. Some analogies between the results of this chapter and the previous one will be then pointed out. The last chapter is the conclusion, where we briefly summarize the main results of the thesis.

Chapter 2

Bosonic Josephson junction coupled to photons: Model

2.1 Interacting Bose-Einstein condensate

The Bose-Einstein condensate in our system is composed of an atomic gas, usually made of alkali or alkali-earth atoms, such as ^{87}Rb or ^{23}Na, which is trapped with an external potential and it is cooled to a temperature of the order of 100 nK. In order for the gas to show a purely quantum behaviour, it needs to be degenerate. A gas is considered degenerate when the de Broglie wavelength of its atoms is larger than their mean interparticle distance. If the gas has density n, the mean interparticle distance is $d \simeq n^{-1/3}$ and the de Broglie wavelength is $\lambda = \sqrt{2\pi\hbar^2/mk_BT}$, where m is the mass of the atoms, T their temperature and k_B is Bolzmann's constant. The condition can therefore be written as $\lambda > d$. When such condition is satisfied the wave function of the atoms overlap, and they show quantum interference. The gas we are studying is weakly interacting and can be considered to be dilute. A gas is weakly interacting when the mean interparticle distance in much larger than the s-wave scattering length, a_s of the atoms: $n|a_s|^3 \ll 1$. This does not mean that the interactions between atoms are weak. The interaction can be strong as long as the interaction energy of the atoms is small compared to their kinetic energy.

When such a gas is cooled to a low enough temperature it becomes a Bose-Einstein condensate. The condensation is a consequence of the statistical properties of bosons, whose wave functions are symmetric for the exchange of any two particles.

2.1.1 External potential

Ultracold atomic gases can be cooled and trapped with the combined use of laser beams and magnetic fields in a so called Magneto-Optical trap [7].

Such a trap is composed of an arrangement of lasers tuned to a frequency just below the resonant frequency of the atoms. In this system, an atom headed toward such a beam will see the photons from the laser as having a frequency closer to the resonance because of the Doppler effect. The oncoming photons will affect the atom more than those coming from the opposite direction, so they will tend to slow down the atom and therefore cool it. Using three pairs of laser beams intersecting in the same point will result in cooling along three orthogonal axis. This arrangement is called optical molasses, because atoms moving in any direction will tend to slow down as if they were in a viscous fluid. A position dependent trapping force can be provided through a spatially dependent magnetic field. Because of it, the resonance frequency of the atoms will experience a Zeeman shift and the interaction of the atoms with the laser photons will result in a spatially dependent force which constitutes the trapping potential.

Another technique for the trapping of the atoms is the optical dipole trap that is based on the interaction of the induced electric dipole moment of the atoms with an external light field. Such kind of traps are used in [8] to build the same type of confining potential we are considering.

In our system the atoms are confined by a double-well (DW) potential, $V_{DW}(x)$, along the x direction and we assume that the confinement is tightly harmonic, with frequency ω_H, in the (y, z) plane, so that the system can be considered almost unidimensional. The total external potential $V(\mathbf{r})$ for the atoms is therefore given by

$$V(\mathbf{r}) = V_{DW}(x) + \frac{1}{2} m\omega_H^2 (y^2 + z^2) \,, \tag{2.1}$$

where m is the mass of the bosons.

2.1.2 Atomic Hamiltonian

The Bose-Einstein condensate we are studying is formed by bosonic alkaline or alkaline-earth-metal atoms having an electronic ground state, which we will label with the subscript g, and an optically accessible excited state, which we will label with e. The atomic transition frequency ω_A is in the optical range, i.e. $\omega_A \approx 10^{15}$ Hz. The Hamiltonian that describes the interacting bosons in the trapping potential can be written as:

$$\hat{H}_A = \sum_{\sigma=g,e} \int d^3\mathbf{r}\ \hat{\Psi}^\dagger_\sigma(\mathbf{r}) \Big[-\frac{\hbar^2}{2m}\nabla^2 + V(\mathbf{r}) + \hbar\omega_A\ \delta_{\sigma,e} + \frac{1}{2}\sum_{\sigma'} g_{\sigma\sigma'} \hat{\Psi}^\dagger_{\sigma'}(\mathbf{r}) \hat{\Psi}_{\sigma'}(\mathbf{r}) \Big] \hat{\Psi}_\sigma(\mathbf{r}), \tag{2.2}$$

where $\hat{\Psi}^\dagger_\sigma(\mathbf{r})$ is the bosonic field operator that creates an atom in the state σ at the position $\mathbf{r}$ and it satisfies the bosonic commutation relations:

$$[\hat{\Psi}_\sigma(\mathbf{r}), \hat{\Psi}^\dagger_{\sigma'}(\mathbf{r}_1)] = \delta(\mathbf{r} - \mathbf{r}_1)\delta_{\sigma,\sigma'}$$
$$[\hat{\Psi}_\sigma(\mathbf{r}), \hat{\Psi}_{\sigma'}(\mathbf{r}_1)] = 0.$$

In principle, the trapping potential could depend on the internal state of the atom, but it will play no role in our considerations.

In our study, atom-atom interaction is modelled by s-wave scattering, with coupling constants g_{gg}, g_{ee} and g_{ge}, where $g_{\sigma,\sigma'} = 4\pi\hbar^2 a_{\sigma,\sigma'}/m$. Here $a_{\sigma,\sigma'}$ is the s-wave scattering length pertaining to collisions between two atoms in the state σ and σ', respectively.

Elementary theory of particle scattering

Let us give a brief introduction to the theory of particle scattering with the sole purpose of explaining why we model the interaction between the atoms with the s-wave scattering.

When studying the scattering of two distinguishable particles it is convenient to use the center of mass coordinates and the relative coordinates. The center of mass behaves like a free particle and can be described using a plane wave. The wave function for the relative system φ_r is made up of the sum of an ingoing wave φ_{in}, described by a plane wave, and of an outgoing wave φ_{out}. If we observe the outgoing wave at a distance much larger than the interatomic distances, the outgoing wave can be described by a spherical wave which is modulated by a function $f(\mathbf{k})$:

$$\varphi_r = \varphi_{in} + \varphi_{out} = e^{ikz} + f(\mathbf{k})\frac{e^{ikr}}{r},$$

where f($\mathbf{k}$) is the scattering amplitude and where we assume that the ingoing wave has a wave number parallel to z. If the interacting potential is spherically symmetric, the scattering amplitude depends only on the angle θ between the relative momentum of the atoms before and after the scattering. The scattering amplitude $f(\theta)$ is linked to the differential cross section $d\sigma/d\Omega$ as:

$$\frac{d\sigma}{d\Omega} = |f(\theta)|^2.$$

Because of the spherical symmetry of the potential, $f(\theta)$ can be expanded using Legendre polynomials:

$$f(\theta) = \frac{1}{2ik}\sum_{l=0}^{\infty}(2l+1)(e^{2i\delta_l} - 1)P_l(\cos\theta),$$

where l is the angular quantum number, $\delta_l(k)$ the scattering phase shift, and $P_l(\cos\theta)$ is the l-th Lengendre polynomial. The total cross section is:

$$\begin{aligned}\sigma &= 2\pi \int_{-\infty}^{\infty} d(\cos\theta)|f(\theta)|^2 \\ &= \frac{4\pi}{k^2}\sum_{l=0}^{\infty}(2l+1)\sin^2(\delta_l).\end{aligned}$$

The calculation of the cross section can be carried out by using some theoretical results regarding the relation between δ_l and k. It can be proven that for a short-range potential, when $k \to 0$ then $\delta_l \sim k^{2l+1}$. For a long-range potential that decays as r^{-n}, when $k \to 0$, then $\delta_l \sim k^{2l+1}$ if $l < \frac{n-3}{2}$ and $\delta_l \sim k^{n-2}$ otherwise. Assuming that the potential between the atoms is Van der Waals-like and it decays as r^{-6}, we see that when $k \to 0$, which is satisfied for an ultracold Bose gas, all the δ_l become very small. The largest contribution to the cross section is given by the s-wave, which is the $l = 0$ term of the sum. Given that $\delta_0 \sim k$, it can be written as:

$$\delta_0 = -a_s k$$

and in the $k \to 0$ limit:

$$f(\theta) = -a_s.$$

where a_s is the s-wave scattering length and it depends only on the interaction potential. The total cross section is:

$$\sigma = 4\pi a_s^2$$

and it depends only on the scattering length. The scattering length allows us to model the actual interaction potential with a simpler pseudo-potential $V(\mathbf{r})$, which describes the interaction between the atoms as:

$$V(\mathbf{r}) = \frac{4\pi\hbar^2 a_s}{m}\delta(\mathbf{r}) \tag{2.3}$$

where m is the mass of the atoms and $\delta(\mathbf{r})$ is the Dirac delta function. This potential well describes the short range of the interaction and also its spherical symmetry. We are justified in using a two-body interaction because the gas we are studying is dilute. This means that the probability of having collisions between more than two atoms is negligible.

2.2 Optical cavity

An optical cavity, or optical resonator is an arrangement of optical components that allows a light beam circulating inside of it to form standing

waves. The type of optical cavity used in our system is a Fabry-Pérot resonator which is made of two highly reflective parallel mirrors.

In general, given an empty cavity we are interesting in knowing its normal modes which are defined as the solutions of the Helmholtz equation:

$$(\nabla^2 + \frac{\omega^2}{c^2})u(\mathbf{r}) = 0,$$

with appropriate boundary conditions. In general, there is a discrete set of eigenfrequencies ω_n and of orthogonal eigenfunctions $u_n(\mathbf{r})$, labelled by an index n. The electric field inside of the cavity can be expanded in terms of its normal modes as:

$$\mathbf{E}(\mathbf{r}, t) = \sum_n \epsilon_n(t) u_n(\mathbf{r}) e^{i\omega_n t} + c.c.,$$

where $\epsilon_n(t)$ are the complex mode amplitudes and $c.c$ is the complex conjugate of the same expression. By explicitly writing the term $e^{i\omega_n t}$, we ensure that $\epsilon_n(t)$ is a slowly varying amplitude. However, since most cavities are open because they are not bounded by closed surfaces, the formal definition of a normal mode is not strictly applicable. Nevertheless, it is customary to use the term cavity mode, because, after many reflections, additional reflections have little effect on the distribution of the cavity field.

For on optical cavity formed by plane mirrors located at positions $y = -L/2$ and $y = L/2$, the eigenfrequencies and eigenfunctions are:

$$\begin{aligned} \omega_n &= \frac{n\pi c}{L} \\ u_n(y) &= \cos\left(\frac{\pi n y}{L}\right) \end{aligned}$$

where $u_n(y)$ vanishes at the surfaces and n is a large number. However for more complicated geometrical configurations, the normal modes cannot be approximated by plane waves.

In our system the cavity axis is perpendicular to the direction of the double-well potential and the resonator is operated at the so called TEM_{00} mode [9]. TEM stands for transverse electromagnetic mode, and has neither electric nor magnetic field in the direction of propagation. Its mode function is:

$$f(\mathbf{r}) = \sqrt{\frac{2}{L}}\, \cos(k\, y)\, \frac{e^{-(x^2+z^2)/(2\sigma^2)}}{\pi^{1/2}\sigma}, \tag{2.4}$$

where $k = \omega_C/c$ is the wave number of the cavity mode, L is the distance between the mirrors and σ is the width of the Gaussian profile in the (x, z) plane.

The Q factor of a resonator is a measure of the strength of the damping of its oscillations, and the average lifetime of a resonant photon in the cavity is proportional to the cavity's Q.

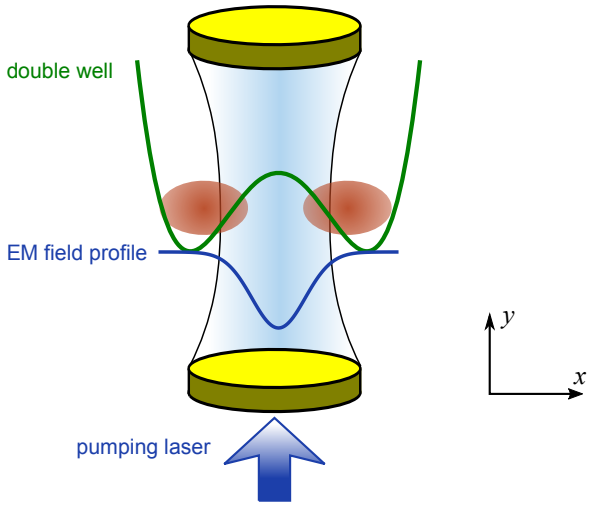

Figure 2.1: Illustration of the setup. The bosonic Josephson Junction is created by magnetic or optical means along the x direction. A Fabry-Pérot cavity is placed around the junction with an axis orthogonal to the junction. The resonator is operated on the TEM_{00} mode.

2.2.1 Cavity Hamiltonian

In our system, the bosonic Josephson Junction is located inside of a high-Q optical cavity with a characteristic frequency ω_C which is close to the atomic transition frequency ω_A of the bosonic atoms. The setup is illustrated in Fig. 2.1.

Moreover, the cavity is pumped through one of its mirrors by a coherent laser light. The single mode of the radiation inside of the cavity can be described by the Hamiltonian [14]

$$\hat{H}_C = \hbar\omega_C\,\hat{a}^\dagger\,\hat{a} - i\hbar\eta\left(e^{i\omega_L t}\hat{a} - e^{-i\omega_L t}\hat{a}^\dagger\right), \tag{2.5}$$

where $\eta > 0$ is the strength of the driving laser, and ω_L is its single-mode frequency.

The first part of the Hamiltonian represents the cavity photons which have frequency ω_C.

The second part of the Hamiltonian describes the laser pumping. Its expression is phenomenological and it models a coherent source of light. However it can be shown that $\hat{H}_C$ is the quantum analogue of a driven harmonic oscillator. Let us show this analogy.

Using the position and momentum operators $\hat{x}$ and $\hat{p}$, the creation and

annihilation $\hat{a}^\dagger$ and $\hat{a}$ operators can be written as:

$$\begin{aligned}\hat{a} &= \sqrt{\frac{\omega_c}{2\hbar}}\left(\hat{q}+\frac{i}{\omega_C}\hat{p}\right)\\ \hat{a}^\dagger &= \sqrt{\frac{\omega_c}{2\hbar}}\left(\hat{q}-\frac{i}{\omega_C}\hat{p}\right)\end{aligned}$$

By substituting these expressions into the Hamiltonian $\hat{H}_C$ we get:

$$\begin{aligned}\hat{H}_C &= \frac{\omega_C^2}{2}\left(\hat{q}^2+\frac{\hat{p}}{\omega_C^2}\right)-i\hbar\eta\sqrt{\frac{\omega_C}{2\hbar}}\left[\left(\hat{q}+\frac{i}{\omega_C}\hat{p}\right)e^{i\omega_L t}-\left(\hat{q}-\frac{i}{\omega_C}\hat{p}\right)e^{-i\omega_L t}\right]\\ &= \frac{p^2}{2}+\frac{\omega_C^2}{2}q^2+\sqrt{2\hbar\omega_C}\,\eta\left[\hat{q}\sin(\omega_L t)+\frac{\hat{p}}{\omega_C}\cos(\omega_L t)\right]\end{aligned}$$

This Hamiltonian leads to the following Hamilton equations:

$$\begin{aligned}\dot{q} &= \frac{\partial H}{\partial p}=p+\sqrt{\frac{2\hbar}{\omega_C}}\,\eta\,\cos(\omega_L t)\\ \dot{p} &= -\frac{\partial H}{\partial q}=-\omega_C^2 q-\sqrt{2\hbar\omega_C}\,\eta\,\sin(\omega_L t)\end{aligned}$$

These equations are equivalent to the second order differential equation:

$$\ddot{q}+\omega_C^2 q+\sqrt{2\hbar\omega_C}\,\eta\left(1+\frac{\omega_L}{\omega_C}\right)\sin(\omega_L t)=0,$$

which is the equation of a driven harmonic oscillator where the driving force is sinusoidal with frequency ω_L.

2.3 Interaction with the cavity

2.3.1 Atom-light interaction

Since the bosonic Josephson junction is inside of an optical cavity, it is very important to model the interaction of the bosonic atoms with the radiation. This can be done through the Jaynes-Cummings Hamiltonian, which describes the interaction of a single two-level atom with a single-mode light field. We will derive this model and understand under which conditions it holds.

As it is the case in our system, let us consider a single bosonic atom which has only two electronic states, a ground state and an excited one and it is interacting with an electromagnetic field. The interaction of the atom with the light field can be modelled by using the minimal substitution. The Hamiltonian of a single atom which interacts with an electromagnetic field

is:

$$\begin{aligned}\hat{H} &= \frac{1}{2m}(\hat{p} - q\hat{A})^2 + U(\hat{r}) + \hat{H}_{el} + \hbar\omega_c \hat{a}^\dagger \hat{a} \\ &= \frac{1}{2m}\hat{p}^2 + U(\hat{r}) + \hat{H}_{el} - \frac{q}{2m}(\hat{p}\cdot\hat{A} + \hat{A}\cdot\hat{p}) + \frac{q}{2m}\hat{A}^2 + \sum_k \hbar\omega_k \hat{a}_k^\dagger \hat{a}_k\end{aligned}$$

where $\hat{p}$, $\hat{r}$, q and m are the momentum, position, charge and mass of the atom. $\hat{A}$ is the vector potential of the field, $\hat{H}_{el}$ is the part of the Hamiltonian that describes the electronic state of the atom, $U(\hat{r})$ is a general external potential that acts on the atom and ω_k, $\hat{a}_k^\dagger$ and $\hat{a}_k$ are the frequency and the creation and annihilation operators for the k-th mode of the quantized electromagnetic field. From the second line of the previous expression we find that

$$\hat{H}_{int} = -\frac{q}{2m}(\hat{p}\cdot\hat{A} + \hat{A}\cdot\hat{p}) + \frac{q}{2m}\hat{A}^2$$

is the interaction Hamiltonian that we are interested in studying. If we use the Coulomb gauge $\nabla\cdot\hat{A} = 0$, then $[\hat{P}, \hat{A}] = 0$ and we can write:

$$\hat{H}_{int} = -\frac{q}{m}\hat{p}\cdot\hat{A} + \frac{q}{2m}\hat{A}^2$$

Moreover, the $\hat{A}^2$ term is usually very small except for very intense fields, so it can be neglected. Thus the interaction Hamiltonian is simply:

$$\hat{H}_{int} = -\frac{q}{m}\hat{p}\cdot\hat{A} \tag{2.6}$$

At this point it is convenient to quantize the atomic field and write the atomic Hamiltonian in terms of the field operators. The atomic Hamiltonian written in the coordinate representation reads:

$$\hat{H}_A = \frac{1}{2m}\hat{p}^2 + U(\hat{r}) + \hat{H}_{el} = -\frac{\hbar^2}{2m}\nabla^2 + U(r) + H_{el},$$

where it is not necessary to explicit the form of H_{el}. The normalized eigenfunctions $\psi_j(r)$ and the eigenvalues E_j of $\hat{H}_A$ satisfy:

$$\hat{H}_A\psi_j(r) = E_j\psi_j(r),$$

and the corresponding atomic field operators can be written as:

$$\hat{\psi}(r) = \sum_j \hat{b}_j\psi_j(r)$$

$$\hat{\psi}^\dagger(r) = \sum_j \hat{b}_j^\dagger\psi_j^*(r),$$

where $\hat{b}_j^\dagger$ and $\hat{b}_j$ are the creation and annihilation operators of an atom in the state j, and they obey bosonic commutation relations $[\hat{b}_i, \hat{b}_j^\dagger] = \delta_{ij}$ and $[\hat{b}_i, \hat{b}_j] = [\hat{b}_i^\dagger, \hat{b}_j^\dagger] = 0$. The atomic Hamiltonian can be written as:

$$\hat{H}_A = \int d^3r \hat{\psi}^\dagger(r) H_A \hat{\psi}(r) = \sum_i E_i \hat{b}_i^\dagger \hat{b}_i.$$

Using the field operators the interaction Hamiltonian can be written as:

$$\hat{H}_{int} = \int d^3r \, \hat{\psi}^\dagger(r) \left[-\frac{q}{m} \hat{A} \cdot \hat{p} \right] \hat{\psi}(r)$$

The quantized vector potential operator $\hat{A}$ can be written as:

$$\hat{A} = \sum_k \sqrt{\frac{\hbar}{2\omega\epsilon_0}} \left[\hat{a}_k \vec{u}_k(r) + \hat{a}_k^\dagger \vec{u}_k^*(r) \right]$$

where $\vec{u}_k(r)$ are the normal modes of the field. After substituting the expression for $\hat{A}$ the interaction Hamiltonian becomes:

$$\hat{H}_{int} = -\frac{q}{m} \sum_{i,j,k} \hat{b}_i^\dagger \hat{b}_j \int d^3r \, \psi_i^*(r) \sqrt{\frac{\hbar}{2\omega\epsilon_0}} \left[\hat{a}_k \vec{u}_k(r) + \hat{a}_k^\dagger \vec{u}_k^*(r) \right] \hat{p} \psi_j(r)$$

After renaming:

$$g_{ijk} = -\frac{q}{m} \sqrt{\frac{1}{2\omega\epsilon_0\hbar}} \int d^3r \, \psi_i^*(r) \left(\vec{u}_k(r) \cdot \hat{p} \right) \psi_j(r)$$

the interaction Hamiltonian can be written as:

$$\hat{H}_{int} = \sum_{i,j,k} \hat{b}_i^\dagger \hat{b}_j \left(g_{ijk} \hat{a}_k + g_{ijk}^* \hat{a}_k^\dagger \right)$$

The expression for g_{ijk} is quite complicated. However, for typical light sources, with a wavelength much larger than the atomic size (the optical part of the light spectrum has a wavelength of about $500nm$, which is 10^4 times larger than the Bohr radius), the form of g_{ijk} can be simplified. Because of this great difference in length scales, we can assume that the light field is constant in space for the atom and so we can substitute $u_k(r) = u_k(r_0)$, where r_0 are the coordinates of the atom. This is the so called dipole approximation. Using this approximation and observing that $\hat{p} = \frac{i}{\hbar} m [\hat{H}_A, \hat{r}]$ the term $\int d^3r \psi_i^*(r) \hat{p} \psi_j(r)$ can be written as:

$$\begin{aligned} \int d^3r \psi_i^*(r) \hat{p} \psi_j(r) &= \frac{i}{\hbar} m (E_i - E_j) \langle i | \hat{r} | j \rangle \\ &= \frac{i}{\hbar} m (E_i - E_j) \vec{d}_{ij} \end{aligned}$$

where $\vec{d}_{ij}$ is the dipole moment for the $j \to i$ transition and where we used the ket notation for the eigenvectors of the Hamiltonian. Then we can write:

$$g_{ijk} = -\frac{q}{m}\sqrt{\frac{1}{2\omega\epsilon_0\hbar}}\vec{u}_k(r_0)\frac{i}{\hbar}m(E_i - E_j)\vec{d}_{ij}.$$

We can simplify the model even more if we consider a sigle mode of the light field and call its frequency ω. By calling $(E_2 - E_1) = \hbar\omega_A$, where ω_A is the atomic transition frequency, we can write:

$$g(r_0) = -iq\sqrt{\frac{1}{2\hbar\omega\epsilon_0}}\omega_A\vec{u}(r_0)\cdot\vec{d}_{ij}$$

where $\vec{u}(r_0)$ can be chosen such that g is real. From now on let us omit the position dependence of g. The interaction Hamiltonian becomes:

$$\hat{H}_{int} = \hbar g\left[\hat{b}_1^\dagger\hat{b}_2(\hat{a} + \hat{a}^\dagger) + \hat{b}_2^\dagger\hat{b}_1(\hat{a} + \hat{a}^\dagger)\right]$$

Let us now use the so called rotating wave approximation. If we work in the interaction picture the operators become:

$$(\hat{H}_{int})_I = e^{i\hat{H}_0 t/\hbar}\hat{H}_{int}e^{-i\hat{H}_0 t/\hbar},$$

where $\hat{H}_0 = \hat{H} - \hat{H}_{int}$. In this picture the operators $\hat{a}$ and $\hat{b}_j$ transform as:

$$\begin{aligned}\hat{b}_j(t) &= \hat{b}_j(0)e^{-iE_j t/\hbar}\\ \hat{a}(t) &= \hat{a}(0)e^{-i\omega t}.\end{aligned}$$

After substituting the values of these operators we can write the interaction Hamiltonian as:

$$(\hat{H}_{int})_I = \hbar g[\hat{b}_1^\dagger\hat{b}_2\hat{a}e^{-i(\omega_A+\omega)t} + \hat{b}_1^\dagger\hat{b}_2\hat{a}^\dagger e^{-i(\omega_A-\omega)t} + \hat{b}_2^\dagger\hat{b}_1\hat{a}e^{i(\omega_A-\omega)t} + \hat{b}_2^\dagger\hat{b}_1\hat{a}^\dagger e^{-i(\omega_A+\omega)t}]$$

If $\omega_A \approx \omega$, which means that the light field is close to the atomic resonance, the exponential terms in the previous equation oscillate with very different frequencies. The terms with $e^{-i(\omega_A+\omega)t} \approx e^{-2i\omega t}$ while the terms $e^{-i(\omega_A-\omega)t}$ oscillate much slower. For typical optical transitions $\omega_A + \omega \approx 10^{14}Hz$ while $\omega_A - \omega \lesssim 10^6 Hz$. The large difference of the time scales allows us to neglect the terms that oscillate very fast because, on any appreciable time scale the oscillations would average to zero. This is the rotating wave approximation. It can also be pointed out that the terms that we are neglecting with the rotating wave approximation are those that largely violate energy conservation. The term $\hat{b}_1^\dagger\hat{b}_2\hat{a}$ denotes the absorption of a photon and the transition from the excited state to the ground state. This process clearly violates energy conservation. Similarly, the term $\hat{b}_2^\dagger\hat{b}_1\hat{a}^\dagger$ represents the transition from

the ground state to the excited state that emits a photon. This process clearly violates energy conservation as well. The two terms that survive are $\hat{b}_1^\dagger \hat{b}_2 \hat{a}^\dagger$ and $\hat{b}_2^\dagger \hat{b}_1 \hat{a}$ which represent respectively the transition from the excited state to the ground state with the emission of a photon and the transition from the ground state to the excited state with the absorption of a photon. Therefore, by switching back from the interaction picture, the interaction Hamiltonian of a single two-level atom with a single-mode electromagnetic field can be written as:

$$\hat{H}_{int} = \hbar g \left[\hat{b}_1^\dagger \hat{b}_2 \hat{a}^\dagger + \hat{b}_2^\dagger \hat{b}_1 \hat{a} \right].$$

2.3.2 Interaction Hamiltonian

In our system we can describe the interaction of the atoms with the cavity photons using a variation of the interaction Hamiltonian we just derived. Using bosonic field operators and writing explicitly the parameter g as $g(\mathbf{r}) = -i\hbar\Omega_R f(\mathbf{r})$, the Hamiltonian can be written as:

$$\hat{H}_I = -i\hbar\Omega_R \int d^3\mathbf{r}\ f(\mathbf{r}) \big[\hat{a}\, \hat{\Psi}_e^\dagger(\mathbf{r}) \hat{\Psi}_g(\mathbf{r}) - \hat{a}^\dagger\, \hat{\Psi}_g^\dagger(\mathbf{r}) \hat{\Psi}_e(\mathbf{r}) \big], \tag{2.7}$$

where $f(\mathbf{r})$ is the mode function of the cavity, and Ω_R is called the single-photon Rabi frequency.

2.4 Complete Hamiltonian

The Hamiltonian that describes the whole system is the sum of the individual contributions $\hat{H} = \hat{H}_A + \hat{H}_C + \hat{H}_I$, and it can be written as:

$$\begin{aligned} \hat{H} = \sum_{\sigma=g,e} \int d^3\mathbf{r}\ \hat{\Psi}_\sigma^\dagger(\mathbf{r}) \Big[& -\frac{\hbar^2}{2m}\nabla^2 + V(\mathbf{r}) + \hbar\omega_A\ \delta_{\sigma,e} \\ & + \frac{1}{2} \sum_{\sigma'} g_{\sigma\sigma'} \hat{\Psi}_{\sigma'}^\dagger(\mathbf{r}) \hat{\Psi}_{\sigma'}(\mathbf{r}) \Big] \hat{\Psi}_\sigma(\mathbf{r}) + \\ & \hbar\omega_C\, \hat{a}^\dagger\, \hat{a} - i\hbar\eta \Big(e^{i\omega_L t} \hat{a} - e^{-i\omega_L t} \hat{a}^\dagger \Big) \\ & - i\hbar\Omega_R \int d^3\mathbf{r}\ f(\mathbf{r}) \big[\hat{a}\, \hat{\Psi}_e^\dagger(\mathbf{r}) \hat{\Psi}_g(\mathbf{r}) - \hat{a}^\dagger\, \hat{\Psi}_g^\dagger(\mathbf{r}) \hat{\Psi}_e(\mathbf{r}) \big] \end{aligned} \tag{2.8}$$

2.4.1 Rotating frame

We notice from Eq. (2.8) that the Hamiltonian of the system is time dependent through $\hat{H}_C$. However, it is possible to eliminate the time dependence of $\hat{H}_C$ by switching to a rotating frame with frequency ω_L, which allows us to work with slowly varying variables. The change of frame is performed

by using a unitary transformation $\hat{U}$ that acts on any given operator $\hat{O}$ and any given state $|\phi\rangle$ in the following manner:

$$\tilde{O} = \hat{U}\hat{O}\hat{U}^\dagger$$

$$|\tilde{\phi}\rangle = \hat{U}|\phi\rangle$$

where the tilde is used to identify the operators and the states in the new frame. Let us now see how the Hamiltonian transforms. The Schrödinger equation in the original frame can be written as:

$$i\hbar\frac{d}{dt}|\phi\rangle = \hat{H}|\phi\rangle$$

Let us now insert the identity $\hat{U}^\dagger\hat{U}$ before the state $|\phi\rangle$ and apply $\hat{U}$ on the left:

$$\begin{aligned}
\hat{U}H\hat{U}^\dagger\hat{U}|\phi\rangle &= \hat{U}i\hbar\frac{d}{dt}\left(\hat{U}^\dagger\hat{U}|\phi\rangle\right) \\
\hat{U}H\hat{U}^\dagger|\tilde{\phi}\rangle &= i\hbar\hat{U}\frac{d}{dt}\left(\hat{U}^\dagger|\tilde{\phi}\rangle\right) \\
&= i\hbar\hat{U}\left(\dot{\hat{U}}^\dagger|\tilde{\phi}\rangle + \hat{U}^\dagger\frac{d}{dt}|\tilde{\phi}\rangle\right) \\
&= i\hbar\left(\hat{U}\dot{\hat{U}}^\dagger + \frac{d}{dt}\right)|\tilde{\phi}\rangle
\end{aligned}$$

Therefore, in the rotating frame, the Schrödinger's equation

$$i\hbar\frac{d}{dt}|\tilde{\phi}\rangle = \tilde{H}|\tilde{\phi}\rangle$$

holds when

$$\tilde{H} = \hat{U}H\hat{U}^\dagger + i\hbar\dot{\hat{U}}\hat{U}^\dagger, \tag{2.9}$$

where the identity $\dot{\hat{U}}\hat{U}^\dagger + \hat{U}\dot{\hat{U}}^\dagger = 0$ was used in the last step.

The unitary transformation we use to eliminate the time dependence of the Hamiltonian is:

$$\hat{U}(t) = \exp\left\{i\omega_L t\left[\hat{a}^\dagger\hat{a} + \int d^3\mathbf{r}\ \hat{\Psi}_e^\dagger(\mathbf{r})\hat{\Psi}_e(\mathbf{r})\right]\right\} \tag{2.10}$$

The photon creation and annihilation operators $\hat{a}$ and $\hat{a}^\dagger$ commute with the field operators $\hat{\Psi}_e(\mathbf{r})$ and $\hat{\Psi}_e^\dagger(\mathbf{r})$ because they act on different Hilbert spaces. We are then allowed to write the unitary transformation as the product of two exponentials:

$$\hat{U}(t) = \hat{U}_a\,\hat{U}_e = \exp\left\{i\omega_L t\ \hat{a}^\dagger\hat{a}\right\}\ \exp\left\{i\omega_L t\int d^3\mathbf{r}\ \hat{\Psi}_e^\dagger(\mathbf{r})\hat{\Psi}_e(\mathbf{r})\right\},$$

where $\hat{U}_a = \exp\left\{i\omega_L t\ \hat{a}^\dagger\hat{a}\right\}$ and $\hat{U}_e = \exp\left\{i\omega_L t \int d^3\mathbf{r}\ \hat{\Psi}_e^\dagger(\mathbf{r})\hat{\Psi}_e(\mathbf{r})\right\}$, and we can compute separately the action of the first and second exponential of the unitary transformation $\hat{U}$ on the Hamiltonian. It is also worth noticing that $\int d^3\mathbf{r}\ \hat{\Psi}_e^\dagger(\mathbf{r})\hat{\Psi}_e(\mathbf{r}) = \hat{N}_e$, where $\hat{N}_e$ is the number operator for the atoms in the excited electronic state.

Let us calculate the transformed Hamiltonian through Eq. (2.9). Let us start by computing its second part: $i\hbar\dot{\hat{U}}\hat{U}^\dagger$. The derivative of the unitary operator $\hat{U}$ is:

$$\dot{\hat{U}} = i\omega_L\left[\hat{a}^\dagger\hat{a} + \int d^3\mathbf{r}\ \hat{\Psi}_e^\dagger(\mathbf{r})\hat{\Psi}_e(\mathbf{r})\right]\ \exp\left\{i\omega_L t\left[\hat{a}^\dagger\hat{a} + \int d^3\mathbf{r}\ \hat{\Psi}_e^\dagger(\mathbf{r})\hat{\Psi}_e(\mathbf{r})\right]\right\}$$

and

$$i\hbar\dot{U}U^\dagger = -\hbar\omega_L\left[\hat{a}^\dagger\hat{a} + \int d^3\mathbf{r}\ \hat{\Psi}_e^\dagger(\mathbf{r})\hat{\Psi}_e(\mathbf{r})\right].$$

Let us now calculate the first term of the transformed Hamiltonian: $\hat{U}\hat{H}\hat{U}^\dagger$. Since the Hamiltonian of the system is the sum of three parts, $\hat{H} = \hat{H}_A + \hat{H}_C + \hat{H}_I$, let us apply the unitary transformation to each of them. Let us start with

$$\hat{H}_C = \hbar\omega_C\,\hat{a}^\dagger\,\hat{a} - i\hbar\eta\left(e^{i\omega_L t}\hat{a} - e^{-i\omega_L t}\hat{a}^\dagger\right) = \hat{H}_0 + \hat{H}_1$$

where $\hat{H}_0 = \hbar\omega_C\,\hat{a}^\dagger\,\hat{a}$ and $\hat{H}_1 = -i\hbar\eta\left(e^{i\omega_L t}\hat{a} - e^{-i\omega_L t}\hat{a}^\dagger\right)$. In $\hat{H}_C$ we find only photon annihilation and creation operators. Therefore it is sufficient to consider only the part of the unitary transformation $\hat{U}$ that depends on these operators, $\hat{U}_a$, as the part that depends on the atomic field operators, $\hat{U}_e$, commutes with $\hat{H}_C$ and gives no contribution. However, $\hat{U}_a$ commutes with $\hat{H}_0$ as well, because they are both functions of $\hat{a}^\dagger\hat{a}$. This means that:

$$\tilde{H}_0 = \hat{U}_a\hat{H}_0\hat{U}_a^\dagger = \hat{H}_0 = \hbar\omega_c\hat{a}^\dagger\hat{a}.$$

The transformed operator of $\hat{H}_1$ is:

$$\tilde{H}_1 = \hat{U}_a\hat{H}_1\hat{U}_a^\dagger = -i\hbar\eta\left(e^{i\omega_L t}\hat{U}_a\hat{a}\hat{U}_a^\dagger - e^{-i\omega_L t}\hat{U}_a\hat{a}^\dagger\hat{U}_a^\dagger\right).$$

Now we need to evaluate $\tilde{a} = \hat{U}_a\hat{a}\hat{U}_a^\dagger$ and $\tilde{a}^\dagger = \hat{U}_a\hat{a}^\dagger\hat{U}_a^\dagger$. We can compute them by using a special case of the Campbell-Baker-Haussdorf equality:

$$e^{\lambda\hat{A}}\hat{B}e^{-\lambda\hat{A}} = e^{\lambda\gamma},$$

where $\hat{A}$ and $\hat{B}$ are operators that satisfy $[\hat{A},\hat{B}] = \gamma\hat{B}$. Since $[\hat{a}^\dagger\hat{a},\hat{a}] = -\hat{a}$ and $[\hat{a}^\dagger\hat{a},\hat{a}^\dagger] = \hat{a}^\dagger$, we find that:

$$\begin{aligned}\tilde{a} &= e^{i\omega_L t}\hat{a}\\ \tilde{a}^\dagger &= e^{-i\omega_L t}\hat{a}^\dagger.\end{aligned}$$

We can now compute $\tilde{H}_1$:

$$\tilde{H}_1 = -i\hbar\eta\left(e^{i\omega_L t}\tilde{a} - e^{-i\omega_L t}\tilde{a}^\dagger\right) = -i\hbar\eta(\hat{a} - \hat{a}^\dagger)$$

Therefore the expression for $\tilde{H}_C$ is:

$$\tilde{H}_C = \hbar\omega_c\hat{a}^\dagger\hat{a} - i\hbar\eta(\hat{a} - \hat{a}^\dagger). \tag{2.11}$$

When applying the unitary transformation to light-matter interaction part of the Hamiltonian, $\hat{H}_I$, we need to compute:

$$\tilde{H}_I = \hat{U}\hat{H}_I\hat{U}^\dagger = -i\hbar\Omega_R \int d^3\mathbf{r}\ f(\mathbf{r})\left[\hat{U}\hat{a}\,\hat{\Psi}_e^\dagger(\mathbf{r})\hat{\Psi}_g(\mathbf{r})\hat{U}^\dagger - \hat{U}\hat{a}^\dagger\,\hat{\Psi}_g^\dagger(\mathbf{r})\hat{\Psi}_e(\mathbf{r})\hat{U}^\dagger\right]$$

The expression between brackets can be written in a more convenient fashion. After inserting $\hat{U}^\dagger\hat{U}$ after the photon operators and reordering the operators we get:

$$\tilde{a}\tilde{\Psi}_e^\dagger(\mathbf{r})\hat{\Psi}_g(\mathbf{r}) - \tilde{a}^\dagger\hat{\Psi}_g^\dagger(\mathbf{r})\tilde{\Psi}_e(\mathbf{r}),$$

where $\tilde{\Psi}_e^\dagger(\mathbf{r}) = \hat{U}\hat{\Psi}_e^\dagger(\mathbf{r})\hat{U}^\dagger$ and $\tilde{\Psi}_e(\mathbf{r}) = \hat{U}\hat{\Psi}_e(\mathbf{r})\hat{U}^\dagger$ are the transformed expressions for the atomic field operators. Using the Campbell-Baker-Haussdorf equality and the commutation relations $[\int d^3\mathbf{r}\ \hat{\Psi}_e^\dagger(\mathbf{r})\hat{\Psi}_e(\mathbf{r}), \hat{\Psi}_e(\mathbf{r})] = -\hat{\Psi}_e(\mathbf{r})$ and $[\int d^3\mathbf{r}\ \hat{\Psi}_e^\dagger(\mathbf{r})\hat{\Psi}_e(\mathbf{r}), \hat{\Psi}_e^\dagger(\mathbf{r})] = \hat{\Psi}_e^\dagger(\mathbf{r})$, we find that:

$$\begin{aligned}\tilde{\Psi}_e(\mathbf{r}) &= e^{i\omega_L t}\,\hat{\Psi}_e(\mathbf{r}) \\ \tilde{\Psi}_e^\dagger(\mathbf{r}) &= e^{-i\omega_L t}\,\hat{\Psi}_e^\dagger(\mathbf{r}).\end{aligned}$$

This means that:

$$\tilde{H}_I = \hat{H}_I. \tag{2.12}$$

The last term of the Hamiltonian we need to calculate is the transformed expression of $\hat{H}_A$. We will show that this part of the Hamiltonian commutes with $\hat{U}$, remembering the commutation relations of the atomic field operators:

$$[\hat{N}_e, \hat{\psi}_\sigma(\mathbf{r})] = -\hat{\psi}_\sigma(\mathbf{r})\delta_{e,\sigma}$$

$$[\hat{N}_e, \hat{\psi}_\sigma^\dagger(\mathbf{r})] = \hat{\psi}_\sigma^\dagger(\mathbf{r})\delta_{e,\sigma},$$

and the fact that $[e^{\hat{A}}, \hat{B}] = 0$ if $[\hat{A}, \hat{B}] = 0$. $\hat{H}_A$ can be separated into its one-body part, which contains two field operators, and its two-body part, which contains four field operators. The one-body part that depends on the ground state field operator is:

$$\int d^3\mathbf{r}\ \hat{\Psi}_g^\dagger(\mathbf{r})T(\mathbf{r})\hat{\Psi}_g(\mathbf{r}),$$

where $T(\mathbf{r}) = -\frac{\hbar^2}{2m}\nabla^2 + V(\mathbf{r}) + \hbar\omega_A\ \delta_{\sigma,e}$ with $\sigma = g$, and it clearly commutes with $\hat{N}_e$. The one-body part that depends on the excited state field operator is:

$$\int d^3\mathbf{r}\ \hat{\Psi}_e^\dagger(\mathbf{r}) T(\mathbf{r}) \hat{\Psi}_e(\mathbf{r}),$$

and for the sake of clarity let us call it $\hat{H}_{A1}$. Let us show that $\hat{H}_{A1}$ commutes with $\hat{N}_e$, by proving that $\hat{H}_{A1}\hat{N}_e = \hat{N}_e\hat{H}_{A1}$:

$$\begin{aligned}
\hat{H}_{A1}\hat{N}_e &= \int d^3\mathbf{r}\ \hat{\Psi}_e^\dagger(\mathbf{r}) T(\mathbf{r}) \hat{\Psi}_e(\mathbf{r}) \hat{N}_e \\
&= \int d^3\mathbf{r}\ \hat{\Psi}_e^\dagger(\mathbf{r}) T(\mathbf{r}) \big[\hat{N}_e \hat{\Psi}_e(\mathbf{r}) + \hat{\Psi}_e(\mathbf{r})\big] \\
&= \int d^3\mathbf{r}\ \hat{\Psi}_e^\dagger(\mathbf{r}) T(\mathbf{r}) \hat{N}_e \hat{\Psi}_e(\mathbf{r}) + \hat{H}_{A1} \\
&= \int d^3\mathbf{r}\ \big[\hat{N}_e \hat{\Psi}_e^\dagger(\mathbf{r}) - \hat{\Psi}_e^\dagger(\mathbf{r})\big] T(\mathbf{r}) \hat{\Psi}_e(\mathbf{r}) + \hat{H}_{A1} \\
&= \int d^3\mathbf{r}\ \hat{N}_e \hat{\Psi}_e^\dagger(\mathbf{r}) T(\mathbf{r}) \hat{\Psi}_e(\mathbf{r}) \\
&= \hat{N}_e \hat{H}_{A1}.
\end{aligned}$$

Therefore the one-body part of $\hat{H}_A$ commutes with $\hat{U}$. With similar, but more tedious calculations, it can be shown that the two-body part of $\hat{H}_A$ commutes with N_e as well. Therefore:

$$\tilde{H}_A = \hat{H}_A. \tag{2.13}$$

At this point we can write the complete Hamiltonian in the rotating frame by summing all the previous terms:

$$\begin{aligned}
\hat{H} = \sum_{\sigma=g,e} \int d^3\mathbf{r}\ \hat{\Psi}_\sigma^\dagger(\mathbf{r}) \Big[&-\frac{\hbar^2}{2m}\nabla^2 + V(\mathbf{r}) - \hbar\Delta_A \delta_{\sigma,e} \\
&+ \frac{1}{2}\sum_{\sigma'} g_{\sigma\sigma'} \hat{\Psi}_{\sigma'}^\dagger(\mathbf{r}) \hat{\Psi}_{\sigma'}(\mathbf{r}) \Big] \hat{\Psi}_\sigma(\mathbf{r}) - \hbar\Delta_C\, \hat{a}^\dagger\, \hat{a} - i\hbar\eta\big(\hat{a} - \hat{a}^\dagger\big) \\
&- i\hbar\Omega_R \int d^3\mathbf{r}\ f(\mathbf{r}) \big[\hat{a}\, \hat{\Psi}_e^\dagger(\mathbf{r}) \hat{\Psi}_g(\mathbf{r}) - \hat{a}^\dagger\, \hat{\Psi}_g^\dagger(\mathbf{r}) \hat{\Psi}_e(\mathbf{r})\big],
\end{aligned} \tag{2.14}$$

where the tilde symbol is no longer used. The Hamiltonian is no longer time dependent. However, the change of frame has another consequence on the expression of the Hamiltonian: the bare frequencies of the atomic transition ω_A, and of the cavity ω_C are substituted by the following detunings: $\Delta_A = \omega_L - \omega_A$ and $\Delta_C = \omega_L - \omega_C$.

2.5 Heisenberg equations

Now that we have written the Hamiltonian of the whole system we can derive the Heisenberg equations of the field operators. The Heisenberg equation for an operator $\hat{O}$ and Hamiltonian $\hat{H}$ are:

$$i\hbar\frac{\partial}{\partial t}\hat{O} = [\hat{O}, \hat{H}].$$

Let us write the equation for the operators $\hat{a}$, $\hat{\Psi}_g(\mathbf{r})$ and $\hat{\Psi}_e(\mathbf{r})$:

$$i\hbar\frac{\partial}{\partial t}\hat{a} = [\hat{a}, \hat{H}] = -\hbar\Delta_C\,\hat{a} + i\hbar\eta + i\hbar\Omega_R\int d^3\mathbf{r} f(\mathbf{r})\hat{\Psi}_g^\dagger(\mathbf{r})\hat{\Psi}_e(\mathbf{r}), \quad (2.15a)$$

$$i\hbar\frac{\partial}{\partial t}\hat{\Psi}_g(\mathbf{r}) = [\hat{\Psi}_g(\mathbf{r}), \hat{H}] = \Bigg[-\frac{\hbar^2}{2m}\nabla^2 + V(\mathbf{r}) + \sum_\sigma g_{g\sigma}\hat{\Psi}_\sigma^\dagger(\mathbf{r})\hat{\Psi}_\sigma(\mathbf{r})\Bigg]\hat{\Psi}_g(\mathbf{r}) + i\hbar\Omega_R f(\mathbf{r})\hat{a}^\dagger\,\hat{\Psi}_e(\mathbf{r}), \quad (2.15b)$$

$$i\hbar\frac{\partial}{\partial t}\hat{\Psi}_e(\mathbf{r}) = [\hat{\Psi}_e(\mathbf{r}), \hat{H}] = \Bigg[-\frac{\hbar^2}{2m}\nabla^2 + V(\mathbf{r}) - \hbar\Delta_A + \sum_\sigma g_{e\sigma}\hat{\Psi}_\sigma^\dagger(\mathbf{r})\hat{\Psi}_\sigma(\mathbf{r})\Bigg]\hat{\Psi}_e(\mathbf{r}) - i\hbar\Omega_R f(\mathbf{r})\hat{a}\,\hat{\Psi}_g(\mathbf{r}). \quad (2.15c)$$

In the limit, when the atomic detuning Δ_A is much larger than the other characteristic frequency scales of the system, the population of the excited state follows adiabatically the ground state. Therefore the excited state field operator can be adiabatically eliminated. In fact, the field operators $\hat{\psi}_g(\mathbf{r})$ and $\hat{a}$ vary on a much larger time scale than $1/\Delta_A$, which is the characteristic time of $\hat{\psi}_e(\mathbf{r})$. Under these conditions the square bracket in Eq. (2.15c) is dominated by the atomic detuning, and the excited state field operator immediately relaxes to its steady-state value. Therefore we can set its time derivative to zero and calculate its value as a function of the slow evolving fields $\hat{\psi}_g(\mathbf{r})$ and $\hat{a}$:

$$\hat{\Psi}_e(\mathbf{r}) \simeq -i\frac{\Omega_R f(\mathbf{r})}{\Delta_A} a\,\hat{\Psi}_g(\mathbf{r}). \quad (2.16)$$

At this point we can substitute the expression (2.16) into the Heisenberg equations for $\hat{\psi}_g(\mathbf{r})$ and $\hat{a}$ and we get:

$$i\hbar\partial_t\hat{a} = -\hbar\Delta_C\,\hat{a} + i\hbar\eta + \hbar\frac{\Omega_R^2}{\Delta_A}\hat{a}\int d^3r f^2(\mathbf{r})\hat{\Psi}_g^\dagger(\mathbf{r})\hat{\Psi}_g(\mathbf{r}), \quad (2.17a)$$

$$i\hbar\partial_t\hat{\Psi}_g(\mathbf{r}) = \Bigg[-\frac{\hbar^2}{2m}\nabla^2 + V(\mathbf{r}) + \hbar\frac{\Omega_R^2}{\Delta_A} f^2(\mathbf{r})\hat{a}^\dagger\hat{a} + g_{gg}\hat{\Psi}_g^\dagger(\mathbf{r})\hat{\Psi}_g(\mathbf{r})\Bigg]\hat{\Psi}_g(\mathbf{r}), \quad (2.17b)$$

where we have neglected the interaction with excited state atoms, assuming that the population of the excited state is much smaller than that of the ground state. At this point we can notice that Equations (2.17) can be thought as the Heisenberg equations that derive from the following effective Hamiltonian:

$$\hat{H}_{\text{eff}} = -\hbar\Delta_C\hat{a}^\dagger\hat{a} - i\hbar\eta(\hat{a} - \hat{a}^\dagger) + \int d^3\mathbf{r}\ \hat{\Psi}_g^\dagger(\mathbf{r})\Bigg[-\frac{\hbar^2}{2m}\nabla^2 + V(\mathbf{r}) + \hbar U_0\,\hat{a}^\dagger\hat{a}f^2(\mathbf{r}) + \frac{1}{2}g_{gg}\hat{\Psi}_g^\dagger(\mathbf{r})\hat{\Psi}_g(\mathbf{r})\Bigg]\hat{\Psi}_g(\mathbf{r}), \quad (2.18)$$

where $U_0 = \Omega_R^2/\Delta_A$ has been introduced. As a result of the adiabatic elimination of the excited state, the atom-photon interaction is represented by the term $\hbar U_0\,\hat{a}^\dagger\hat{a}f^2(\mathbf{r})$, which has the form of a new optical potential with position dependence $f^2(\mathbf{r})$ and an effective amplitude $U_0\,a^\dagger a$. When the atomic transition is red detuned from the pumping ($\Delta_A < 0$ and therefore $U_0 < 0$), the atoms are attracted to the intensity maximum of the cavity field, which effectively lowers the double-well barrier. When the atomic transition is blue detuned ($\Delta_A > 0$ and therefore $U_0 > 0$) the atoms are repelled from the intensity maximum of the cavity field [12]. This effect is proportional to the photon number $\hat{a}^\dagger\hat{a}$ and therefore the state of the cavity influences the parameters of the Josephson junction.

2.6 Two-Mode Hamiltonian

It is convenient to transform the Hamiltonian into a simpler form. In order for us to do this we take advantage of the properties of the eigenfunctions of a double well potential, and therefore use a two-mode description of the system. The Hamiltonian of a double well potential in one dimension is:

$$\hat{H}_{DW} = -\frac{\hbar^2}{2m}\frac{d^2}{dx^2} + V_{DW}(x).$$

If the double well potential is symmetric with respect to x, then the Hamiltonian $\hat{H}_{DW}$ commutes with with the parity operator $\hat{P}$. This means that the eigenfunctions of the system must be eigenstates of both $\hat{H}_{DW}$ and $\hat{P}$, and so they must have a defined parity. By solving the Schrödinger equation of the system it can be found that the ground state $|\varphi_s\rangle$ is symmetric and

the first excited state $|\varphi_a\rangle$ is antisymmetric. From these two eigenstates it is possible to build local Wannier-like states $w_1(x)$ and $w_2(x)$, which are highly localized eigenstates, centered around the minima of the unperturbed double-well potential $V_{DW}(x)$. The Wannier states are linear combinations of the ground and first excited states of the system:

$$\begin{aligned} w_1(x) &= \frac{|\varphi_s\rangle + |\varphi_a\rangle}{\sqrt{2}} \\ w_2(x) &= \frac{|\varphi_s\rangle - |\varphi_a\rangle}{\sqrt{2}}. \end{aligned}$$

We assume that the Wannier states remain unchanged when the cavity field is turned on. This assumption means that the second excited state of the double well potential stays away from the low-energy doublet even when a classical cavity field is present. If Δ_{DW} is the difference in energy between the second excited state and the first one, the condition that makes the assumption hold can be written as: $\Delta_{DW} \gg -U_0\xi^2\langle f^2(\mathbf{r})\rangle$, where ξ^2 is the average number of photons in the cavity and the average $\langle f^2(\mathbf{r})\rangle$ is calculated with respect to the condensate wave function [11].

The atomic field operator can then be approximated as:

$$\hat{\Psi}_g(\mathbf{r}) = \Big(w_1(x)\ \hat{b}_1 + w_2(x)\ \hat{b}_2\Big)\ \frac{e^{-(y^2+z^2)/(2l_H^2)}}{\pi^{1/2} l_H}\ , \tag{2.19}$$

where $\hat{b}_1$ and $\hat{b}_2$ are the bosonic annihilation operators of the Wannier-like functions centered around the two minima of the double well potential, $\frac{e^{-(y^2+z^2)/(2l_H^2)}}{\pi^{1/2} l_H}$ is the lowest energy eigenfunction of the 2D harmonic potential in the (y, z) plane, and $l_H = \sqrt{\hbar/(m\omega_H)}$ is the characteristic length of the strong harmonic confinement.

For the sake of simplicity we can write the atomic field operator as:

$$\hat{\Psi}_g(\mathbf{r}) = \hat{\phi}(x)\varphi(y, z)$$

in which we have separated the part of the field operator that depends on the coordinate x and on the coordinates (y, z).

In order for us to write the two-mode description of the Hamiltonian we need to substitute the new expression for $\hat{\Psi}_g(\mathbf{r})$ into the effective Hamiltonian. The part of the effective Hamiltonian $\hat{H}_{eff}$ that depends on the atomic field operator is:

$$\int d^3\mathbf{r}\ \hat{\Psi}_g^\dagger(\mathbf{r})\Bigg[-\frac{\hbar^2}{2m}\nabla^2 + V(\mathbf{r}) + \hbar U_0\,\hat{a}^\dagger\hat{a} f^2(\mathbf{r}) + \frac{1}{2}g_{gg}\hat{\Psi}_g^\dagger(\mathbf{r})\hat{\Psi}_g(\mathbf{r})\Bigg]\hat{\Psi}_g(\mathbf{r}).$$

This integral can be divided into three parts:

$$\hat{H}_1^{eff} = \int d^3\mathbf{r}\ \hat{\Psi}_g^\dagger(\mathbf{r})\left[-\frac{\hbar^2}{2m}\nabla^2 + V(\mathbf{r})\right]\hat{\Psi}_g(\mathbf{r}) \tag{2.20}$$

$$\hat{H}_2^{eff} = \int d^3\mathbf{r}\ \hat{\Psi}_g^\dagger(\mathbf{r})\left[\hbar U_0\, \hat{a}^\dagger\hat{a} f^2(\mathbf{r})\right]\hat{\Psi}_g(\mathbf{r}) \tag{2.21}$$

$$\hat{H}_3^{eff} = \int d^3\mathbf{r}\ \hat{\Psi}_g^\dagger(\mathbf{r})\left[\frac{1}{2}g_{gg}\hat{\Psi}_g^\dagger(\mathbf{r})\hat{\Psi}_g(\mathbf{r})\right]\hat{\Psi}_g(\mathbf{r}). \tag{2.22}$$

Let us start by evaluating the first part. Between brackets in $\hat{H}_1^{eff}$ we find the kinetic part of the Hamiltonian and the external potential. The explicit expression of the external potential is $V(\mathbf{r}) = V_{DW}(x) + \frac{1}{2}m\omega_H^2(y^2+z^2)$. We can separate the terms inside of the brackets in $\hat{H}_1^{eff}$ into its x-dependent part and (y,z)-dependent part:

$$H_{1,x}^{eff} = -\frac{\hbar^2}{2m}\frac{d^2}{dx^2} + V_{DW}(x)$$

and

$$H_{1,yz}^{eff} = -\frac{\hbar^2}{2m}(\frac{d^2}{dy^2} + \frac{d^2}{dz^2}) + \frac{1}{2}m\omega_H^2(y^2+z^2)$$

Let us now integrate H_1^{eff}. The integral can be written as:

$$\begin{aligned}
\hat{H}_{eff,1} &= \int dx\, dy\, dz\ \left[\hat{\phi}^\dagger(x)\varphi(y,z)\left(H_{1x}^{eff} + H_{1yz}^{eff}\right)\hat{\phi}(x)\varphi(y,z)\right] \\
&= \int dx\, dy\, dz\ \left[\hat{\phi}^\dagger(x)\varphi(y,z)H_{1x}^{eff}\hat{\phi}(x)\varphi(y,z) + \hat{\phi}^\dagger(x)\varphi(y,z)H_{1yz}^{eff}\hat{\phi}(x)\varphi(y,z)\right] \\
&= \int dx\ \left[\hat{\phi}^\dagger(x)H_{1x}^{eff}\hat{\phi}(x)\right] + \int dx\ \left[\hat{\phi}^\dagger(x)\hat{\phi}(x)\right]\int dy\, dz\ \left[\varphi(y,z)H_{1yz}^{eff}\varphi(y,z)\right]
\end{aligned} \tag{2.23}$$

In the last line we used the fact that $\varphi(y,z)$ is normalized. The last term of the last integral in the y,z variables can be calculated explicitly:

$$\int dy\, dz\ \left[\varphi(y,z)H_{1yz}^{eff}\varphi(y,z)\right] = \hbar\omega_H,$$

and the integral in the variable x becomes:

$$\int dx\, \hat{\phi}^\dagger(x)\hat{\phi}(x) = \int dx\ \left[\left(w_1^*(x)\ \hat{b}_1^\dagger + w_2^*(x)\ \hat{b}_2^\dagger\right)\left(w_1(x)\ \hat{b}_1 + w_2(x)\ \hat{b}_2\right)\right].$$

Using the fact that the $w_1(x)$ and $w_2(x)$ are orthonormal functions we find that the integral becomes simply:

$$\hat{b}_1^\dagger\hat{b}_1 + \hat{b}_2^\dagger\hat{b}_2 = \hat{n}_1 + \hat{n}_2 = \hat{N}_A,$$

where $\hat{b}_1^\dagger \hat{b}_1 = \hat{n}_1$ is the number operator of atoms in the left well, $\hat{b}_2^\dagger \hat{b}_2 = \hat{n}_2$ is the number operator of atoms in the right well and $\hat{N}_A$ is the operator of the total number of atoms. As for the first integral in Eq. (2.23), we can write it as:

$$\int dx \left[\hat{\phi}^\dagger(x) H_{1x}^{eff} \hat{\phi}(x)\right] = \int dx \left(w_1^*(x)\ \hat{b}_1^\dagger + w_2^*(x)\ \hat{b}_2^\dagger\right) \left[-\frac{\hbar^2}{2m}\frac{d^2}{dx^2} + V_{DW}(x)\right] \left(w_1(x)\ \hat{b}_1 + w_2(x)\ \hat{b}_2\right)$$

This integral is made of four terms which can be written as:

$$\begin{aligned}
\int dx\, \hat{\phi}^\dagger(x) H_{eff,1x} \hat{\phi}(x) &= \hat{b}_1^\dagger \hat{b}_1 \int dx\, w_1^*(x) \left[-\frac{\hbar}{2m}\frac{d^2}{dx^2} + V_{DW}(x)\right] w_1(x) \\
&+ \hat{b}_2^\dagger \hat{b}_2 \int dx\, w_2^*(x) \left[-\frac{\hbar}{2m}\frac{d^2}{dx^2} + V_{DW}(x)\right] w_2(x) \\
&+ \hat{b}_1^\dagger \hat{b}_2 \int dx\, w_1^*(x) \left[-\frac{\hbar}{2m}\frac{d^2}{dx^2} + V_{DW}(x)\right] w_2(x) \\
&+ \hat{b}_2^\dagger \hat{b}_1 \int dx\, w_2^*(x) \left[-\frac{\hbar}{2m}\frac{d^2}{dx^2} + V_{DW}(x)\right] w_1(x).
\end{aligned}$$

Now we can rename the integrals:

$$\epsilon' = \int dx\, w_j^*(x) \left[-\frac{\hbar^2}{2m}\frac{d^2}{dx^2} + V_{DW}(x)\right] w_j(x),$$

where $j = 1, 2$, and

$$J = -\int dx\, w_i^*(x) \left[-\frac{\hbar^2}{2m}\frac{d^2}{dx^2} + V_{DW}(x)\right] w_j(x),$$

where $i \neq j$. The Wannier functions can be chosen so that J is real and positive. Since the double well is symmetric, both ϵ' and J do not depend on the i or j index. Therefore the whole integral $\hat{H}_1^{eff}$ can be written as:

$$\begin{aligned}
\hat{H}_1^{eff} &= \hbar\omega_H \hat{N}_A + \epsilon' \hat{N}_A - J\left(\hat{b}_2^\dagger \hat{b}_1 + \hat{b}_1^\dagger \hat{b}_2\right) \\
&= \epsilon \hat{N}_A - J\left(\hat{b}_2^\dagger \hat{b}_1 + \hat{b}_1^\dagger \hat{b}_2\right), \qquad (2.24)
\end{aligned}$$

where $\epsilon = \hbar\omega_H + \epsilon'$ is the on-site energy of a single well and J represents the tunneling amplitude.

Let us now evaluate $\hat{H}_2^{eff}$. By writing the mode function as the product of its x-dependent part and its (y, z)-dependent part we can write:

$$\begin{aligned}
\hat{H}_2^{eff} &= \int dx\, dy\, dz \left[\hat{\phi}^\dagger(x)\varphi(y,z) \left(\frac{2\hbar U_0}{\pi L \sigma^2} \hat{a}^\dagger \hat{a} f_x(x) f_{yz}(y,z)\right) \hat{\phi}(x)\varphi(y,z)\right] \\
&= \frac{2\hbar U_0}{\pi L \sigma^2} \hat{a}^\dagger \hat{a} \int dx \left[\hat{\phi}^\dagger(x) f_x(x) \hat{\phi}(x)\right] \int dy\, dz \left[\varphi(y,z) f_{yz}(y,z) \varphi(y,z)\right],
\end{aligned}$$

where $f_x(x) = e^{-x^2/\sigma^2}$ and $f_{yz}(y,z) = \cos^2(k\,y)e^{-z^2/\sigma^2}$. The second integral in the last line can be carried out explicitly:

$$\int dy\,dz\;[\,\varphi(y,z)f_{yz}(y,z)\varphi(y,z)] = \frac{\sigma}{2}\frac{(e^{-k^2l_H^2}+1)}{\sqrt{\sigma^2+l_H^2}}.$$

The complete integral then becomes:

$$\hat{H}_2^{eff} = \frac{(e^{-k^2l_H^2}+1)}{\sqrt{\sigma^2+l_H^2}}\frac{\hbar U_0}{\pi L\sigma}\hat{a}^\dagger\hat{a}\int dx\;\left[\hat{\phi}^\dagger(x)f_x(x)\hat{\phi}(x)\right]. \tag{2.25}$$

The last integral is made of four parts:

$$\begin{aligned}\int dx\;\left[\hat{\phi}^\dagger(x)f_x(x)\hat{\phi}(x)\right] &= \hat{b}_1^\dagger\hat{b}_1\int dx\,|w_1(x)|^2\left[e^{-\frac{x^2}{\sigma^2}}\right]\\ &+ \hat{b}_2^\dagger\hat{b}_2\int dx\,|w_2(x)|^2\left[e^{-\frac{x^2}{\sigma^2}}\right]\\ &+ \hat{b}_1^\dagger\hat{b}_2\int dx\,w_1^*(x)\left[e^{-\frac{x^2}{\sigma^2}}\right]w_2(x)\\ &+ \hat{b}_2^\dagger\hat{b}_1\int dx\,w_2^*(x)\left[e^{-\frac{x^2}{\sigma^2}}\right]w_1(x).\end{aligned}$$

Now we can rename:

$$W_0 = \frac{\hbar U_0\left(1+e^{-k^2l_H^2}\right)}{L\pi\sigma\sqrt{l_H^2+\sigma^2}}\int dx|w_j(x)|^2\,e^{-x^2/\sigma^2} \tag{2.26}$$

$$W_{12} = \frac{\hbar U_0\left(1+e^{-k^2l_H^2}\right)}{L\pi\sigma\sqrt{l_H^2+\sigma^2}}\int dx w_1^*(x)\,w_2(x)\,e^{-x^2/\sigma^2}, \tag{2.27}$$

where both W_0 and W_{12} do not depend on the indices i,j because the double well is symmetric. The parameters W_0 and W_{12} are the AC-Stark shift and the cavity assisted tunneling amplitude, respectively [22]. Since the Wannier functions are highly localized, and the expressions for W_0 and W_{12} are those of overlap integrals of these functions, the magnitude of the parameter W_0 is always larger than that of W_{12}, therefore $|W_{12}| < |W_0|$. The setup of the system, in particular the direction of the cavity axis relative to the Josephson junction, is such that W_0 and W_{12} can have values close to each other (see Eqs. (2.26), (2.27) and Fig. 2.2). The ratio between W_{12} and W_0 depends on the width σ of the TEM_{00} mode function [11].

Therefore $\hat{H}_2^{eff}$ becomes:

$$\hat{H}_2^{eff} = \hat{N}_L\left[W_0\hat{N}_A + W_{12}(\hat{b}_1^\dagger\hat{b}_2 + \hat{b}_2^\dagger\hat{b}_1)\right], \tag{2.28}$$

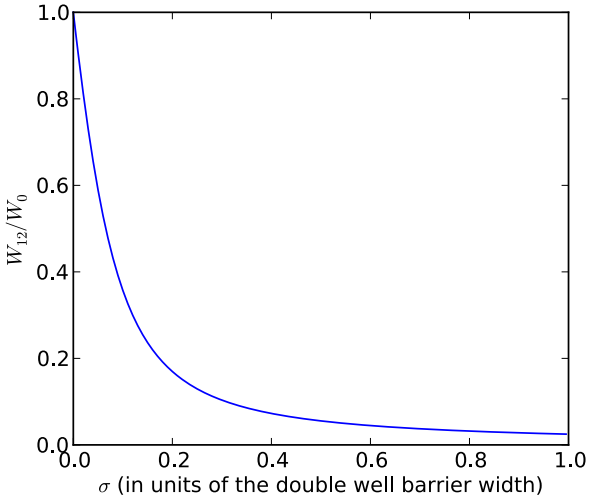

Figure 2.2: The ratio between W_{12} and W_0 as a function of the ratio between the width of the cavity waist and the width of the double-well barrier. The parameters are chosen in such a way that the Wannier functions have some small but non-zero overlap ($J \approx 0.1\epsilon$).

where $\hat{N}_L = \hat{a}^\dagger \hat{a}$ is the photon number operator.

As for the last part of the Hamiltonian, $\hat{H}_3^{eff}$, which describes the interaction between the atoms, it can be written as:

$$\hat{H}_3^{eff} = \int dx\, \hat{\phi}^\dagger(x)\hat{\phi}^\dagger(x)\hat{\phi}(x)\hat{\phi}(x)\, \frac{g_{gg}}{2} \int dx\, dy\, \varphi^4(y,z).$$

The (y,z)-dependent part of the integral can be carried out explicitly:

$$\int dx\, dy\, \varphi^4(y,z) = \frac{1}{2\pi l_H^2}.$$

Remembering that $\hat{\phi}(x)$ is written in terms of the operators $\hat{b}_1$ and $\hat{b}_2$ and of the Wannier functions $w_1(x)$ and $w_2(x)$, we can see that the first part of the integral is made of a sum of the overlap integrals of powers of the Wannier functions. The first part of the integral can be written as:

$$\frac{1}{2} \sum_{i,j,k,l=1,2} U_{ijkl} \hat{b}_i^\dagger \hat{b}_j^\dagger \hat{b}_k \hat{b}_l,$$

where

$$U_{ijkl} = \int dx\, w_i^*(x) w_j^*(x) w_k(x) w_l(x).$$

However, since the Wannier function are highly localized, we can omit the off-site terms, i.e. the ones where i, j, k, l are not all equal, because they are typically two orders of magnitude smaller than the in-site interaction terms

[16]. Therefore we only keep the terms that contain $\hat{b}_1^\dagger\hat{b}_1^\dagger\hat{b}_1\hat{b}_1$ and $\hat{b}_2^\dagger\hat{b}_2^\dagger\hat{b}_2\hat{b}_2$. By doing this $\hat{H}_3^{eff}$ becomes:

$$\hat{H}_3^{eff} = \frac{g_{gg}}{4\pi l_H^2}\left(\hat{b}_1^\dagger\hat{b}_1^\dagger\hat{b}_1\hat{b}_1\int dx\,|w_1(x)|^4 + \hat{b}_2^\dagger\hat{b}_2^\dagger\hat{b}_2\hat{b}_2\int dx\,|w_2(x)|^4\right).$$

And by calling:

$$U = \frac{g_{gg}}{2\pi l_H^2}\int dx\,|w_j(x)|^4, \tag{2.29}$$

we can write $\hat{H}_3^{eff}$ as:

$$\hat{H}_3^{eff} = \frac{U}{2}\left(\hat{b}_1^\dagger\hat{b}_1^\dagger\hat{b}_1\hat{b}_1 + \hat{b}_2^\dagger\hat{b}_2^\dagger\hat{b}_2\hat{b}_2\right), \tag{2.30}$$

where U is the on-site interaction energy, and because of the symmetry of the double well potential it does not depend on the index j.

Finally, combining all the parts of the Hamiltonian we find that, after substituting Eq. (2.19) into the effective Hamiltonian Eq. (2.18) we get the new Hamiltonian:

$$\hat{H} = \hat{H}_L + \hat{H}_J + \hat{H}_{JL},$$

where the cavity is described by

$$\hat{H}_L = -\hbar\Delta_C\,\hat{a}^\dagger\hat{a} - i\hbar\eta\left(\hat{a} - \hat{a}^\dagger\right), \tag{2.31}$$

the bosonic Josephson junction is described by

$$\hat{H}_J = \epsilon\,\hat{N}_A - J\left(\hat{b}_1^\dagger\hat{b}_2 + \hat{b}_2^\dagger\hat{b}_1\right) + \frac{U}{2}\left(\hat{b}_1^\dagger\hat{b}_1^\dagger\hat{b}_1\hat{b}_1 + \hat{b}_2^\dagger\hat{b}_2^\dagger\hat{b}_2\hat{b}_2\right), \tag{2.32}$$

and the interaction between the atoms and the cavity photons is modelled by

$$\hat{H}_{JL} = \hat{N}_L\left[W_0\hat{N}_A + W_{12}(\hat{b}_1^\dagger\hat{b}_2 + \hat{b}_2^\dagger\hat{b}_1)\right]. \tag{2.33}$$

The Hamiltonian of a isolated bosonic Josephson junction is given by only $\hat{H}_J$. The effect of the cavity field is to change the parameters of this Hamiltonian, which can be written as:

$$\hat{H}'_J = \tilde{\epsilon}\,\hat{N}_A - \tilde{J}\left(\hat{b}_1^\dagger\hat{b}_2 + \hat{b}_2^\dagger\hat{b}_1\right) + \frac{U}{2}\left(\hat{b}_1^\dagger\hat{b}_1^\dagger\hat{b}_1\hat{b}_1 + \hat{b}_2^\dagger\hat{b}_2^\dagger\hat{b}_2\hat{b}_2\right), \tag{2.34}$$

where $\tilde{\epsilon} = \epsilon + W_0\hat{N}_L$ is the shifted on-site energy and $\tilde{J} = J - W_{12}\hat{N}_L$ is the assisted tunneling amplitude. For red detuned atoms ($\Delta_A < 0$) both W_0 and W_{12} are negative. This means that the cavity field shifts the on-site energies downwards and assists the tunneling by increasing the effective tunneling amplitude. When the atoms are blue detuned ($\Delta_A < 0$), W_0 and W_{12} are positive and the cavity field has the effect of shifting the on-site energies upwards and lowering the effective tunneling amplitude.

These parameters, $\tilde{\epsilon}$ and $\tilde{J}$ depend on the number of photons in the system $\hat{N}_L$ and therefore become, in general, dynamical quantities.

Heisenberg equations

From the new expression of the two-mode Hamiltonian we can derive the Heisenberg equations of motion for the operators $\hat{b}_j$ $(j = 1, 2)$ and $\hat{a}$. When writing the equations, the on-site energy term $\epsilon\hat{N}_A$ can be dropped from the Hamiltonian, since $\hat{N}_A$ is a constant of motion and therefore gives no relevant contribution to the equations. The Heisenberg equations then become:

$$i\hbar\frac{d}{dt}\hat{b}_1 = W_0\,\hat{a}^\dagger\hat{a}\,\hat{b}_1 - (J - W_{12}\,\hat{a}^\dagger\hat{a})\hat{b}_2 + U\,\hat{n}_1\hat{b}_1, \tag{2.35a}$$

$$i\hbar\frac{d}{dt}\hat{b}_2 = W_0\,\hat{a}^\dagger\hat{a}\,\hat{b}_2 - (J - W_{12}\,\hat{a}^\dagger\hat{a})\hat{b}_1 + U\,\hat{n}_2\hat{b}_2, \tag{2.35b}$$

$$i\hbar\frac{d}{dt}\hat{a} = -[\hbar\Delta_C - W_0\hat{N}_A - W_{12}(\hat{b}_1^\dagger\hat{b}_2 + \hat{b}_2^\dagger\hat{b}_1)]\hat{a} + i\hbar\eta, \tag{2.35c}$$

where $\hat{n}_j = \hat{b}_j^\dagger\hat{b}_j$ is the atomic population in the well j.

2.7 Semiclassical approximation

We can study the set of equation we have found by using the semiclassical (or mean-field) approximation. Under this approximation we assume that the system is in a full coherent state (FCS). This means that we describe the atoms in the left and right well, as well as the photons in the cavity with coherent states. The full coherent state can be written as:

$$|FCS\rangle = |\beta_1\rangle_A \otimes |\beta_2\rangle_A \otimes |\alpha\rangle_L; \tag{2.36}$$

where $\hat{b}_j|\beta_j\rangle_A = \beta_j|\beta_j\rangle_A$ and $\hat{a}|\alpha\rangle_L = \alpha|\alpha\rangle_L$. It is convenient to write the eigenvalues of the atomic coherent state as:

$$\beta_j = \sqrt{N_j(t)}\,e^{i\theta_j(t)},$$

where $N_j(t)$ the average number of atoms in the j-th well at time t and $\theta_j(t)$ the corresponding phase. Similarly:

$$\alpha = \xi(t)\,e^{i\phi(t)},$$

where $N_L(t) = \xi(t)^2$ is the average number of photons in the cavity at time t and $\phi(t)$ the corresponding phase. At this point we can evaluate the Heisenberg equations of the system in the full coherent state by substituting the creation an annihilation operators with the corresponding coherent state c-numbers. The Heisenberg equation for the $\hat{a}$ operator becomes:

$$i\hbar\frac{d}{dt}\alpha = -[\hbar\Delta_C - W_0N_A - W_{12}(\sqrt{N_1N_2}(e^{i(\theta_2-\theta_1)} + e^{-i(\theta_2-\theta_1)})]\alpha + i\hbar\eta,$$

where the t-dependence of the c-numbers has been omitted. By defining

$$z(t) = \frac{N_1(t) - N_2(t)}{N_A} \tag{2.37}$$

as the fractional imbalance of the atomic population of the left and right wells, and

$$\theta(t) = \theta_2(t) - \theta_1(t) \tag{2.38}$$

as the atomic relative phase, we can write:

$$\sqrt{N_1 N_2} = \frac{1}{2} N_A \sqrt{1 - z^2}.$$

The equation becomes:

$$\frac{d}{dt}\alpha = i\left(\Delta_C - \frac{W_0}{\hbar}N_A - \frac{W_{12}}{\hbar}N_A\sqrt{1-z^2}\cos\theta\right)\alpha + \eta.$$

By writing α explicitly and using a dot to represent the time derivative, $d\alpha/dt$ becomes:

$$\dot{\alpha} = e^{i\phi}\dot{\xi} + i\xi e^{i\phi}\dot{\phi},$$

and the equation can be written as:

$$\dot{\xi}e^{i\phi} + i\xi e^{i\phi}\dot{\phi} = i\left(\Delta_C - \frac{W_0}{\hbar}N_A - \frac{W_{12}}{\hbar}N_A\sqrt{1-z^2}\cos\theta\right)\xi\, e^{i\phi} + \eta.$$

Dividing both sides by $e^{i\phi}$ the equation becomes:

$$\dot{\xi} + i\xi\dot{\phi} = i(\Delta_C - \frac{W_0}{\hbar}N_A - \frac{W_{12}}{\hbar}N_A\sqrt{1-z^2}\cos\theta)\xi + \eta\cos\phi - i\eta\sin\phi.$$

The real and imaginary parts of the equation are:

$$\dot{\xi} = \eta\cos\phi \tag{2.39}$$

$$\xi\dot{\phi} = \left(\Delta_C - \frac{W_0}{\hbar}N_A - \frac{W_{12}}{\hbar}N_A\sqrt{1-z^2}\cos\theta\right)\xi - \eta\sin\phi. \tag{2.40}$$

This pair of equations describes the dynamics of the cavity photons.

As for the Heisenberg equations of the atomic operators $\hat{b}_1$ and $\hat{b}_2$, after substituting the operators with the c-numbers we get:

$$i\hbar\frac{d}{dt}(\sqrt{N_1}e^{i\theta_1}) = W_0\xi^2\sqrt{N_1}e^{i\theta_1} - \tilde{J}\sqrt{N_2}e^{i\theta_2} + UN_1\sqrt{N_1}e^{i\theta_1}$$

$$i\hbar\frac{d}{dt}(\sqrt{N_2}e^{i\theta_2}) = W_0\xi^2\sqrt{N_2}e^{i\theta_2} - \tilde{J}\sqrt{N_1}e^{i\theta_1} + UN_2\sqrt{N_2}e^{i\theta_2}$$

where $\tilde{J} = J - W_{12}\xi^2$. After writing the time derivatives explicitly using the dot notation we get:

$$i\hbar(\frac{\dot{N}_1}{2\sqrt{N_1}}e^{i\theta_1} + i\sqrt{N_1}\dot{\theta}_1 e^{i\theta_1}) = W_0\xi^2\sqrt{N_1}e^{i\theta_1} - \tilde{J}\sqrt{N_2}e^{i\theta_2} + UN_1\sqrt{N_1}e^{i\theta_1}$$

$$i\hbar(\frac{\dot{N}_2}{2\sqrt{N_2}}e^{i\theta_2} + i\sqrt{N_2}\dot{\theta}_2 e^{i\theta_2}) = W_0\xi^2\sqrt{N_2}e^{i\theta_2} - \tilde{J}\sqrt{N_1}e^{i\theta_1} + UN_2\sqrt{N_2}e^{i\theta_2}.$$

Let us now multiply the first and second equation by $\sqrt{N_1}e^{-i\theta_1}$ and $\sqrt{N_2}e^{-i\theta_2}$ respectively, and take the imaginary part of the equations:

$$\begin{aligned}\frac{\hbar}{2}\dot{N}_1 &= -\tilde{J}\sqrt{N_1N_2}\sin\theta \\ \frac{\hbar}{2}\dot{N}_2 &= +\tilde{J}\sqrt{N_1N_2}\sin\theta.\end{aligned}$$

Taking the difference of the two equations, dividing by N_A and remembering the definition of z we get:

$$\dot{z} = -\frac{4}{\hbar}\tilde{J}\frac{\sqrt{N_1N_2}}{N_A}\sin\theta.$$

Since $\sqrt{N_1N_2} = \frac{1}{2}N_A\sqrt{1-z^2}$ and defining $\nu = \tilde{J}/\hbar$, we can write the equation as:

$$\dot{z} = -2\nu\sqrt{1-z^2}\sin\theta.$$

By taking the real part of the two equations we get:

$$\begin{aligned}-\hbar N_1\dot{\theta}_1 &= W_0\xi^2N_1 - \tilde{J}\sqrt{N_1N_2}\cos\theta + UN_1^2 \\ -\hbar N_2\dot{\theta}_2 &= W_0\xi^2N_2 - \tilde{J}\sqrt{N_1N_2}\cos\theta + UN_2^2\end{aligned}$$

dividing the first equation by $\hbar N_1$, the second by $\hbar N_2$ and taking their difference we find:

$$\dot{\theta} = \frac{\tilde{J}}{\hbar}\left(\frac{N_1-N_2}{\sqrt{N_1N_2}}\right)\cos\theta + \frac{U}{\hbar}(N_1-N_2),$$

which can be written as:

$$\dot{\theta} = \frac{1}{\hbar}\left(\frac{2\tilde{J}\cos\theta}{\sqrt{1-z^2}} + N_AU\right)z.$$

Therefore the Heisenberg equations for the field operators $\hat{a}$, $\hat{b}_1$ and $\hat{b}_2$, in the semiclassical approximation, can be written as the following set of ordinary differential equations (ODEs) for the variables z, θ, ξ and ϕ:

$$\dot{z} = -2\nu\sqrt{1-z^2}\sin\theta, \tag{2.41a}$$

$$\dot{\theta} = \left(\tilde{g} + \frac{2\,\nu}{\sqrt{1-z^2}}\cos\theta\right)z, \tag{2.41b}$$

$$\dot{\xi} = \eta\cos\phi, \tag{2.41c}$$

$$\dot{\phi} = \delta_C - \frac{\eta}{\xi}\sin\phi, \tag{2.41d}$$

We have here introduced the following parameters which have the physical dimensions of a frequency: $\tilde{g} = UN_A/\hbar$, which is the mean-field frequency shift due to atomic collisions; $\nu = (J - W_{12}\xi^2)/\hbar$, standing for the effective tunneling strength modified by the photon assisted process; $\delta_C = \Delta_C - N_A(W_0 + W_{12}\sqrt{1-z^2}\cos\theta)/\hbar$ is the effective cavity detuning. The parameters $\nu(t)$ and $\delta_C(t)$ are shorthand notations that actually depend on the mean-field variables. Moreover, also the tunneling amplitude J, which is a constant in the bare BJJ, is now replaced by the time-dependent term $\nu(t)$. In the absence of radiation fields, i.e. $\xi(t) = \phi(t) = 0$ at any time t, the above ODEs reduce to those of the standard BJJ dynamics [10]:

$$\begin{aligned} \dot{z} &= -2\frac{J}{\hbar}\sqrt{1-z^2}\sin\theta, \\ \dot{\theta} &= \left(\tilde{g} + \frac{2\,J}{\hbar}\frac{\cos\theta}{\sqrt{1-z^2}}\right) z. \end{aligned}$$

Chapter 3

Dynamics of the system in the semiclassical approximation

In this chapter we will be studying some features of the dynamics of the system in the semiclassical approximation. In the first part we will find the fixed point of the system and we will study how it behaves close to them.

In the second part we will study the system when the photon field can be considered to be constant. This will allow us to perform a better analytical study of the problem and to show how the presence of the cavity photons can change the kind of dynamics the Bosonic Josephson junction can perform.

3.1 Fixed points

In order for us to study the the system (2.41), it is convenient to use a vector notation, in which $\mathbf{X} = (X_1, X_2, X_3, X_4) = (z, \theta, \xi, \phi)$. The fixed points of the ODEs (2.41), can be found by solving $d\mathbf{X}/dt = 0$. We expect to find two different types of equilibria: the ones with $z = 0$ are called zero imbalance equilibria, because $z = 0$ implies that there is the same number of bosons in the left and right well, while the ones with $z \neq 0$ are called finite imbalance equilibria, because $z \neq 0$ implies that one of the wells is more populated than the other.

3.1.1 Zero imbalance equilibria

Let us start with the zero imbalance equilibria. The second equation $\dot{\theta} = 0$ is already met because $z = 0$. The condition $\dot{z} = 0$ is satisfied when $\theta = 0$, or $\theta = \pi$. The third equation $\dot{\xi} = 0$ leads to $\phi = \pm\pi/2$. Solving the last

equation $\dot{\phi} = 0$ with respect to ξ, we can find its value at equilibrium:

$$\xi = \pm \frac{\hbar\eta}{\hbar\Delta_C - N_A(W_0 \pm W_{12})} = \pm \frac{\eta}{\delta_C(0)} \tag{3.1}$$

The first $\pm$ sign depends on the value of ϕ: there is a $+$ when $\phi = \pi/2$ and a $-$ when $\phi = -\pi/2$. The second $\pm$ sign depends on the value of θ: there is a $+$ when $\theta = 0$ and a $-$ when $\theta = \pi$.

So we can write the stationary points with zero imbalance as:

$$\mathbf{X_1} = \left(0, 0, \frac{\hbar\eta}{\hbar\Delta_C - N_A(W_0 + W_{12})}, \frac{\pi}{2}\right), \tag{3.2a}$$

$$\mathbf{X_2} = \left(0, 0, \frac{\hbar\eta}{N_A(W_0 + W_{12}) - \hbar\Delta_C}, -\frac{\pi}{2}\right), \tag{3.2b}$$

$$\mathbf{X_3} = \left(0, \pi, \frac{\hbar\eta}{\hbar\Delta_C - N_A(W_0 - W_{12})}, \frac{\pi}{2}\right), \tag{3.2c}$$

$$\mathbf{X_4} = \left(0, \pi, \frac{\hbar\eta}{N_A(W_0 - W_{12}) - \hbar\Delta_C}, -\frac{\pi}{2}\right). \tag{3.2d}$$

Since ξ is the amplitude of the photon field, $\xi > 0$. Therefore, for $\delta_C > 0$ the actual fixed points are $\mathbf{X}_1$ and $\mathbf{X}_3$; while for $\delta_C < 0$ $\mathbf{X}_2$ and $\mathbf{X}_4$ are the fixed points.

Let us now study how the system behaves close to these equilibria. We can do this by linearizing the system (2.41). Using the vector notation the system can be written as:

$$\dot{\mathbf{X}} = \mathbf{f}(\mathbf{X}),$$

where $\mathbf{f}(\mathbf{X})$ is a vector of four functions such that:

$$\begin{aligned} \dot{z} &= f_1(\mathbf{X}), \\ \dot{\theta} &= f_2(\mathbf{X}), \\ \dot{\xi} &= f_3(\mathbf{X}), \\ \dot{\phi} &= f_4(\mathbf{X}). \end{aligned}$$

The Jacobian matrix of the system is made of the derivatives of the functions f_i with respect to the variables z, θ, ξ, ϕ:

$$J = \begin{pmatrix} \frac{\partial f_1}{\partial z} & \frac{\partial f_1}{\partial \theta} & \frac{\partial f_1}{\partial \xi} & \frac{\partial f_1}{\partial \phi} \\ \frac{\partial f_2}{\partial z} & \frac{\partial f_2}{\partial \theta} & \frac{\partial f_2}{\partial \xi} & \frac{\partial f_2}{\partial \phi} \\ \frac{\partial f_3}{\partial z} & \frac{\partial f_3}{\partial \theta} & \frac{\partial f_3}{\partial \xi} & \frac{\partial f_3}{\partial \phi} \\ \frac{\partial f_4}{\partial z} & \frac{\partial f_4}{\partial \theta} & \frac{\partial f_4}{\partial \xi} & \frac{\partial f_4}{\partial \phi} \end{pmatrix}.$$

When taking the derivatives of the functions $f_i(\mathbf{X})$, whose explicit formulas can be seen in (2.41), it is important to remember that ν and δ_C are functions

of $\mathbf{X}$. The elements of the Jacobian matrix are:

$$\begin{aligned}
\frac{\partial f_1}{\partial z} &= \frac{2z\left(J - W_{12}\xi^2\right)\sin(\theta)}{\hbar\sqrt{1-z^2}} \\
\frac{\partial f_1}{\partial \theta} &= -\frac{2\sqrt{1-z^2}\left(J - W_{12}\xi^2\right)\cos(\theta)}{\hbar} \\
\frac{\partial f_1}{\partial \xi} &= \frac{4W_{12}\sqrt{1-z^2}\xi\sin(\theta)}{\hbar} \\
\frac{\partial f_1}{\partial \phi} &= 0 \\
\frac{\partial f_2}{\partial z} &= \frac{2\left(J - W_{12}\xi^2\right)\cos(\theta)z^2}{\hbar\left(1-z^2\right)^{3/2}} + \frac{N_A U}{\hbar} + \frac{2\left(J - W_{12}\xi^2\right)\cos(\theta)}{\hbar\sqrt{1-z^2}} \\
\frac{\partial f_2}{\partial \theta} &= -\frac{2z\left(J - W_{12}\xi^2\right)\sin(\theta)}{\hbar\sqrt{1-z^2}} \\
\frac{\partial f_2}{\partial \xi} &= -\frac{4W_{12}z\xi\cos(\theta)}{\hbar\sqrt{1-z^2}} \\
\frac{\partial f_2}{\partial \phi} &= 0 \\
\frac{\partial f_3}{\partial z} &= 0 \\
\frac{\partial f_3}{\partial \theta} &= 0 \\
\frac{\partial f_3}{\partial \xi} &= 0 \\
\frac{\partial f_3}{\partial \phi} &= -\eta\sin(\phi) \\
\frac{\partial f_4}{\partial z} &= \frac{N_A W_{12} z\cos(\theta)}{\hbar\sqrt{1-z^2}} \\
\frac{\partial f_4}{\partial \theta} &= \frac{N_A W_{12}\sqrt{1-z^2}\sin(\theta)}{\hbar} \\
\frac{\partial f_4}{\partial \xi} &= \frac{\eta\sin(\phi)}{\xi^2} \\
\frac{\partial f_4}{\partial \phi} &= -\frac{\eta\cos(\phi)}{\xi}
\end{aligned}$$

In order to find the small oscillations frequencies of the system we need to evaluate the Jacobian matrix J in one of the equilibria.

Let us start with the equilibrium $\mathbf{X_1}$. The Jacobian matrix becomes:

$$J(\mathbf{X_1}) = \begin{pmatrix}
0 & -\frac{2\left(J - \frac{\hbar^2 W_{12}\eta^2}{(\hbar\Delta_C - N_A(W_{12}+W_0))^2}\right)}{\hbar} & 0 & 0 \\
\frac{N_A U}{\hbar} + \frac{2\left(J - \frac{\hbar^2 W_{12}\eta^2}{(\hbar\Delta_C - N_A(W_{12}+W_0))^2}\right)}{\hbar} & 0 & 0 & 0 \\
0 & 0 & 0 & -\eta \\
0 & 0 & \frac{(\hbar\Delta_C - N_A(W_{12}+W_0))^2}{\hbar^2\eta} & 0
\end{pmatrix}$$

It is very interesting to notice how, in the linearized system resulting from this Jacobian matrix, the atomic and photon degrees of freedom are no longer coupled. For the sake of simplicity we can write $J(\mathbf{X_1})$ as:

$$J(\mathbf{X_1}) = \begin{pmatrix} 0 & a & 0 & 0 \\ b & 0 & 0 & 0 \\ 0 & 0 & 0 & c \\ 0 & 0 & d & 0 \end{pmatrix}$$

where

$$\begin{aligned} a &= -\frac{2\left(J - \frac{\hbar^2 W_{12}\eta^2}{(\hbar\Delta_C - N_A(W_{12}+W_0))^2}\right)}{\hbar} \\ b &= \frac{N_A U}{\hbar} + \frac{2\left(J - \frac{\hbar^2 W_{12}\eta^2}{(\hbar\Delta_C - N_A(W_{12}+W_0))^2}\right)}{\hbar} \\ c &= -\eta \\ d &= \frac{(\hbar\Delta_C - N_A(W_{12}+W_0))^2}{\hbar^2\eta} \end{aligned}$$

Such a matrix has eigenvalues

$$\begin{aligned} \lambda_{1,2} &= \pm\sqrt{ab} \\ \lambda_{3,4} &= \pm\sqrt{cd} \end{aligned}$$

The equilibrium is stable when all the eigenvalues are purely imaginary. The corresponding frequencies are:

$$\begin{aligned} \omega_{1,at} &= \sqrt{|ab|} \\ \omega_{1,ph} &= \sqrt{|cd|} \end{aligned}$$

where the subscripts at and ph stand for the atomic and photon degrees of freedom respectively; the two vertical bars represent the absolute value of the expression. The linearized system at $\mathbf{X_1}$ takes the form:

$$\begin{aligned} \dot{z} &= a\,\theta \\ \dot{\theta} &= b\,z \\ \dot{\xi} &= c\,(\phi - \frac{\pi}{2}) \\ \dot{\phi} &= d\,(\xi - \bar{\xi}_1) \end{aligned}$$

where $\bar{\xi}_1 = X_{1,4}$. This system is made of four equations which are coupled in pairs.

The system of ODEs for any given variables x and y:

$$\begin{aligned} \dot{x} &= p\,(y - y_0) \\ \dot{y} &= q\,(x - x_0) \end{aligned}$$

with initial conditions $x(0) = x_0 + \delta x$, with δx small and $y(0) = y_0$, has solutions:

$$\begin{aligned} x(t) &= x_0 + \frac{\delta x}{2}(e^{\sqrt{pq}\ t} + e^{-\sqrt{pq}\ t}) \\ y(t) &= y_0 + \sqrt{\frac{q}{p}}\frac{\delta x}{2}(e^{\sqrt{pq}\ t} - e^{-\sqrt{pq}\ t}). \end{aligned}$$

When all the eigenvalues $\pm\sqrt{pq}$ are purely imaginary the solutions clearly represent oscillations around (x_0, y_0).

$$x(t) = x_0 + \delta x \cos(\sqrt{|pq|}\ t) \tag{3.3}$$

$$y(t) = y_0 - \delta x\sqrt{|\frac{q}{p}|}\sin(\sqrt{|pq|}\ t) \tag{3.4}$$

The linearized system at $\mathbf{X_1}$ is made of two pairs coupled ODEs of this kind. Two ODEs for the photon degrees of freedom and two for the atomic degrees of freedom.

Looking at to pair of equations that describe the linearized dynamics of the photon viariables we notice that the product $cd = -\frac{(\hbar\Delta_C - N_A(W_{12}+W_0))^2}{\hbar^2}$ is always negative. This means that the dynamics of the photon degrees of freedom, close to the fixed point, is made of small oscillations for every value of the parameters that appear in the equations.

As for the dynamics of the atomic degrees of freedom we need to study the sign of the product ab. Let us analyze how the various parameters affect the sign of the product. First of all, as mentioned before, $\mathbf{X_1}$ is a valid equilibrium only when $\delta_c > 0$. This implies that $\Delta_C > \frac{N_A}{\hbar}(W_0 + W_{12})$. Let us start by separating the case when $W_{12} > 0$ and $W_{12} < 0$.

When $W_{12} < 0$, $a < 0$. The sign of the product ab is then determined by the sign of b. If we write b as $b = \frac{N_A U}{\hbar} - a$, then $b > 0$ if $U > \frac{\hbar a}{N_A}$.

Solutions of the system equations with initial conditions close to $\mathbf{X_1}$, with $ab > 0$ and $ab < 0$ respectively, and $W_{12} < 0$ can be seen in the two plots of Fig. (3.1). The green dashed lines represent the analytical solutions as in Eq. (3.3). It can be clearly seen from the plots that when $ab < 0$ the system displays small oscillations around the equilibrium, as expected from the analysis of the eigenvalues. On the other hand, when $ab > 0$ the equilibrium is no longer stable and the solutions move away from the initial values.

For $W_{12} > 0$, the value of a can be either positive or negative.
$a > 0$ when $J < \frac{\hbar^2 W_{12}\eta^2}{(\hbar\Delta_C - N_A(W_{12}+W_0))^2}$. If we write b as $b = \frac{N_A U}{\hbar} - a$, then $b > 0$ when $U > \frac{\hbar a}{N_A}$.
The two plots in Fig. (3.2) depict the solutions of the equations when $ab < 0$ and when $ab > 0$ respectively.
$a < 0$ when $J > \frac{\hbar^2 W_{12}\eta^2}{(\hbar\Delta_C - N_A(W_{12}+W_0))^2}$. By writing b as $b = \frac{N_A U}{\hbar} - a$, then

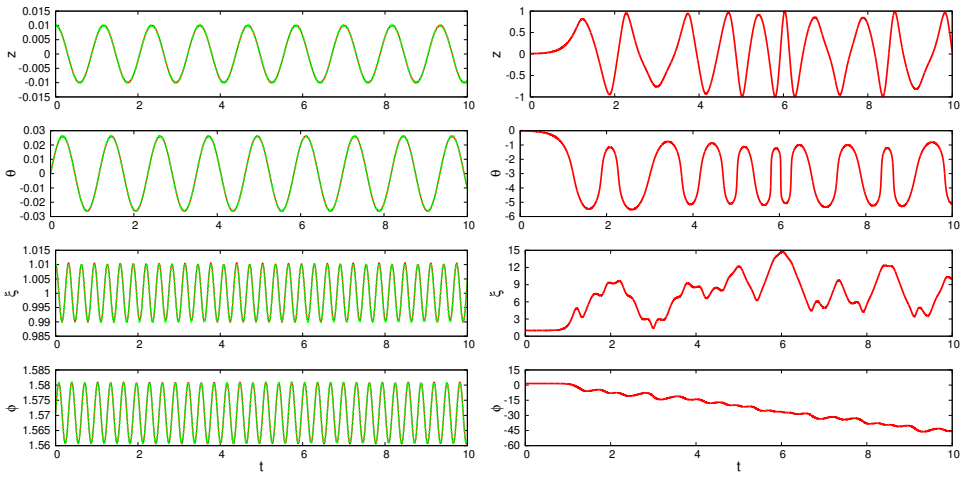

(a) (b)

Figure 3.1: Time evolution of the variables (z, θ, ξ, ϕ) around the fixed point $\mathbf{X}_1$. Time is measured in units of $\hbar/J$. The red lines represent the numerical solution of the system. The green dashed line represents the analytical solution as in Eq. (3.3). In panel (a) the parameters of the system are such that the equilibrium is stable, and the green and red lines overlap. In panel (b) the parameters of the system are such that the equilibrium is not stable and only the numerical solution is showed. In both panels $W_{12} < 0$. The four panels correspond to the four components of the state vector $\mathbf{X}$. The parameters for (a) are: $\hbar\Delta_C = -100J$, $W_0 N_A = -90J$, $W_{12} N_A = -30J$, $UN_A = 12J$, $N_A = 1000$, $\hbar\eta = 20J$. The initial condition is $\mathbf{X}(t = 0) = (0.01, 0, 1.01, \pi/2)$.The parameters for (b) are: $\hbar\Delta_C = -100J$, $W_0 N_A = -90J$, $W_{12} N_A = -30J$, $UN_A = -12J$, $N_A = 1000$, $\hbar\eta = 20J$. The initial condition is $\mathbf{X}(t = 0) = (0.01, 0, 1.01, \pi/2)$.

$b > 0$ when $U > \frac{\hbar a}{N_A}$. The two plots in Fig. (3.3) depict the solutions of the equations when $ab < 0$ and when $ab > 0$ respectively.

It can be seen from all the plots that the analytical solution is very similar to the numerical one, and that near the equilibrium, when $ab < 0$, the system shows small oscillations.

A similar analysis can be carried out for the other zero imbalance equilibria because their Jacobian matrix has exactly the same structure as $J(\mathbf{X_1})$. Therefore we only write the corresponding Jacobian matrices and the conditions for the equilibria to be stable, without making other plots. Since the frequency of the small oscillations for the photon degrees of freedom is always real, we only need to study the product ab. When it is negative the atomic frequency of the small oscillations is real, otherwise it is imaginary and the equilibrium is not stable.

The Jacobian matrix for $\mathbf{X_3}$ is:

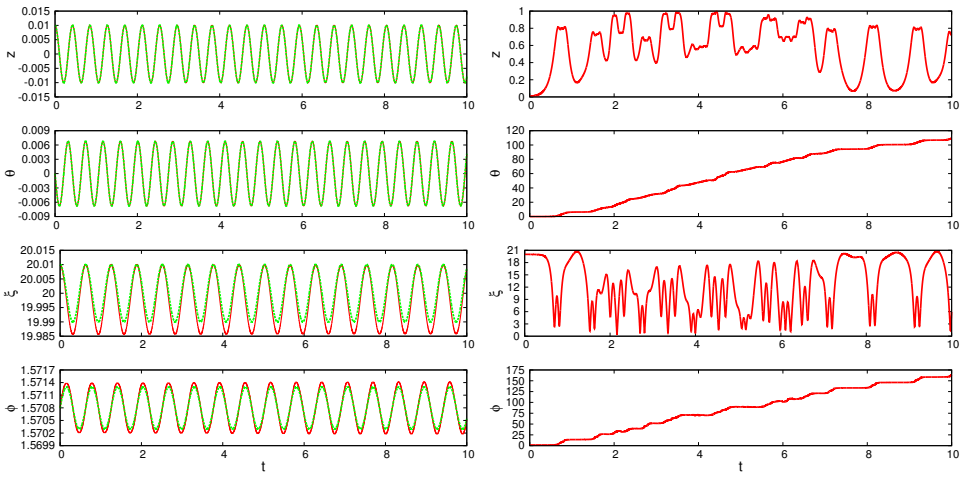

(a) (b)

Figure 3.2: Time evolution of the variables (z, θ, ξ, ϕ) around the fixed point $\mathbf{X}_1$. Time is measured in units of $\hbar/J$. The red lines represent the numerical solution of the system. The green dashed line represents the analytical solution. In panel (a) the parameters of the system are such that the equilibrium is stable, and the green and red lines overlap. In panel (b) the parameters of the system are such that the equilibrium is not stable and only the numerical solution is showed. In both panels $W_{12} > 0$ and $a > 0$. The four panels correspond to the four components of the state vector $\mathbf{X}$. The parameters for (a) are: $\hbar\Delta_C = 130J$, $W_0 N_A = 90J$, $W_{12} N_A = 30J$, $UN_A = 12J$, $N_A = 1000$, $\hbar\eta = 200J$. The initial condition is $\mathbf{X}(t = 0) = (0.01, 0, 20.01, \pi/2)$. The parameters for (b) are: $\hbar\Delta_C = 130J$, $W_0 N_A = 90J$, $W_{12} N_A = 30J$, $UN_A = 25J$, $N_A = 1000$, $\hbar\eta = 200J$. The initial condition is $\mathbf{X}(t = 0) = (0.01, 0, 20.01, \pi/2)$.

$$J(\mathbf{X_3}) = \begin{pmatrix} 0 & \frac{2\left(J - \frac{\hbar^2 W_{12}\eta^2}{(\hbar\Delta_C - N_A(W_0 - W_{12}))^2}\right)}{\hbar} & 0 & 0 \\ \frac{N_A U}{\hbar} - \frac{2\left(J - \frac{\hbar^2 W_{12}\eta^2}{(\hbar\Delta_C - N_A(W_0 - W_{12}))^2}\right)}{\hbar} & 0 & 0 & 0 \\ 0 & 0 & 0 & -\eta \\ 0 & 0 & \frac{(\hbar\Delta_C - N(W_0 - W_{12}))^2}{\hbar^2\eta} & 0 \end{pmatrix}$$

When $W_{12} < 0$, then $a > 0$. The sign of the product ab is then determined by the sign of b. Writing $b = \frac{N_A U}{\hbar} - a$, then $b < 0$ when $U < \frac{\hbar a}{N_A}$.

For $W_{12} > 0$, a can have both signs. When $W_{12} > 0$ then also $W_0 > 0$. Since $\delta_c > 0$, $\Delta_C > 0$.

$a > 0$ when $J > \frac{\hbar^2 W_{12}\eta^2}{(\hbar\Delta_C - N_A(W_{12}+W_0))^2}$. Writing $b = \frac{N_A U}{\hbar} - a$, $b < 0$ when $U < \frac{\hbar a}{N_A}$.

$a < 0$ when $J < \frac{\hbar^2 W_{12}\eta^2}{(\hbar\Delta_C - N_A(W_{12}+W_0))^2}$. Writing $b = \frac{N_A U}{\hbar} - a$, then $b > 0$ when $U > \frac{\hbar a}{N_A}$.

Let us now write the Jacobian matrix for the equilibrium $\mathbf{X_2}$:

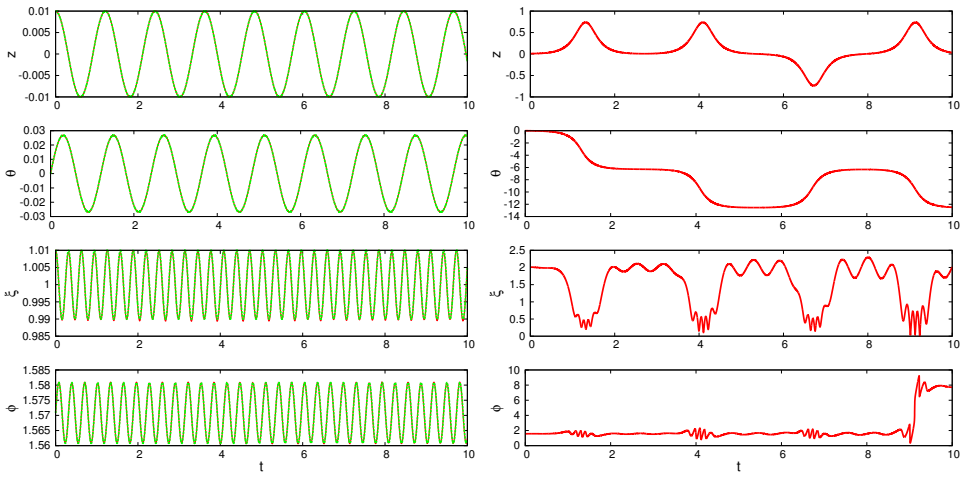

(a) (b)

Figure 3.3: Time evolution of the variables (z, θ, ξ, ϕ) around the fixed point $\mathbf{X}_1$. Time is measured in units of $\hbar/J$. The red lines represent the numerical solution of the system. The green dashed line represents the analytical solution. In panel (a) the parameters of the system are such that the equilibrium is stable, and the green and red line overlap. In panel (b) the parameters of the system are such that the equilibrium is not stable and only the numerical solution is showed. In both panels $W_{12} > 0$ and $a < 0$. The four panels correspond to the four components of the state vector $\mathbf{X}$. The parameters for (a) are: $\hbar\Delta_C = 140J$, $W_0 N_A = 90J$, $W_{12} N_A = 30J$, $UN_A = 12J$, $N_A = 1000$, $\hbar\eta = 20J$. The initial condition is $\mathbf{X}(t=0) = (0.01, 0, 1.01, \pi/2)$. The parameters for (b) are: $\hbar\Delta_C = 130J$, $W_0 N_A = 90J$, $W_{12} N_A = 30J$, $UN_A = -12J$, $N_A = 1000$, $\hbar\eta = 20J$. The initial condition is $\mathbf{X}(t=0) = (0.01, 0, 2.01, \pi/2)$.

$$J(\mathbf{X_2}) = \begin{pmatrix} 0 & -\frac{2\left(J - \frac{\hbar^2 W_{12}\eta^2}{(\hbar\Delta_C - N_A(W_{12}+W_0))^2}\right)}{\hbar} & 0 & 0 \\ \frac{N_A U}{\hbar} + \frac{2\left(J - \frac{\hbar^2 W_{12}\eta^2}{(\hbar\Delta_C - N_A(W_{12}+W_0))^2}\right)}{\hbar} & 0 & 0 & 0 \\ 0 & 0 & 0 & \eta \\ 0 & 0 & -\frac{(\hbar\Delta_C - N_A(W_{12}+W_0))^2}{\hbar^2\eta} & 0 \end{pmatrix}$$

When $W_{12} < 0$ $a < 0$. The sign of the product ab is then determined by the sign of b. $b > 0$ if $U > \frac{\hbar a}{N_A}$. If $U > 0$ then $b > 0$.

For $W_{12} > 0$ a can have both signs. When $W_{12} > 0$ then also $W_0 > 0$. Since $\delta_c > 0$, then $\Delta_C > 0$. $a > 0$ when $J < \frac{\hbar^2 W_{12}\eta^2}{(\hbar\Delta_C - N_A(W_{12}+W_0))^2}$. Writing $b = \frac{N_A U}{\hbar} - a$, then $b > 0$ when $U > \frac{\hbar a}{N_A}$.

$a < 0$ when $J > \frac{\hbar^2 W_{12}\eta^2}{(\hbar\Delta_C - N_A(W_{12}+W_0))^2}$. Writing $b = \frac{N_A U}{\hbar} - a$, then $b > 0$ when $U > \frac{\hbar a}{N_A}$.

The Jacobian matrix for $\mathbf{X_4}$ is:

$$J(\mathbf{X_4}) = \begin{pmatrix} 0 & \frac{2\left(J-\frac{\hbar^2 W_{12}\eta^2}{(\hbar\Delta_C - N(W_0-W_{12}))^2}\right)}{\hbar} & 0 & 0 \\ \frac{N_A U}{\hbar} - \frac{2\left(J-\frac{\hbar^2 W_{12}\eta^2}{(\hbar\Delta_C - N_A(W_0-W_{12}))^2}\right)}{\hbar} & 0 & 0 & 0 \\ 0 & 0 & 0 & \eta \\ 0 & 0 & -\frac{(\hbar\Delta_C - N_A(W_0-W_{12}))^2}{\hbar^2\eta} & 0 \end{pmatrix}$$

When $W_{12} < 0$ $a > 0$. The sign of the product ab is then determined by the sign of b. $b < 0$ if $U < \frac{\hbar a}{N_A}$.

For $W_{12} > 0$ a can have both signs. When $W_{12} > 0$ then also $W_0 > 0$. Since $\delta_c > 0$ $\Delta_C > 0$. $a > 0$ when $J > \frac{\hbar^2 W_{12}\eta^2}{(\hbar\Delta_C - N_A(W_{12}+W_0))^2}$. Writing $b = \frac{N_A U}{\hbar} - a$, then $b < 0$ when $U < \frac{\hbar a}{N_A}$.

$a < 0$ when $J < \frac{\hbar^2 W_{12}\eta^2}{(\hbar\Delta_C - N_A(W_{12}+W_0))^2}$. Writing $b = \frac{N_A U}{\hbar} - a$, then $b > 0$ when $U > \frac{\hbar a}{N_A}$.

3.1.2 Finite imbalance equilibria

Now let us turn to the finite imbalance equilibrium solutions, where $0 < |z| \leq 1$. These equilibria can be found by solving $d\mathbf{X}/dt = 0$. The first equation of the system implies that $\theta = 0$ or $\theta = \pi$. The third is met when $\phi = \pm\pi/2$.

Let us first consider the case when $\theta = 0$. The second equation becomes

$$\frac{UN_A}{\hbar} + \frac{2\nu}{\sqrt{1-z^2}} = 0.$$

This means that

$$\sqrt{1-z^2} = -\frac{2\hbar\nu}{UN_A}.$$

Since the left hand side of the equation is positive, ν/U needs to be negative. This is a condition that must be satisfied in order for this equilibrium to exist. Solving the equation for z we find:

$$\bar{z} = \pm\sqrt{1 - \left(\frac{2\hbar\nu}{UN_A}\right)^2} \tag{3.5}$$

The last equation of $d\mathbf{X}/dt = 0$ leads to the equilibrium value for ξ:

$$\xi = \pm\frac{\eta}{\delta_C(0)} = \pm\frac{\hbar\eta}{\hbar\Delta_C - N_A(W_0 + W_{12}\sqrt{1-\bar{z}^2})} \tag{3.6}$$

Let us now consider the case when $\theta = \pi$. The second equation becomes

$$\frac{UN_A}{\hbar} - \frac{2\nu}{\sqrt{1-z^2}} = 0$$

This means that

$$\sqrt{1-z^2} = \frac{2\hbar\nu}{UN_A}$$

Since the left hand side of the equation is positive, ν/U needs to be positive. This is a condition that must be satisfied to have this equilibrium. Solving the equation for z we find:

$$\bar{z} = \pm\sqrt{1 - \left(\frac{2\hbar\nu}{UN_A}\right)^2} \tag{3.7}$$

where we have used $\bar{z}$ to label the equilibrium value of z. The last equation leads to the equilibrium value for ξ:

$$\xi = \pm\frac{\eta}{\delta_C(0)} = \pm\frac{\hbar\eta}{\hbar\Delta_C - N_A(W_0 - W_{12}\sqrt{1-\bar{z}^2})} \tag{3.8}$$

The $\pm$ sign depends on the value of ϕ: there is a $+$ when $\phi = \pi/2$ and a $-$ when $\phi = -\pi/2$.

For $\theta = 0$, the condition we have found for the existence of the equilibrium is that $\nu/U = (J - W_{12}\bar{\xi}^2)/U \leq 0$. This is different from the bare BJJ, in which this condition can be satisfied only when $U < 0$ since $\tilde{J} = J$ is always positive. However, because of the light-matter interaction, the numerator can change sign for a large enough number of photons, so this equilibrium configuration can occur both for a positive and negative interaction between the atoms: $U > 0$ when $J - W_{12}\bar{\xi}^2 < 0$ and $U < 0$ when $J - W_{12}\bar{\xi}^2 > 0$.

Similar calculations can be carried out when $\theta = \pi$. The condition for the existence of the equilibrium becomes $U < 0$ when $J - W_{12}\bar{\xi}^2 < 0$ and $U > 0$ when $J - W_{12}\bar{\xi}^2 > 0$. The finite imbalance equilibria we find are:

$$\mathbf{X}_5 = \left(\bar{z}, 0, \frac{\hbar\eta}{\hbar\,\Delta_C - N_A\left(W_0 + W_{12}\sqrt{1-\bar{z}^2}\right)}, \frac{\pi}{2}\right), \tag{3.9a}$$

$$\mathbf{X}_6 = \left(\bar{z}, 0, \frac{\hbar\eta}{N_A\left(W_0 + W_{12}\sqrt{1-\bar{z}^2}\right) - \hbar\,\Delta_C}, -\frac{\pi}{2}\right), \tag{3.9b}$$

and similarly for $\theta = \pi$,

$$\mathbf{X}_7 = \left(\bar{z}, \pi, \frac{\hbar\eta}{\hbar\,\Delta_C - N_A\left(W_0 - W_{12}\sqrt{1-\bar{z}^2}\right)}, \frac{\pi}{2}\right), \tag{3.9c}$$

$$\mathbf{X}_8 = \left(\bar{z}, \pi, \frac{\hbar\eta}{N_A\left(W_0 - W_{12}\sqrt{1-\bar{z}^2}\right) - \hbar\,\Delta_C}, -\frac{\pi}{2}\right). \tag{3.9d}$$

In these equations

$$\bar{z} = \pm\sqrt{1 - \left(\frac{2(J - W_{12}\,\bar{\xi}^2)}{UN_A}\right)^2}. \tag{3.10}$$

where $\bar{\xi}$ is a formal shorthand notation referring to the third component of the vectors $\mathbf{X}_5 \dots \mathbf{X}_8$, and it is a function of $\bar{z}$. This means that the value of $\bar{z}$ is the solution of Eq. (3.10), which is a third degree equation in $\sqrt{1-z^2}$. A cubic equation has either 1 or 3 real solutions, and the condition for $\bar{z}$ to be real is that the expression under the square root in Eq. (3.10) is positive. This happens when $-UN_A/2 \leq (J - W_{12}\xi^2) \leq UN_A/2$ for repulsive interactions ($U > 0$), and $(J - W_{12}\xi^2) \geq -UN_A/2$ for attractive interactions ($U < 0$). As ξ has to be positive, it follows that for $\delta_C > 0$ the two finite imbalance fixed points are $\mathbf{X}_5$ and $\mathbf{X}_7$, while for $\delta_C < 0$ the finite imbalance fixed points are $\mathbf{X}_6$ and $\mathbf{X}_8$.

The study of small oscillations is more complicated for the finite imbalance equilibria, because of the form of the Jacobian matrix. Let us show what the Jacobian matrix looks like for $\mathbf{X_5}$:

$$J(\mathbf{X_5}) = \begin{pmatrix} 0 & e & 0 & 0 \\ f & 0 & g & 0 \\ 0 & 0 & 0 & h \\ i & 0 & j & 0 \end{pmatrix} \tag{3.11}$$

where

$$\begin{aligned}
e &= -\frac{2\sqrt{1-z^2}\left(J - \frac{\hbar^2 W_{12}\eta^2}{\left(\hbar\Delta_C - N\left(W_0 + W_{12}\sqrt{1-z^2}\right)\right)^2}\right)}{\hbar} \\
f &= \frac{2\left(J - \frac{\hbar^2 W_{12}\eta^2}{\left(\hbar\Delta_C - N\left(W_0 + W_{12}\sqrt{1-z^2}\right)\right)^2}\right) z^2}{\hbar\left(1-z^2\right)^{3/2}} + \frac{NU}{\hbar} \\
&+ \frac{2\left(J - \frac{\hbar^2 W_{12}\eta^2}{\left(\hbar\Delta_C - N\left(W_0 + W_{12}\sqrt{1-z^2}\right)\right)^2}\right)}{\hbar\sqrt{1-z^2}} \\
g &= -\frac{4W_{12} z\eta}{\sqrt{1-z^2}\left(\hbar\Delta_C - N\left(W_0 + W_{12}\sqrt{1-z^2}\right)\right)} \\
h &= -\eta \\
i &= \frac{NW_{12} z}{\hbar\sqrt{1-z^2}} \\
j &= \frac{\left(\hbar\Delta_C - N\left(W_0 + W_{12}\sqrt{1-z^2}\right)\right)^2}{\hbar^2\eta}
\end{aligned}$$

In these equations $\bar{z}$ is the solution of Eq. (3.10).

It can be seen from the form of the Jacobian matrix that the atomic and photon degrees of freedom are no longer independent of each other but are coupled. Moreover the study of the stability of the equilibria is no longer straightforward as it was before, and can not be carried out analitically as

before The dynamics of the system around these equilibria will be carried out later, by using a simplifying assumption.

3.2 Adiabatic elimination of the photon dynamics

In the system we are studying the characteristic frequency of the photon dynamics is the effective detuning δ_C, while the characteristic frequency for tunneling processes is given by $\hbar^{-1}\nu$ and usually δ_C is orders of magnitude larger than $\hbar^{-1}\nu$ [14]. When such a relation holds between the two characteristic frequencies, that is to say when $\delta_C \gg \hbar^{-1}\nu$, the time scales of photon and atom dynamics separate and the photon field can be adiabatically eliminated. This means that the photon field evolves on a time scale much smaller than the atom field and therefore we can assume that it relaxes quickly to its steady state value when the atomic variables change. This allows us to calculate the photon degrees of freedom ξ and ϕ as a function of the atomic degrees of freedom z and θ by formally setting the derivative of ξ and ϕ to zero and solving for ξ and ϕ.

Looking at the full system (2.41), and using the bar symbol to indicate the value of the variables in this approximation, it can be seen that $\dot{\xi} = 0$ implies that $\eta \cos\phi = 0$ and so $\bar{\phi}(t) = \pm\frac{\pi}{2}$. Thus $\bar{\xi}(t) = \eta\cos\bar{\phi}(t)/\delta_C(t)$, where $\bar{\phi}$ is chosen so that $\bar{\xi}$ is positive, and where we remind that $\delta_C(t) = \Delta_C - N_A(W_0 + W_{12}\sqrt{1-z^2(t)}\cos\theta(t))/\hbar$. This means that, in this approximation, the photon degrees of freedom can be written as a function of the atomic variables of the system. Substituting the expression for $\bar{\xi}$ into the system (2.41), we get a new set of two equations which describe the dynamics of the system:

$$\dot{z} = -2\bar{\nu}\sqrt{1-z^2}\sin\theta, \tag{3.12a}$$

$$\dot{\theta} = \left(\tilde{g} + \frac{2\,\bar{\nu}}{\sqrt{1-z^2}}\cos\theta\right) z, \tag{3.12b}$$

with $\bar{\nu} = \bar{\nu}(t) = (J - W_{12}\bar{\xi}^2(t))/\hbar = (J - W_{12}\eta^2/\delta_C^2(t))/\hbar$.

It is important to notice that this set of equations has the same form as the equations that describe the dynamics of a bare BJJ, however there is a quite relevant difference. The assisted tunneling amplitude $\bar{\nu}$ is not a constant but a function of z and θ, and therefore it varies with time.

3.3 Constant photon field

When the cavity detuning Δ_C is much larger than $N_A W_0$ and $N_A W_{12}$, the photon amplitude ξ, as it appears in Eqs. (3.12), depends only weakly on the atomic varables z and θ. Therefore, when this condition is satisfied, the photon field amplitude ξ can be considered to be constant in time and have value $\xi = \eta/|\Delta_C|$. The new set of equations that describes our system is:

$$\dot{z} = -2\tilde{\nu}\sqrt{1-z^2}\sin\theta, \tag{3.13a}$$

$$\dot{\theta} = \left(\tilde{g} + \frac{2\,\tilde{\nu}}{\sqrt{1-z^2}}\cos\theta\right) z, \tag{3.13b}$$

where $\tilde{\nu} = (J - W_{12}\bar{\xi}^2)/\hbar = (J - W_{12}\eta^2/\delta_C^2)/\hbar = \tilde{J}/\hbar$ and $\xi = \eta/|\Delta_C|$.

This set of equations is very similar to the Josephson equations for a bare Josephson junction. But here, because of the cavity photons, the tunneling amplitude J is substituted with the assisted tunneling amplitude $\tilde{J}$. The assisted tunneling $\tilde{J}$ clearly depends on the number of photons ξ^2. Since the tunneling amplitude J is assumed to be positive, the presence of the cavity photons can have three consequences. When $W_{12} < 0$ the assisted tunneling amplitude $\tilde{J}$ can only get larger. When $W_{12} > 0$, for $\xi^2 < J/W_{12}$, the assisted tunneling becomes smaller, but remains positive, and for $\xi^2 > J/W_{12}$, $\tilde{J}$ changes sign and becomes negative.

At this point it is convenient to rewrite Eqs. (3.13) as:

$$\dot{z} = -2\tilde{J}\sqrt{1-z^2}\sin\theta, \tag{3.14a}$$

$$\dot{\theta} = \left(UN_A + \frac{2\,\tilde{J}}{\sqrt{1-z^2}}\cos\theta\right) z, \tag{3.14b}$$

where we used $\hbar = 1$ and we have written explicitly the expression $\tilde{g} = UN_A$ to show more clearly how U and N_A influence the dynamics.

These two equations are the Hamilton equations that derive from the Hamiltonian that describes the total energy of the system:

$$H(z,\theta) = \frac{UN_A^2}{2}\,z^2 - 2N_A\tilde{J}\sqrt{1-z^2}\,\cos\theta \tag{3.15}$$

as

$$\begin{aligned} \dot{z} &= -\frac{1}{N_A}\frac{\partial H}{\partial \theta} \\ \dot{\theta} &= \frac{1}{N_A}\frac{\partial H}{\partial z} \end{aligned}$$

3.3.1 Equilibria

We can now study the main features of the dynamics of the system by finding the equilibria of the system and studying how the system behaves close to them. By solving the equations $\dot{z} = 0$ and $\dot{\phi} = 0$ we can find the stationary points of the system, and using Eq. (3.15) we can calculate the energy of the system at the equilibria. It is easy to see that the system has four equilibria.

Using a vector notation in which $\mathbf{Y} = (Y_1, Y_2) = (z, \theta)$, we can write the equilibria as:

$$\mathbf{Y}_1 = (0, 0), \tag{3.16a}$$

$$\mathbf{Y}_2 = (0, \pi), \tag{3.16b}$$

$$\mathbf{Y}_3 = \left(\pm\sqrt{1 - \left(\frac{2\tilde{J}}{UN_A} \right)^2}, 0 \right), \tag{3.16c}$$

$$\mathbf{Y}_4 = \left(\pm\sqrt{1 - \left(\frac{2\tilde{J}}{UN_A} \right)^2}, \pi \right). \tag{3.16d}$$

In order for the last two equilibria to exist the expression under the square root must be positive and this implies that $(UN_A)^2 > (2\tilde{J})^2$. We don't consider $\mathbf{Y}_3$ and $\mathbf{Y}_4$ as two equilibria each for the clear $z \to -z$ symmetry of the system. The first two equilibria are the only ones we can have if there is no interaction between the atoms ($U = 0$). The last two equilibria are characterized by a non zero value of z. This means that there is an imbalance in the occupation of the wells. This phenomena is called self trapping and it is a consequence of the interaction between the bosons. In particular we can separate the solution to the equations in two classes. One is characterized by oscillations around $z = 0$ and therefore the time average of the population imbalance is zero: $\langle z(t) \rangle = 0$. The second class of solutions is characterized by an average imbalance in the population of the wells and therefore $\langle z(t) \rangle \neq 0$, where the angular brackets represent the time average. When $\langle z(t) \rangle \neq 0$ the system is said to be in the self trapping regime.

3.3.2 Equilibrium stability

To study the stability of the equilibria we can use the Jacobian matrix of the system:

$$J(\mathbf{Y}) = \begin{pmatrix} \frac{2\tilde{J}z\sin\theta}{\sqrt{1-z^2}} & -2\tilde{J}\sqrt{1-z^2}\cos\theta \\ UN_A + \frac{2\tilde{J}z^2\cos\theta}{(1-z^2)^{3/2}} + \frac{2\tilde{J}\cos\theta}{\sqrt{1-z^2}} & -\frac{2\tilde{J}z\sin\theta}{\sqrt{1-z^2}} \end{pmatrix} \tag{3.17}$$

Now we need to calculate the Jacobian matrix at the equilibria and find its eigenvalues.

Zero imbalance equilibria

Let us start with the equilibrium $\mathbf{Y_1}$:

$$J(\mathbf{Y_1}) = \begin{pmatrix} 0 & -2\tilde{J} \\ UN_A + 2\tilde{J} & 0 \end{pmatrix} \tag{3.18}$$

This matrix has eigenvalues

$$\lambda_1 = \pm i\sqrt{4\tilde{J}^2 + 2UN_A\tilde{J}}.$$

The equilibrium is stable when the eigenvalues are purely imaginary. The frequency of the small oscillations around $\mathbf{Y_1}$, written in the actual physical dimensions, is therefore:

$$\omega_1 = \frac{1}{\hbar}\sqrt{4\tilde{J}^2 + 2UN_A\tilde{J}}. \tag{3.19}$$

The frequency ω_1 is real when:

$$4\tilde{J}^2 + 2UN_A\tilde{J} > 0,$$

which can be written as:

$$4\tilde{J}^2\left(1 + \frac{UN_A}{2\tilde{J}}\right) > 0.$$

Therefore this equilibrium is stable when

$$\frac{UN_A}{2\tilde{J}} > -1. \tag{3.20}$$

For the equilibrium $\mathbf{Y_2}$ we can follow the same steps:

$$J(\mathbf{Y_2}) = \begin{pmatrix} 0 & 2\tilde{J} \\ UN_A - 2\tilde{J} & 0 \end{pmatrix} \tag{3.21}$$

After calculating the eigenvalues of the matrix we find that the frequency of the small oscillations around $\mathbf{Y_2}$ is:

$$\omega_2 = \frac{1}{\hbar}\sqrt{4\tilde{J}^2 - 2UN_A\tilde{J}}, \tag{3.22}$$

and we can write it as:

$$\omega_2 = \frac{1}{\hbar}\sqrt{4\tilde{J}^2\left(1 - \frac{UN_A}{2\tilde{J}}\right)}.$$

The frequency is real when:

$$\frac{UN_A}{2\tilde{J}} < 1. \tag{3.23}$$

Let us now show some examples of how the cavity photons influence the frequency of small oscillations for the zero imbalance equilibria. Let us choose $\mathbf{Y_1}$. When the in-site interaction is positive, $U > 0$, the condition that gives the stability of the equilibrium is always satisfied when $W_{12} < 0$. In this case the presence of the photon field only modifies the frequency of

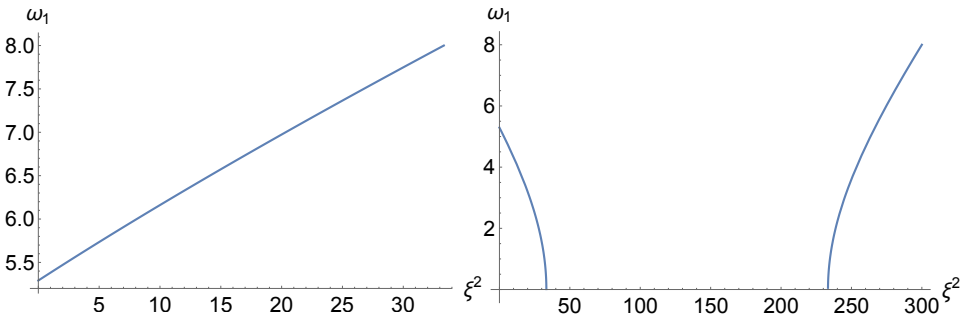

Figure 3.4: Frequency ω_1 (3.19) written as a function of the number of photons ξ^2. ω_1 is in units of $J/\hbar$. $W_{12} = -0.03J$ in the first panel and $W_{12} = 0.03J$ in the second. In the second panel, the frequency is not real when $33.33 < \xi^2 < 233.33$. The other parameters are $N_A = 1000$ and $U = 0.012J$.

the small oscillations. This can be seen in the first panel of Fig. (3.4). On the other hand, when $W_{12} > 0$, there exists a range of number of photons for which the frequency is no longer real and the system no longer performs small oscillations around the equilibrium. This happens when

$$\frac{J}{W_{12}} < \bar{\xi}^2 < \frac{1}{W_{12}}\left(\frac{UN_A}{2} + J\right). \tag{3.24}$$

This can be seen in the second panel of Fig. (3.4).

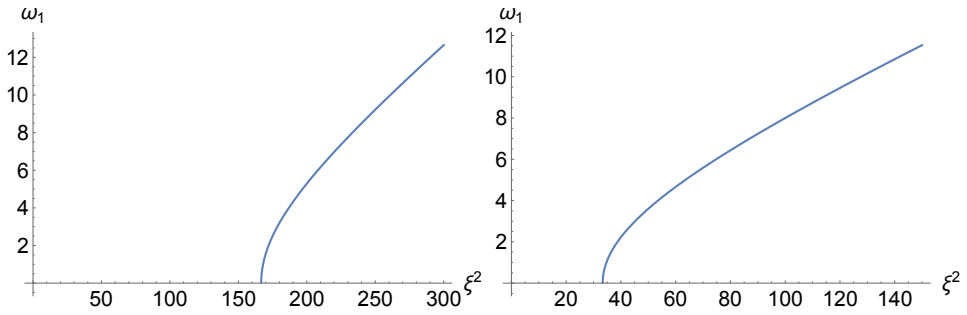

Figure 3.5: Frequency ω_1 (3.19) written as a function of the number of photons ξ^2. ω_1 is in units of $J/\hbar$. $W_{12} = -0.03J$ in the first panel and $W_{12} = 0.03J$ in the second. The other parameters are $N_A = 1000$ and $U = -0.012J$.

When $U < 0$ the equilibrium is not always stable. When it is not, however, it can be made stable by increasing the number of photons. When $W_{12} < 0$ the equilibrium is stable when:

$$\xi^2 > \frac{1}{W_{12}}\left(\frac{UN_A}{2} + J\right), \tag{3.25}$$

and when $W_{12} > 0$ it becomes stable for:

$$\xi^2 > \frac{J}{W_{12}} \tag{3.26}$$

The frequency ω_1 as a function of ξ^2 for this case can be seen in Fig. (3.5).

Finite imbalance equilibria

For the finite imbalance equilibrium $\mathbf{Y_3}$ the Jacobian matrix reads:

$$J(\mathbf{Y_3}) = \begin{pmatrix} 0 & \frac{4\tilde{J}^2}{UN_A} \\ UN_A - \frac{U^3N_A^3}{4\tilde{J}^2} & 0 \end{pmatrix} \tag{3.27}$$

where we have used the fact that in order for this equilibrium to exist $UN_A/2\tilde{J} < -1$ and therefore the ratio $U/\tilde{J}$ must be negative. The corresponding frequency is:

$$\omega_3 = \frac{1}{\hbar}\sqrt{U^2N_A^2 - 4\tilde{J}^2}, \tag{3.28}$$

which is real when:

$$\frac{UN_A}{2\tilde{J}} < -1. \tag{3.29}$$

This condition is the same as the one that describes the existence of this equilibrium. Therefore, when this equilibrium exists, it is also stable.

For the other finite imbalance equilibrium $\mathbf{Y_4}$ the Jacobian matrix reads:

$$J(\mathbf{Y_4}) = \begin{pmatrix} 0 & \frac{4\tilde{J}^2}{UN_A} \\ UN_A - \frac{U^3N_A^3}{4\tilde{J}^2} & 0 \end{pmatrix} \tag{3.30}$$

where in this cased we have used $UN_A/2\tilde{J} > 1$. The corresponding frequency is:

$$\omega_4 = \frac{1}{\hbar}\sqrt{U^2N_A^2 - 4\tilde{J}^2}, \tag{3.31}$$

which is real when:

$$\frac{UN_A}{2\tilde{J}} > 1 \tag{3.32}$$

In this case as well, the existence condition for the equilibrium is the same that gives its stability, and thus, when this equilibrium exisits, it is also stable. In Fig. (3.6) we can see how the number of cavity photons influences the frequency ω_4.

When there is no interaction between the atoms $U = 0$. In this case the only possible equilibria are $\mathbf{Y_1}$ and $\mathbf{Y_2}$ the equations of the system describe oscillations with frequency:

$$\omega_R = \frac{2}{\hbar}|\tilde{J}| = \frac{2}{\hbar}|J - W_{12}\bar{\xi}^2|, \tag{3.33}$$

where ω_R is called Rabi frequency and the osciallations Rabi oscillations. The presence of the photon field modifies the Rabi frequency of the oscillations as can be seen from Fig. (3.7).

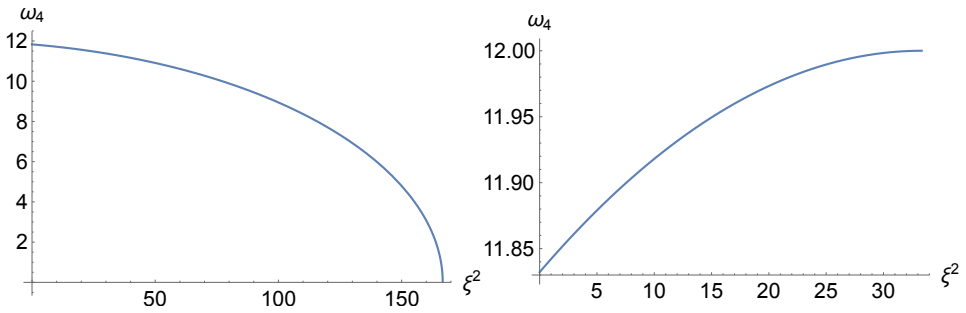

Figure 3.6: Frequency ω_4 (3.31) written as a function of the number of photons ξ^2. ω_4 is in units of $J/\hbar$ and $W_{12} = -0.03J$ in the first panel and $W_{12} = 0.03J$ in the second. In both panels the range of ξ^2 is given by the condition for the stability of the equilibrium. The other parameters are $N_A = 1000$ and $U = 0.012J$

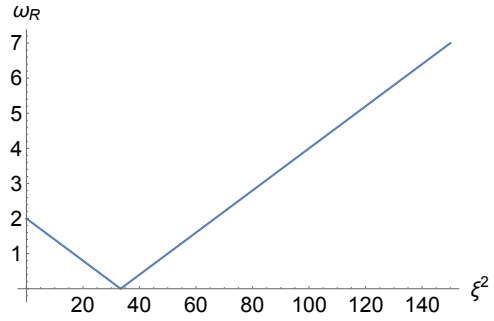

Figure 3.7: Rabi frequency ω_R (3.33) written as a function of the number of photons ξ^2. ω_R is in units of $J/\hbar$ and $W_{12} = 0.03J$.

Energies

The energies of the stationary points can be calculated by substituting their values for z and θ into the expression of the Hamiltonian (3.15). The energies of the equailibria with zero imbalance can be computed straightforwardly and they are:

$$E_1 = -2N_A\tilde{J} \tag{3.34}$$

$$E_2 = 2N_A\tilde{J}. \tag{3.35}$$

As for the energy of the finite imbalance equilibria, it is necessary to pay attention to the relative signs of the in-site interaction U and of the assisted tunneling amplitude $\tilde{J}$.

Let us start with the stationary point $\mathbf{Y}_4$. In order for $\mathbf{Y}_4$ to exist, $UN_A/2\tilde{J} > 0$. This is a clear consequence of $\dot{\theta} = 0$, when $\theta = \pi$ and $z \neq 0$ and it implies that U and $\tilde{J}$ need to have the same sign. This allows us to write the condition $(UN_A)^2 > (2\tilde{J})^2$, as $UN_A/2\tilde{J} > 1$. It is convenient to rename $UN_A/2\tilde{J} = \Lambda$, and the condition we have just mentioned becomes

$\Lambda > 1$. Using this new variable we can write the energy of the equilibrium as:

$$E_4 = N_A \tilde{J} \left(\Lambda + \frac{1}{\Lambda} \right). \tag{3.36}$$

Since $\Lambda > 1$ the quantity $\left(\Lambda + \frac{1}{\Lambda}\right) > 2$.

Now let us calculate the energy for $\mathbf{Y}_3$. From the equation $\dot{\theta} = 0$ we find that this equilibrium exists only when $UN_A/2\tilde{J} < 0$ which means that U and $\tilde{J}$ need to have opposite signs. The condition $(UN_A)^2 > (2\tilde{J})^2$ becomes $UN_A/2\tilde{J} < -1$. Using Λ as before we find that:

$$E_3 = N_A \tilde{J} \left(\Lambda + \frac{1}{\Lambda} \right). \tag{3.37}$$

The expression for the energy of E_3 is the same as the one we have found for E_4, however, for E_3, Λ is negative. Since $\Lambda < -1$ the quantity $\left(\Lambda + \frac{1}{\Lambda}\right) < -2$.

Energy ranking

At this point we can compare the energies of the equilibria of the system and and rank them to find out which one has the lowest energy. In particular we are interested in understanding when the equilibria with a finite imbalance are the most energetically convenient. The relevant parameters of the system, for a fixed N_A, are U and $\tilde{J}$. The ranking order of the energies is different depending on the sign of these parameters, so we need to separate all the different cases. Let us write again the formulas for the energy of the equilibria we have previously calculated:

$$E_1 = -2N_A\tilde{J}, \tag{3.38}$$

$$E_2 = 2N_A\tilde{J}, \tag{3.39}$$

$$E_{3,4} = N_A \tilde{J} \left(\Lambda + \frac{1}{\Lambda} \right), \tag{3.40}$$

where E_3 and E_4 have the same expression, but can not both exist for the same values of the parameters U and $\tilde{J}$.

Let us start with the case with repulsive interaction, $U > 0$. We can consider two cases: $\tilde{J} > 0$ and $\tilde{J} < 0$.

When $\tilde{J} > 0$, $\tilde{J}$ and U have the same sign and therefore E_3 does not exist. E_4 is positive and clearly larger $2N_A\tilde{J}$. E_1 is the only equilibrium with negative energy and therefore it has the lowest energy.

When $\tilde{J} < 0$, $\tilde{J}$ and U have opposite signs and E_4 does not exist. E_3 is positive and clearly larger than $2N_A\tilde{J}$. E_2 in the only equilibrium with negative energy and it has the lowest energy. Therefore we see that when the interaction is positive the zero imbalance equilibria are always the most energetically favourable.

When the interaction is attractive $U < 0$ we get different results.

When $\tilde{J} > 0$, $\tilde{J}$ and U have opposite signs and E_4 does not exist. E_3 is negative and clearly smaller than $-2N_A\tilde{J}$. Therefore E_3 is the equilibrium with the lowest energy. However, for this equilibrium to exist, the condition $(UN_A)^2 > (2\tilde{J})^2$ needs to be satisfied.

When $\tilde{J} < 0$, $\tilde{J}$ and U have the same sign and E_3 does not exist. E_4 is negative and clearly smaller than $-2N_A\tilde{J}$. Therefore E_4 is the equilibrium with the lowest energy. However, for this equilibrium to exist, the condition $(UN_A)^2 > (2\tilde{J})^2$ needs to be satisfied.

Therefore we can see that when the interaction is negative the energies of the equilibria with a finite imbalance, when they exist, are the most favourable for the system.

Photon induced self trapping

Using the fact that the energy is a constant of motion of the system, the expression of the energy for the finite imbalance equilibria allows us to find a general condition that describes when the system can display the self trapping [10]. Let us remind that when the system is in the self trapping regime there is an imbalance in the population of the wells and $\langle z(t)\rangle \neq 0$, where the angular brackets represent the time average.

When U and $\tilde{J}$ have the same sign we need to consider the equilibrium $\mathbf{Y}_4$ and when the have opposite signs $\mathbf{Y}_3$. Let us show how the cavity photons in the system can induce self trapping solutions for the first case.

When both U and $\tilde{J}$ are positive the condition $\Lambda > 1$ tells us that the energy of the system must satisfy $E_4 > 2N_A\tilde{J}$. This means that self trapping can occur when the initial energy of the system H_0 satisfies:

$$\begin{aligned} H_0 = H(z(0),\theta(0)) &= N_A\Lambda\tilde{J}z^2(0) - 2N_A\tilde{J}\sqrt{1-z^2(0)}cos\theta(0) \\ &= 2N_A\tilde{J}\left[\frac{\Lambda}{2}z^2(0) - \sqrt{1-z^2(0)}cos\theta(0)\right] > 2N_A\tilde{J}, \end{aligned} \tag{3.41}$$

and since we have assumed that $\tilde{J}$ is positive, this expression can be written as:

$$\frac{\Lambda}{2}z^2(0) - \sqrt{1-z^2(0)}\cos\theta(0) > 1. \tag{3.42}$$

This inequality allows us to find relations between $z(0)$, $\theta(0)$ and Λ for which the system can show the self trapping.

If we assume to fix the initial conditions $z(0)$ and $\theta(0)$, the self trapping can occur only when Λ is larger than a critical value Λ_C. Solving for Λ we find that:

$$\Lambda_C = 2\frac{1+\sqrt{1-z^2(0)}cos\theta(0)}{z^2(0)}. \tag{3.43}$$

While in a bare Josephson junction, the tunneling amplitude $\tilde{J} = J$ is fixed, in our system it can be modified, by changing the number of the cavity photons. This means that in our system we have one more relevant parameter that allows us to switch between different regimes. Remembering that $\Lambda = UN_A/2\tilde{J}$, we can see that in a bare BJJ with a fixed number of atoms, Λ can be changed to satisfy this condition only by changing the interaction strength U and making it larger. In our system however we can keep the interaction constant and satisfy this condition by making $\tilde{J}$ smaller. This can be done when $W_{12} > 0$ by increasing the number of photons.

By writing explicitly $\tilde{J}$, we can see that for fixed initial values $z(0)$, $\theta(0)$ and a value of U that would not allow the self trapping in the absence of photons, the condition that the photon number ξ^2 has to satisfy in order for the self trapping to occur is:

$$\xi^2 > \frac{J}{W_{12}}\left(1 - \frac{UN_A}{J}\frac{z^2(0)}{4(1+\sqrt{1-z^2(0)}cos\theta(0)}\right), \tag{3.44}$$

with $\xi^2 \leq \frac{J}{W_{12}}$ for $\tilde{J}$ to be positive.

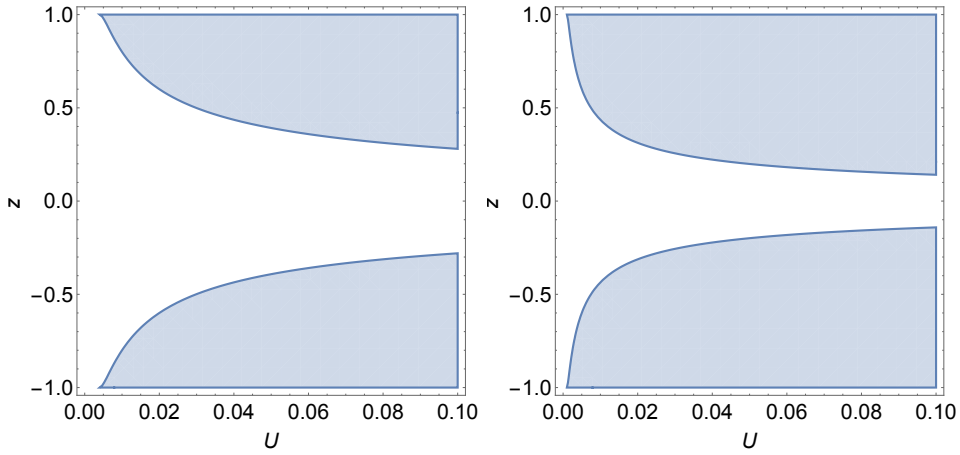

Figure 3.8: The two panels show, highlighted in blue, the values of z and U that allow self trapping for a fixed $\theta = 0$. The differences in the panels depend on the number of photons in the cavity. In the first one $\xi^2 = 0$ and $\tilde{J} = J$, in the second $\xi^2 = 25$ and $\tilde{J} = 0.25J$. The other parameters are $N_A = 1000$, $N_A W_{12} = 30J$. U is written in units of J.

Instead of fixing both $z(0)$ and $\theta(0)$, we can fix $\theta(0)$ and Λ. This leads to a critical value of the initial atomic imbalance $z_c = z_c(\theta(0), \Lambda)$ for which the system shows self trapping. The condition for the self trapping to occur (3.42), by fixing $\theta(0) = 0$ and Λ can be written as:

$$|z(0)| > z_c = \frac{2\sqrt{\Lambda - 1}}{\Lambda} \tag{3.45}$$

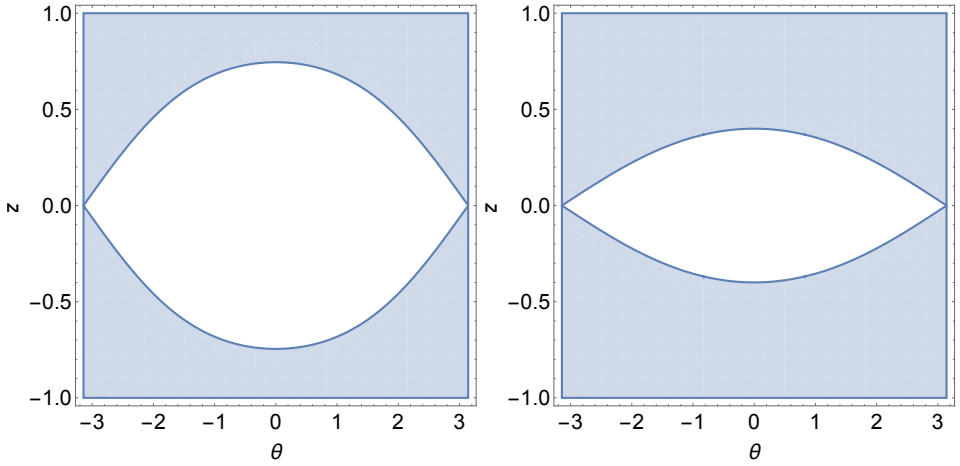

Figure 3.9: The two panels show, highlighted in blue, the values of z and θ that allow the self trapping. The differences in the graphics depend on the number of photons in the cavity. In the first one $\xi^2 = 0$ and $\tilde{J} = J$, in the second $\xi^2 = 25$ and $\tilde{J} = 0.25J$. The other parameters are $N_A = 1000$, $N_A W_{12} = 30J$, $N_A U = 12J$

Remembering that Λ depends on the number of photons through $\tilde{J}$ it is clear that the value of z_c depends on ξ^2. This effect can be seen in Fig. (3.8), where we can notice that the value of z that allows the self trapping gets smaller when the number of photons in the system is increased.

In Fig. (3.9) we can see for which values if $z(0)$ and $\theta(0)$ the self trapping can occur, for a fixed interaction strength U. The area of the plot highlighted in blue represents the initial values from which the system is in the self trapping regime. By comparing the two panels, it can be clearly seen what the effect of changing the number of photons is. In particular we can notice that increasing the number of photons widens the area that allows the self trapping.

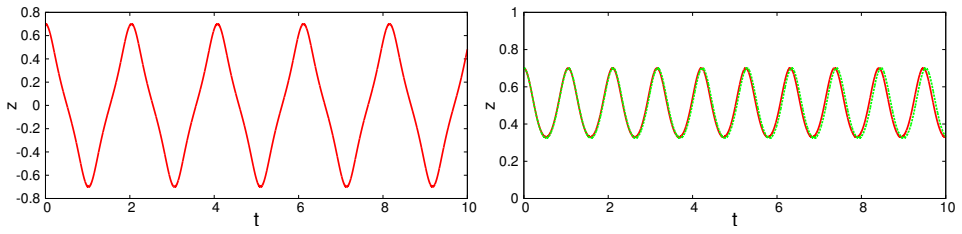

Figure 3.10: Time evolution of the variable z. Time is measured in units of $\hbar/J$. The first panel represents the bare junction in the absence of the cavity. The second one shows the junction inside of the cavity. The red lines represent the numerical solution of the simplified system, where the photon degrees of freedom are constant. The green dashed line represents the solution of the complete system. The parameters for the second panel are: $\hbar\Delta_C = 300J$, $W_0 N_A = 4J$, $W_{12} N_A = 3J$, $U N_A = 12J$, $N_A = 1000$, $\hbar\eta = 3000J$. The initial conditions for the first panel are for $(z, \theta) = (0.7, 0)$. The initial conditions for the second panel are $(z, \theta, \xi, \phi) = (0.7, 0, 10.17, \pi/2)$

The change of regime can be clearly seen from Fig. (3.10). In the left panel we can see the time evolution of the system in the absence of photons and how the population of the wells has a zero average value. The right panel shows the time evolution when the cavity photons are present in the system: it can be clearly seen that the photons induce oscillations around a non-zero average value of z.

Chapter 4

Ground state of the system in the half-semiclassical approximation

So far we have studied the system in the semiclassical approximation that allowed us to describe the photon field and the condensate in the left and right well through coherent states. Now we want to study the static properties of the system, i.e. calculating its ground state, when we do not use the semiclassical approximation for the atoms in the wells. We call this description of the system "half-semiclassical" because the cavity photons are still described with a coherent state, but the atoms are studied in a purely quantum way.

Our intent in studying the system in the half semiclassical approximation is twofold.

On the one hand we are interested in finding out how the presence of the cavity photons influences the ground states of the system. In particular we want to see how the photon field modifies the transition between the atomic coherent state and the "macroscopic cat" state for attractive interaction, and between the atomic coherent state and the separable Fock state for repulsive interaction. This study will make use of some quantum indicators to better identify when the transitions take place.

On the other hand we are also interested in finding out if there is some analogy between the half-semiclassical study of the system and the semiclassical study we have carried out in the previous chapter. In particular we would like to compare the transitions we have seen when studying the equilibria of the Josephson equations and the transitions we find in the ground state of the system.

4.1 Bare Josephson junction

Let us start by studying the ground states of the bare Josephson junction following [13]. The Hamiltonian of the system is:

$$\hat{H}_J = -J\left(\hat{b}_1^\dagger \hat{b}_2 + \hat{b}_2^\dagger \hat{b}_1\right) + \frac{U}{2}\left(\hat{b}_1^\dagger \hat{b}_1^\dagger \hat{b}_1 \hat{b}_1 + \hat{b}_2^\dagger \hat{b}_2^\dagger \hat{b}_2 \hat{b}_2\right). \tag{4.1}$$

It is worth noticing that the number operator $\hat{N}_A = \hat{n}_1 + \hat{n}_2$ commutes with the Hamiltonian and therefore the total number of particles is conserved. Given a fixed number of atoms N in the Josephson junction we want to see how the ground state of the system changes when we vary the ratio $\zeta = U/J$. In order to do this we need to solve the eigenvalue problem for the Hamiltonian $\hat{H}_J$:

$$\hat{H}_J|E_j\rangle = E_j|E_j\rangle, \tag{4.2}$$

where E_j is the j-th eigenvalue and $|E_j\rangle$ the corresponding eigenvector. To solve this problem numerically, we want to write the Hamiltonian $\hat{H}_J$ in its matrix form. By using the Fock basis $\{|n\rangle, n = 0, 1, ..., N\}$, where $|n\rangle = |N-n, n\rangle = |N-n\rangle_1 \otimes |i\rangle_2$, the Hamiltonian is represented by a $(N+1)\times(N+1)$ matrix. The element of the Fock basis $|n\rangle$ describes the state where there are n atoms in the right well and $N-n$ in the left well. The matrix elements of the Hamiltonian are:

$$(H_J)_{nm} = \langle n|\hat{H}_J|m\rangle. \tag{4.3}$$

The eigenstate $|E_j\rangle$ for a given eigenvalue E_j, can be written as:

$$|E_j\rangle = \sum_{n=0}^{N} c_n^{(j)} |n\rangle \ . \tag{4.4}$$

where the square module of the coefficient $|c_n^{(j)}|^2$ is the probability to have n atoms in the right well and $N-n$ in the left one when the system is in the jth eigenstate of the Hamiltonian.

Since we are interested in the ground state of the system we will only need the lowest eignevalue E_0 and eigenvector $|E_0\rangle$.

4.1.1 Coherent, Fock and "macroscopic cat" states

The ground state of the Hamiltonian (4.1) at a fixed N shows different configurations depending on the relative strength of the in-site interaction U and the tunneling amplitude J that can be represented with the dimensionless parameter $\xi = U/J$. Let us start by listing the theoretical results in some limit cases.

- When there is zero interaction $U = 0$, and therefore $\xi = 0$, the ground-state of the Hamiltonian $\hat{H}_J$ is the atomic coherent state (ACS)

$$|ACS\rangle = \frac{1}{\sqrt{N!}}\left[\frac{1}{\sqrt{2}}(\hat{b}_1^\dagger + \hat{b}_2^\dagger)\right]^N |0,0\rangle \ , \tag{4.5}$$

  where $|0,0\rangle = |0\rangle_1 \otimes |0\rangle_2$ is the tensor product between the vacuum of the operator $\hat{b}_1$ and the vacuum of and $\hat{b}_2$, which is the state with no atoms in either well [23, 24].

- When the interaction is repulsive, $U > 0$ and $\zeta > 0$. the ground-state of the Hamiltonian can be found into two different regimes depending on the value of the parameter ζ [25, 26, 27, 28]. When $\zeta \ll N$ the ground-state is close to $|ACS\rangle$. If $\zeta \gg N$, the ground-state is close to the separable Fock state

$$|FOCK\rangle = |\frac{N}{2}, \frac{N}{2}\rangle \ . \tag{4.6}$$

  where half of the atoms are in the right well and half in the left one.

- When the interaction is attractive, $U < 0$ and $\zeta < 0$ the ground-state of the Hamiltonian can be close to the atomic coherent state $|ACS\rangle$ or in a entangled superposition of macroscopic states, i.e. macroscopic Schrödinger cat states [29, 30, 31, 32, 33]. By changing the parameter $\zeta = U/J < 0$ towards smaller values the ground-state of the system evolves towards the following macroscopic superposition state

$$|CAT\rangle = \frac{1}{\sqrt{2}}(|N,0\rangle + |0,N\rangle) \tag{4.7}$$

  which is the linear combination of the states with all particles in the left or in the right well. This entangled macroscopic superposition state is also known as "$NOON$ state" or "macroscopic cat state".

4.2 Quantum indicators

The coherence and entanglement properties of the ground states can be better described by using some estimators, that allow to identify the transitions between the various regimes the ground state can be found in. The estimators we will be using are the Fisher information [34], the coherence visibility [28] and the entanglement entropy [35]. Let us briefly define this quantities and their relation to our system.

4.2.1 Quantum Fisher information

For pure states, such as our ground state $|E_0\rangle$, the quantum version of the Fisher information F_{QFI}, is defined as the variance of the difference of the number of atoms in the right and left well [36, 34, 37]:

$$F_{QFI} = (\Delta\hat{n}_{1,2})^2 = \langle(\hat{n}_1 - \hat{n}_2)^2\rangle - \big(\langle\hat{n}_1 - \hat{n}_2\rangle\big)^2, \tag{4.8}$$

where the expectation value $\langle ...\rangle$ is calculated with respect to the ground state $|E_0\rangle$. Since the Hamiltonian $\hat{H}_J$ is left-right symmetric, the ground state has s definite parity and therefore it satisfies the condition $\langle\hat{n}_1\rangle = \langle\hat{n}_2\rangle$. At this point the Fisher Information F_{QFI} of the state can be written in terms of the coefficients $c_i^{(0)}$ as:

$$F_{QFI} = \sum_{i=0}^{N} \big[2i - N\big]^2 |c_i^{(0)}|^2 \, . \tag{4.9}$$

F_{QFI} can be normalized with respect to its maximum value N^2 by defining the Fisher information F as:

$$F = \frac{F_{QFI}}{N^2} \, . \tag{4.10}$$

F gives the width of the distribution $|c_i^{(0)}|^2$ centered at $i/N = 1/2$. We can observe that $F = 1$ holds for the "macroscopic cat state" $|CAT\rangle$, $F = 1/N$ for the atomic coherent state $|ACS\rangle$ and $F = 0$ for the "separable Fock state" $|FOCK\rangle$. It is also worth mentioning that there exists a sufficient condition to have entanglement between the atoms and it reads $F > 1/N$ [34].

4.2.2 Coherence visibility

In cold atom physics, the coherence properties of condensates are usually studied in terms of their momentum distribution $n(p)$. The momentum distribution is defined as the Fourier transform of the one-body density matrix $\rho_1(x, x')$ [25, 26, 28]:

$$n(p) = \int dx dx' \exp\big(-ip(x - x')\big)\, \rho_1(x, x') \, , \tag{4.11}$$

where

$$\rho_1(x, x') = \langle\hat{\phi}(x)^\dagger \hat{\phi}(x')\rangle \, . \tag{4.12}$$

Here the operators $\hat{\phi}(x)$ and $\hat{\phi}(x)^\dagger$ are the operators defined in Eq. (2.19) and the average $\langle ...\rangle$ is the ground-state average. It was proven [25, 26, 28] that the momentum distribution $n(p)$ can be written as:

$$n(p) = n_0(p)\Big(1 + \alpha_v \cos\big(pd\big)\Big) \, , \tag{4.13}$$

where $n_0(p)$ is the momentum distribution in the fully incoherent regime (which depends on the shape of the double-well potential $V_{DW}(x)$), and d is the distance between the two minima of $V_{DW}(x)$. α_v is a real quantity which measures the visibility of the interference fringes of the distribution $n(p)$. When calculated in our system, the coherence visibility α_v can be written as

$$\alpha_v = \frac{2\,|\langle \hat{a}_1^\dagger \hat{a}_2 \rangle|}{N} \tag{4.14}$$

and it characterizes the degree of coherence between the two wells.

When evaluated in the ground-state $|E_0\rangle$ and written in terms of the coefficients $c_i^{(0)}$, the visibility α becomes:

$$\alpha_v = \frac{2}{N} \left| \sum_{i=0}^{N} c_i^{(0)} c_{i+1}^{(0)} \sqrt{(i+1)(N-i)} \right| . \tag{4.15}$$

The coherence visibility has its maximum value when the ground state of the system is the atomic coherent state $|ACS\rangle$ and it equal to 1.

Density operator and entangled states

We quickly remind some of the properties of the density operator, because it will be useful when defining the entanglement entropy of the system.

Given a system in the state $|\psi(t)\rangle$, the density operator associated with the state of the system is $\hat{\rho}(t) = |\psi(t)\rangle\langle\psi(t)|$. The expectation value of an observable $\hat{O}$ in the state $|\psi(t)\rangle$ can be calculated as:

$$\langle \hat{O} \rangle(t) = \langle \psi(t) | \hat{O} | \psi(t) \rangle,$$

or using the density operator:

$$\langle \hat{O} \rangle(t) = Tr[\hat{\rho}(t)\hat{O}].$$

When $\hat{\rho}(t)$ represents a pure state, then $\hat{\rho}^2 = \hat{\rho}$ and $Tr\hat{\rho}^2 = 1$.

Let us now briefly intorduce the concept of entangled state. Let us consider a system composed of two parts, (1) and (2), with Hilbert spaces $\mathcal{H}_1$ and $\mathcal{H}_2$ respectively. The global system (1) + (2) has as Hilbert space the tensor product $\mathcal{H} = \mathcal{H}_1 \otimes \mathcal{H}_2$. If $\{|u_m\rangle_1\}$ is an orthonormal basis for $\mathcal{H}_1$, and $\{|v_n\rangle_2\}$ is an orthonormal basis for $\mathcal{H}_2$, then $\mathcal{H}$ has as basis $\{|w_{mn}\rangle\} = \{|u_m\rangle_1 \otimes |v_n\rangle_2\}$. A pure state of system (1) can be written as: $|\varphi\rangle_1 = \sum_m a_m |u_m\rangle_1$, and a pure state of system (2) as: $|\chi\rangle_2 = \sum_n b_n |v_n\rangle_2$. A pure state of the complete system can be written as: $|\Phi\rangle = \sum_{m,n} c_{m,n} |u_m\rangle_1 \otimes |v_n\rangle_2 = \sum_{m,n} c_{m,n} |w_m n\rangle$. A pure state is used when the state of the system is perfectly well known. However, when there is only incomplete information about a system, we describe it through a mixed state. In this case, the state of the system may be $|\psi_1\rangle$ with probability p_1, or the state $|\psi_2\rangle$ with

probability p_2, etc, with $\sum_i p_i = 1$. In this case we are dealing with a statistical mixture of states. Such a state can not be described with an average state vector. However it is possible to define a density operator for such a state as: $\hat{\rho}(t) = \sum_i p_i(t)|\psi_i(t)\rangle\langle\psi_i(t)|$. Since we are studying the properties of the ground state of the system, which is obtained from the diagonalization of the system Hamiltonian, and it is a pure state, from now on we will be using only pure states. A pure state of a combined sysytem is said to be separable if it can be written as the tensor product of the states of its subsystems, that is to say: $|\Phi\rangle = |\varphi\rangle_1 \otimes |\chi\rangle_2$. When such a decomposition of the state $|\Phi\rangle$ is not possible, the state of the complete system is said to be entangled. The density operator $\hat{\rho}$ of the complete system is separable if it can be written as $\hat{\rho} = \hat{\rho}_1 \otimes \hat{\rho}_2$. In fact if $|\Phi\rangle = |\varphi\rangle_1 \otimes |\chi\rangle_2$, then $\hat{\rho}_1 = |\varphi\rangle_1\langle\varphi|_1$ and $\hat{\rho}_2 = |\chi\rangle_2\langle\chi|_2$. For a separable state $\hat{\rho}_1$ and $\hat{\rho}_2$ can be calculated from $\hat{\rho}$ by taking the partial trace:

$$\begin{aligned} \hat{\rho}_1 &= \mathrm{Tr}_2\hat{\rho} \\ \hat{\rho}_2 &= \mathrm{Tr}_1\hat{\rho}. \end{aligned}$$

When the state is not separable than the product of $\hat{\rho}_1$ and $\hat{\rho}_2$ obtained after taking the partial trace is not equal to $\hat{\rho}$. However taking the partial trace can be used to measure the correlations between the two parts of the system.

4.2.3 Entanglement entropy

The third and last indicator we will use to analyze the quantum entanglement of the the ground state $|E_0\rangle$ is the entanglement entropy S, which measures the quantum correlations between the atoms in the two wells [35]. If the system is in the state $|E_0\rangle$, its density matrix $\hat{\rho}$ is

$$\hat{\rho} = |E_0\rangle\langle E_0| \,. \tag{4.16}$$

The entanglement entropy of this state is defined as the von Neumann entropy of the reduced density matrix $\hat{\rho}_1$ defined by

$$\hat{\rho}_1 = Tr_2\hat{\rho} \,, \tag{4.17}$$

that is a matrix obtained by partial tracing the total density matrix (4.16) over the basis vectors of the right well. The entanglement entropy S can be written as:

$$S = -Tr\hat{\rho}_1 \log_2 \hat{\rho}_1. \tag{4.18}$$

The expression for the entanglement entropy written in terms of the coeffiencients of the ground state is:

$$S = -\sum_{i=0}^{N} |c_i^{(0)}|^2 \log_2 |c_i^{(0)}|^2 \,. \tag{4.19}$$

The maximum value S can have, for a given number of bosons N, is $\log_2(N+1)$. This value is achieved when all the coefficients of the ground state take the same value: $c_i^{(0)} = 1/\sqrt{N+1}$.

4.3 Crossover between the ground states

We will briefly rederive the results obtained in [13] that describe how the ground state of the system changes regimes when changing the value of ζ. The results here provided will serve as a baseline for the study of the same problem in the presence of cavity photons.

4.3.1 Repulsive interaction

Let us start by numerically solving the eigenvalue problem of Eq. (4.2) for different values of the positive interaction, and therefore of $\zeta = U/J$, to find out what the ground state of the system is. In panel (b) of Fig. (4.1) we can see the plot of the coefficients $|c_n^{(0)}|^2$ for $N = 1000$ for various values of the positive interaction. When the interaction is $U = 0$, as expected, the state of the system is the $|ACS\rangle$ which has a Gaussian profile. We notice that when the interaction becomes stronger, the width of the distribution of the coefficients $|c_n^{(0)}|^2$ becomes narrower. This is related to the aforementioned fact that when ζ is large, the ground state becomes close to the separable Fock state, in which half of the atoms are in the left well and half in the right well. In this configuration only the coefficient $|c_n^{(0)}|^2$ with $n = N/2$ is non zero.

4.3.2 Attractive interaction

In panel (a) of Fig. (4.1) we can see what happens when the interaction is attractive. When increasing the absolute value of ζ we see a change of regime. When $|\zeta|$ is close to zero the ground state is close to an atomic coherent state and the plot of the coefficients $|c_n^{(0)}|^2$ shows a single maximum. The width of the distribution of the gets wider when $|\zeta|$ increases. However for a large enough $|\zeta|$ ($\zeta_{cr} \simeq -0.00203$ for $N = 1000$), a valley appears in the middle of the distribution of the coefficients. The distribution has two maxima which are symmetric with respect to $n/N = 1/2$. This means that the system is most likely to be found in a state where there is an imbalance in the population of the right and left well. The emergence of this kind of ground state can be interpreted as the onset of the self trapping equilibria in the semiclassical dynamics. For an even larger $|\zeta|$, the two maxima move away from each other and the ground state goes toward the "macroscopic quantum cat" state, in which only the coefficients $|c_0^{(0)}|^2$ and $|c_N^{(0)}|^2$ have a non-zero value. When the ground state of the system shows

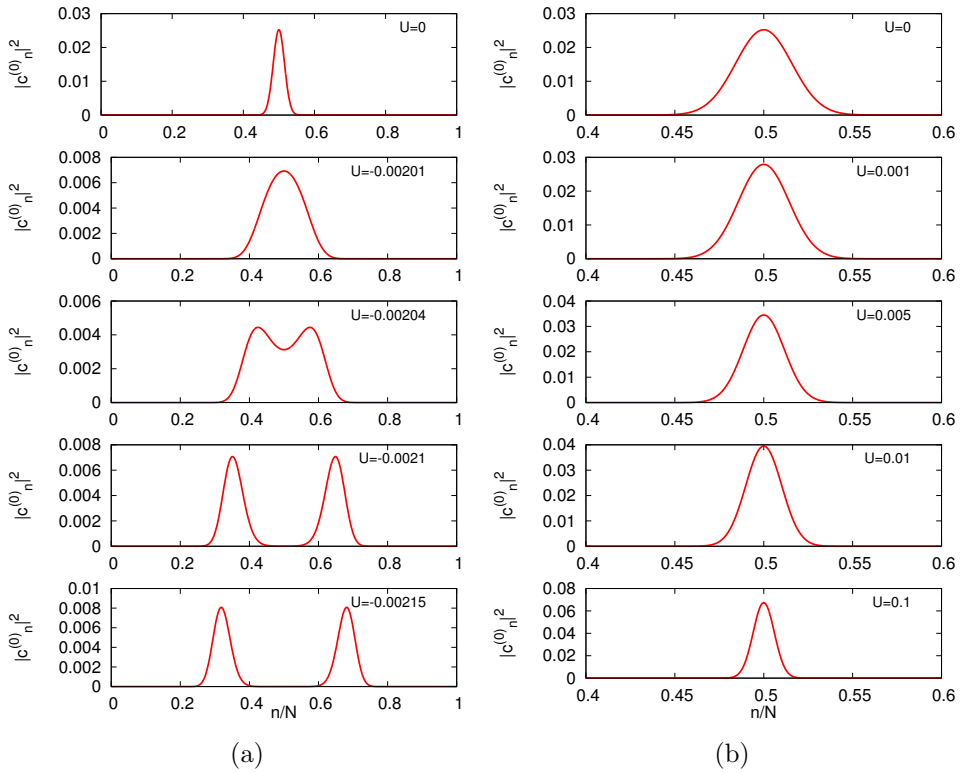

Figure 4.1: Coefficients $|c_n^{(0)}|^2$ as a function of n/N for $N = 1000$. In panel (a) the interaction is negative $U < 0$ and in panel (b) it is positive $U > 0$. In both cases the ground state is showed for 5 values of U, which is written in units of J and therefore equivalent to $\zeta = U/J$. The coefficients $c_n^{(0)}$ are normalized so that $\sum_{n=0}^{N} |c_n^{(0)}|^2 = 1$. n/N is adimensional.

the two symmetric maxima, we will say that it is in the "cat state regime", remembering however that the terminology "cat state" is only used for the aforementioned state.

4.3.3 Quantum indicators

Let us now see how the quantum indicators we have previously mentioned can help us describe the change of regimes of the ground state. The values of the quantum indicators are plotted in Fig. (4.2) as a function of U; since U is written in units of J, in this case, $\zeta = U/J$ and U are equivalent.

As for the Fisher information, we can see from Fig. (4.2) that it is a monotonic decreasing function of U. This is in agreement with the fact that F assumes its maximum value $F = 1$ for the "macroscopic cat state" and and its minimum value $F = 0$ for the separable Fock state. As expected we can see that $F = 1/N = 0.001$ when $U = 0$. From the analysis of the plot we can notice that there is a value of ζ for which the second derivative of the

Fisher information changes sign $\zeta_F \simeq -0.002$, and above which F plateaus.

In Fig. (4.2) we can see the coherence visibility α_v as a function of U. When $\zeta = U/J = 0$ the ground state is the atomic coherent state and α_v has its maximum value. For smaller values of ζ the coherence visibility shows a plateau but for larger values of $|\zeta|$, α_v gets smaller. It is worth noticing that on the attractive side of the interaction there is a value of ζ for which the second derivative of α_v changes sign. This value of ζ, which we can call ζ_α turns out to be the same as ζ_F, and it is close to ζ_{cr}.

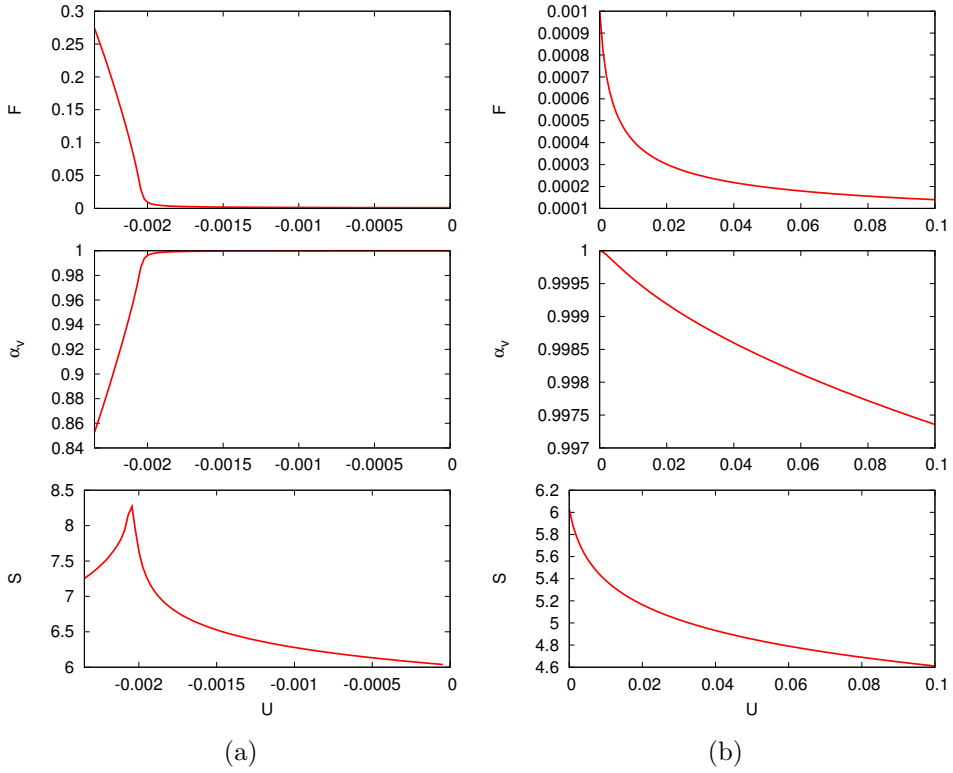

Figure 4.2: Fisher information F, coherence visibility α_v and entanglement entropy S, plotted as a function of U, which is written in units of J, for $N = 1000$. In panel (a) the interaction is attractive $U < 0$ and in panel (b) it is repulsive $U > 0$. F, α and S are adimensional.

Lastly, let us plot in Fig. (4.2) the entanglement entropy of the ground state. We can notice that S shows a maximum for a finite value of ζ when the interaction is attractive; we can call this value ζ_S. We see that this ground state has a larger S than the cat state for which $S = 1$. This means that for a Bosonic Josephson junction the cat state is not the most entangled. Moving away from ζ_S in both directions, S assumes monotonically smaller values. ζ_S is close to ζ_{cr} that identifies the onset of the coherence loss and the transition to the cat state regime.

Because of the close analogy between the critical points of these quantum

indicators and the change of regimes in the ground states, the quantum indicators can also be used to discriminate the transitions between the cat, coherent and Fock state regimes instead of needing to plot the coefficients of the ground state.

4.4 Complete system

Let us now study the ground state of the complete system, that is to say the Bosonic Josephson junction inside of the optical cavity.

In the previous chapter, when studying the dynamics of the system, we used the semiclassical approximation. This meant that both the atoms in the left and right well and the photons in the cavity were described with coherent states. We now use a different approximation, in which we describe only the photons as a coherent state, but we describe the atoms in the wells in a purely quantum way, by using Fock states.

We call the photon coherent state $|\alpha\rangle$, with $\hat{a}|\alpha\rangle = \alpha|\alpha\rangle$. Furthermore, in the same way as we stated when we described the adiabatic elimination of the photon dynamics in the previous chapter, we assume that the photon field relaxes quickly and this allows us to consider the photon coherent state to be a parameter on which the atomic ground state depends.

The ground state of the atomic field for a given photon field strength can be written as:

$$|GS\rangle_\alpha = \sum_n c_n(\alpha)|n\rangle \tag{4.20}$$

where $|n\rangle = |N-n, n\rangle$ is an element of the Fock basis $\{|n\rangle, n = 0, 1, ..., N\}$, as defined before and the coefficients $c_n(\alpha)$ clearly depend on the photon field strength.

So the ground state of the complete system can be written as:

$$|GS\rangle = |\alpha\rangle \otimes |GS\rangle_\alpha, \tag{4.21}$$

which is the tensor product of the coherent state of the photon field and of the atomic ground state for that field strength. Since the Hamiltonian $\hat{H}$ of the complete system commutes with the number operator of the atoms, $\hat{N}_A$, the atomic ground state is also an eigenstate of the number operator and therefore $\hat{N}_A|GS\rangle_\alpha = N|GS\rangle_\alpha$.

To perform the numerical diagonalization of the Hamiltonian we need to calculate its matrix elements in the basis of the Fock states. The Hamiltonian of the Bosonic Josephson junction inside of the cavity is given by Eq. (2.34). We can substitute the photon operators with the corresponding

c-numbers since we are using a coherent state, and we get:

$$\hat{H}(\alpha) = -\left(\hbar\Delta_C - W_0 N\right)|\alpha|^2 - i\hbar\eta\left(\alpha - \alpha^*\right) - \left(J - W_{12}|\alpha|^2\right)\left(\hat{b}_1^\dagger\hat{b}_2 + \hat{b}_2^\dagger\hat{b}_1\right) + \\ + \frac{U}{2}\left(\hat{b}_1^\dagger\hat{b}_1^\dagger\hat{b}_1\hat{b}_1 + \hat{b}_2^\dagger\hat{b}_2^\dagger\hat{b}_2\hat{b}_2\right). \quad (4.22)$$

The Hamiltonian that needs to be diagonalized is such that:

$$\hat{H}|GS\rangle = \hat{H}\left(|\alpha\rangle \otimes |GS\rangle_\alpha\right) = H(\alpha)|GS\rangle_\alpha, \quad (4.23)$$

which can also be written as:

$$H(\alpha)|GS\rangle_\alpha = H(\alpha)\sum_{n=0}^{N} c_n(\alpha)|n\rangle = \sum_{m,n=0}^{N} |m\rangle\langle m|H(\alpha)|n\rangle c_n(\alpha) \quad (4.24)$$

where we inserted the completeness relation: $\sum_{m=0}^{N}|m\rangle\langle m| = \mathbb{I}$.

Therefore the matrix elements of the Hamiltonian are:

$$H_{m,n}(\alpha) = \langle m|H(\alpha)|n\rangle \quad (4.25)$$

To write explicitly the matrix elements of the Hamiltonian we use the fact that:

$$\begin{aligned}
\langle m|\hat{b}_1^\dagger\hat{b}_2|n\rangle &= \sqrt{N-m}\sqrt{n}\,\delta_{m,n-1} \\
\langle m|\hat{b}_2^\dagger\hat{b}_1|n\rangle &= \sqrt{N-n}\sqrt{m}\,\delta_{m,n+1} \\
\langle m|\hat{b}_1^\dagger\hat{b}_1^\dagger\hat{b}_1\hat{b}_1|n\rangle &= (N-n)(N-n-1)\delta_{m,n} \\
\langle m|\hat{b}_2^\dagger\hat{b}_2^\dagger\hat{b}_2\hat{b}_2|n\rangle &= n(n-1)\delta_{m,n}
\end{aligned}$$

Finally the matrix elements of the Hamiltonian can be written as:

$$H_{m,n}(\alpha) = -\left[\left(\hbar\Delta_C - W_0 N\right)|\alpha|^2 + i\hbar\eta\left(\alpha - \alpha^*\right)\right]\delta_{m,n} - \\ - \left(J - W_{12}|\alpha|^2\right)\left(\sqrt{N-m}\sqrt{n}\,\delta_{m,n-1} + \sqrt{N-n}\sqrt{m}\,\delta_{m,n+1}\right) + \\ + \frac{U}{2}\left[(N-n)(N-n-1) + n(n-1)\right]\delta_{m,n} \quad (4.26)$$

By numerically diagonalizing this matrix we can find the value of the coefficients $c_n(\alpha)$. We can notice that the first part of the matrix that reads:

$$-\left[\left(\hbar\Delta_C - W_0 N\right)|\alpha|^2 + i\hbar\eta\left(\alpha - \alpha^*\right)\right]\delta_{m,n}$$

is proportional to the identity matrix, as it does not depend either m or n. Therefore it gives no contribution to the calculation of the eigenstates and we can diagonalize the simpler matrix:

$$H'_{m,n}(\alpha) = -\left(J - W_{12}|\alpha|^2\right)\left(\sqrt{N-m}\sqrt{n}\,\delta_{m,n-1} + \sqrt{N-n}\sqrt{m}\,\delta_{m,n+1}\right) + \\ + \frac{U}{2}\left[(N-n)(N-n-1) + n(n-1)\right]\delta_{m,n} \quad (4.27)$$

If we assume that the photon field relaxes fast then $i\hbar \frac{d}{dt}\alpha = 0$. The expression for $i\hbar \frac{d}{dt}\alpha$ calculated for the ground state reads:

$$i\hbar \frac{d}{dt}\alpha = -\left[\hbar\Delta_C - W_0 N - W_{12} \sum_{n,m=0}^{N} c_m^*(\alpha) c_n(\alpha) \langle m|(\hat{b}_1^\dagger \hat{b}_2 + \hat{b}_2^\dagger \hat{b}_1)|n\rangle\right] \alpha + i\hbar\eta. \quad (4.28)$$

By setting this expression equal to zero we find that:

$$\begin{aligned} \alpha &= \frac{i\hbar\eta}{\hbar\Delta_C - W_0 N - W_{12} \sum_{n,m=0}^{N} c_m^*(\alpha) c_n(\alpha) \langle m|(\hat{b}_1^\dagger \hat{b}_2 + \hat{b}_2^\dagger \hat{b}_1)|n\rangle} \\ &= \frac{i\eta}{\Delta_C - \hbar^{-1}\left[W_0 N + W_{12} \sum_{n=1}^{N} \sqrt{N-n-1}\sqrt{n}\left(c_{n-1}^*(\alpha) c_n(\alpha) + c_n^*(\alpha) c_{n-1}(\alpha)\right)\right]} \end{aligned} \quad (4.29)$$

Therefore, in order for this procedure to be consistent the coefficients $c_n(\alpha)$ of the eigenstates of the Hamiltonian obtained as result of the diagonalization must give the same value of α we started with.

The procedure here described is carried out numerically through a C++ program. The program starts with a trial value of the initial α, calculates the coefficients of the ground state $c_n(\alpha)$ and using them it computes a new value of α. This procedure is repeated for several values of α until the α calculated from the coefficients is equal to the starting one. From this α the actual ground state coefficients are calculated.

The analysis of the ground state can be simplified using the same approximation we have used in the previous chapter when studying the assisted Josephson Junction. When $\Delta_C \gg W_0 N$ and $\Delta_C \gg W_{12} N$, then α depends weakly on the coefficients $c_n(\alpha)$. Therefore, for any starting number of photons $|\alpha|^2$ the above procedure gives as result the starting $|\alpha|^2$. The number of photons in the system can thus be modified by changing the parameters η and Δ_C.

Under this approximation we need to study how the ground states of the Hamiltonian with the assisted tunneling is influenced by the presence of the photons.

4.5 Ground states of the assisted Hamiltonian

The matrix elements (4.26) of the Hamiltonian of the system differ from those of the bare Josephson junction just for the modified tunneling amplitude. The assisted tunneling amplitude becomes $\tilde{J} = \left(J - W_{12}|\alpha|^2\right)$.

The assisted amplitude $\tilde{J}$ can now change its magnitude and also its sign when W_{12} is positive.

Let us now calculate the ground state of the system as we have done for the bare cavity, but this time showing what the effect of the cavity photons is.

4.5.1 $W_{12} < 0$

When $W_{12} < 0$ the assisted tunneling amplitude $\tilde{J}$ is always positive and its magnitude gets larger as the number of photons in the system $|\alpha|^2$ increases.

Let us choose $W_{12} = -0.03J$ and plot together the ground states for various values of U for $|\alpha|^2 = 1$ and $\tilde{J} = 1.03J$. We always plot the ground state of the bare junction, which correspond to $|\alpha|^2 = 0$ to use as a reference.

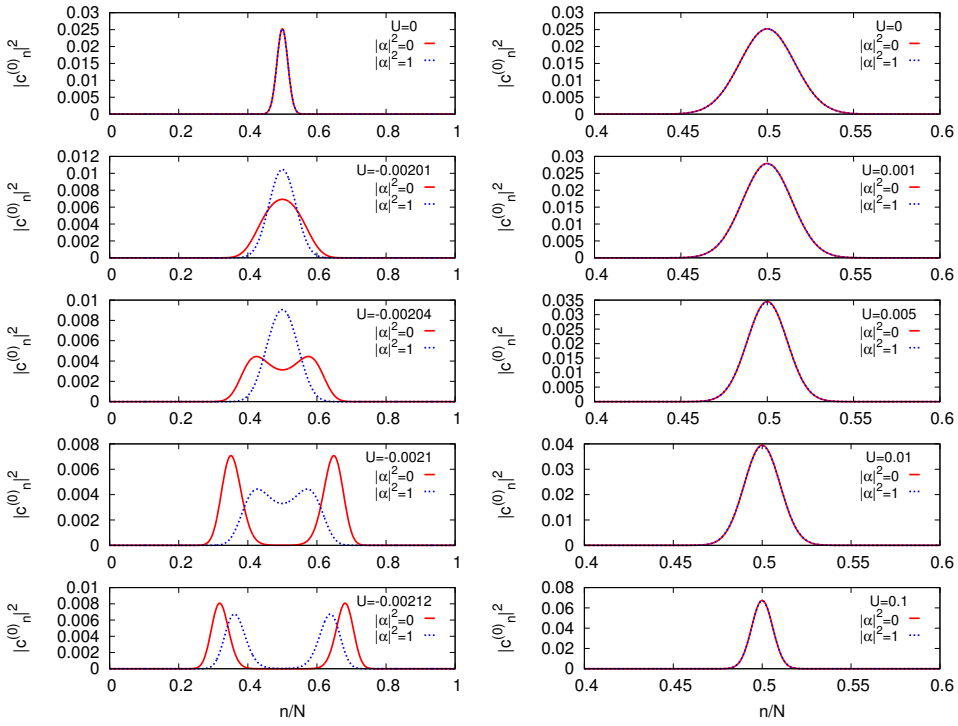

Figure 4.3: Coefficients $|c_n^{(0)}|^2$ as a function of n/N for $W_{12} = -0.03J$ and $N = 1000$. In panel (a) the interaction is negative $U < 0$ and in panel (b) it is positive $U > 0$. U is written in units of J. The red line represents the system with $|\alpha|^2 = 0$, while the blue dashed line the system with $|\alpha|^2 = 1$. In both cases the ground state is showed for 5 values of U. The coefficients $c_n^{(0)}$ are normalized so that $\sum_{n=0}^{N} |c_n^{(0)}|^2 = 1$. n/N is adimensional.

In panel (a) of Fig. (4.3) we can see what happens when the in-site interaction U is negative. The valley in the middle of the distribution appears only for a larger value of $|U|$. This means that the photons have the effect of increasing the coherence of the state, and the transition to the "cat state" regime is delayed. This effect can be clearly seen also from Fig. (4.4) where the plot of the entanglement entropy shows its maximum for a larger $|U|$, and from the Fisher information, which is smaller and therefore represents a narrower width in the distribution for the coefficients $|c_n^{(0)}|^2$.

When the interaction is positive, the effect of the photons is still to delay

the transition to the separable Fock state. While the effect can not be seen from Fig. (4.3), because it is very small, it can be clearly seen in Fig. (4.4) where the coherence visibility of the ground state in the presence of photons is always larger that the state without them.

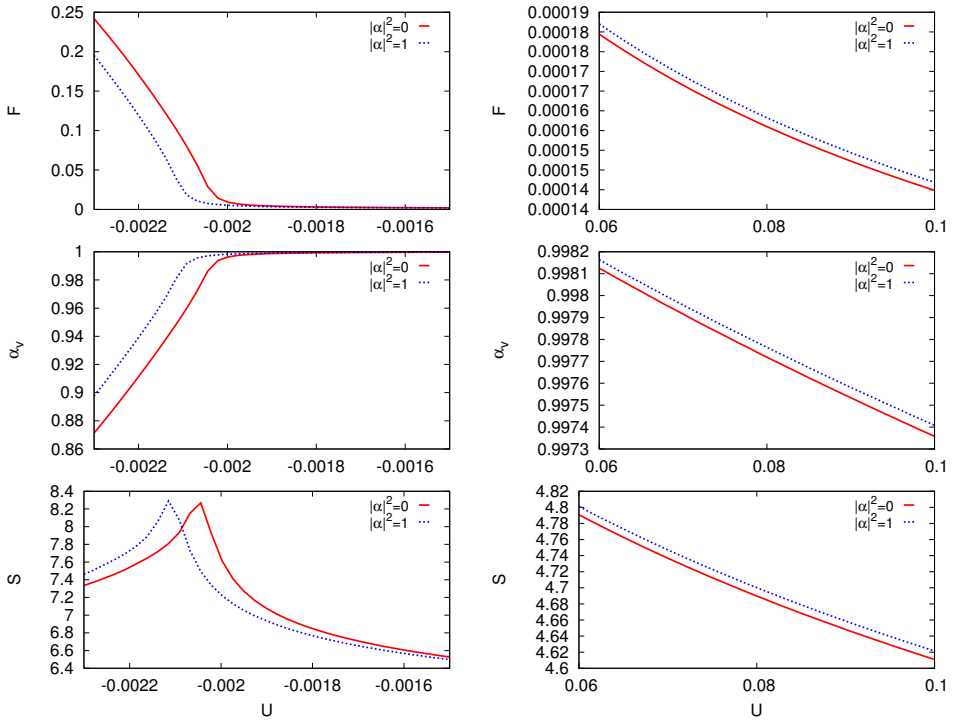

Figure 4.4: Fisher information F, coherence visibility α and entanglement entropy S, plotted as a function of U, which is written in units of J, for $W_{12} = -0.03J$ and $N = 1000$. The red line represents the system with $|\alpha|^2 = 0$, while the blue dashed line the system with $|\alpha|^2 = 1$. In panel (a) the interaction is attractive $U < 0$ and in panel (b) it is repulsive $U > 0$. F, α and S are adimensional.

4.5.2 $W_{12} > 0$

When $W_{12} > 0$ the assisted tunneling amplitude $\tilde{J}$ gets smaller when increasing the number of photons in the cavity. This can lead to two main consequences. On the one hand, if the number of photons is sufficiently small, $\tilde{J}$ maintains its positive sign but its magnitude gets smaller $0 < \tilde{J}/J < 1$. On the other hand if the number of photons is large enough the assisted tunneling can become negative $\tilde{J}/J < 0$.

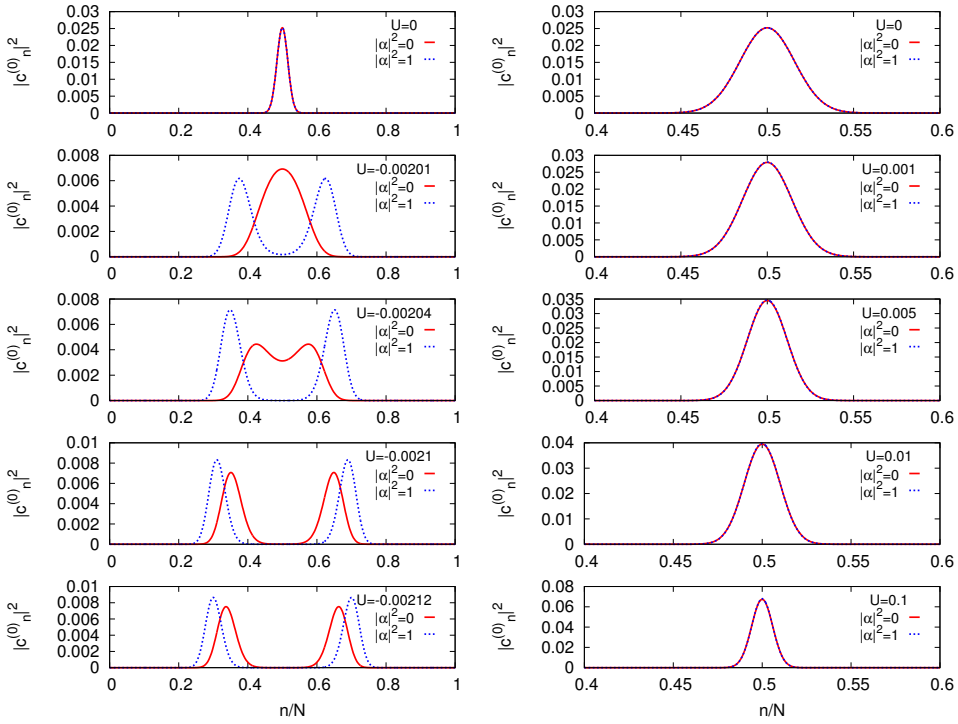

Figure 4.5: Coefficients $|c_n^{(0)}|^2$ as a function of n/N for $W_{12} = 0.03J$ and $N = 1000$. In panel (a) the interaction is negative $U < 0$ and in panel (b) it is positive $U > 0$. U is written in units of J. The red line represents the system with $|\alpha|^2 = 0$, while the blue dashed line the system with $|\alpha|^2 = 1$. In both cases the ground state is showed for 5 values of U. The coefficients $c_n^{(0)}$ are normalized so that $\sum_{n=0}^{N} |c_n^{(0)}|^2 = 1$. Both ζ and n/N are adimensional.

$0 < \tilde{J}/J < 1$

Let us start with the case when $0 < \tilde{J}/J < 1$. We can plot the ground states of the system, for different values of U, and for $|\alpha|^2 = 1$, and $\tilde{J} = 0.97J$. We can see from Fig (4.5) that the effect of the photons in this case is opposite to the effect in the previous section where W_{12} was negative. Since the ratio $U/\tilde{J}$ gets larger in magnitude, the transition from the atomic coherent state to the separable Fock state, when the interaction U is positive, appears more rapidly. The same holds for the transition to the "cat state" regime, when U is negative, which occurs for a negative U with smaller magnitude. This effect can also be seen from the quantum indicators in Fig. (4.6). In particular the maximum of the entanglement entropy can be used to observe the transition to the "cat state" regime, and how it appears for a smaller $|U|$. The plot of the coherence visibility α can be used to see how the coherence of the system is always smaller.

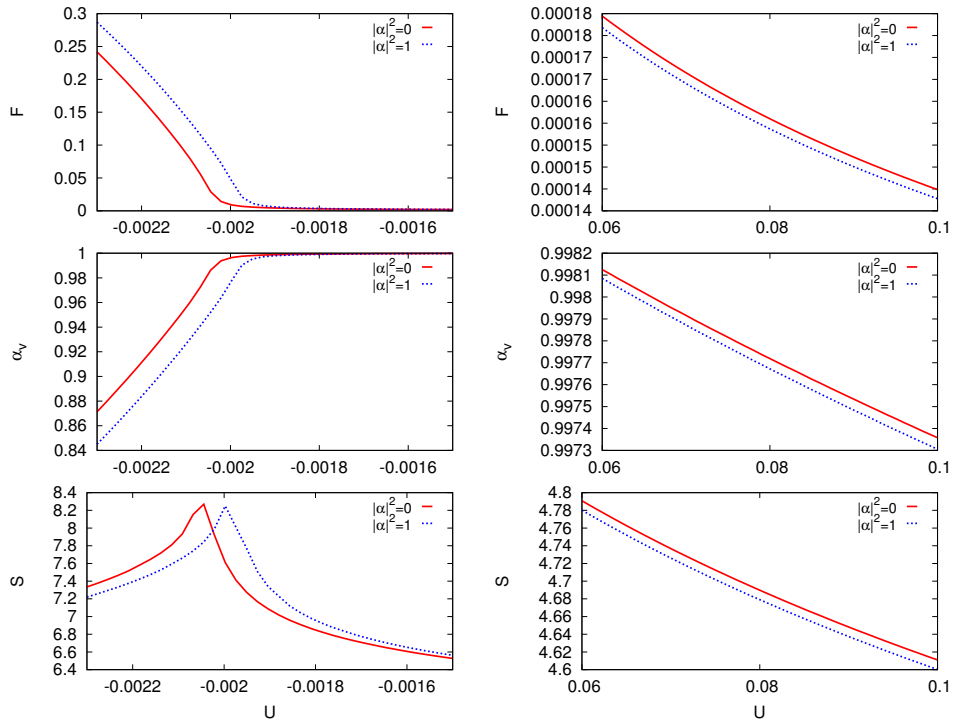

Figure 4.6: Fisher information F, coherence visibility α and entanglement entropy S, plotted as a function of U which is written in units of J, for $W_{12} = 0.03J$ and $N = 1000$. The red line represents the system with $|\alpha|^2 = 0$, while the blue dashed line the system with $|\alpha|^2 = 1$. In panel (a) the interaction is attractive $U < 0$ and in panel (b) it is repulsive $U > 0$. F, α, S and ζ are adimensional.

It is worth mentioning that this result is actually more interesting then the sole rescaling of the ratio U/J. Focusing our attention on the attractive in-site interaction and on the emergence of the "cat state" regime we can notice a fundamental difference. For a fixed number of atoms in the system, in the bare Josephson junction, the transition to the "cat state" regime happens for a definite value of $\zeta = U/J$. However, in the complete system, with a positive W_{12}, by fine tuning the number of cavity photons the transition to the "cat state" regime can happen for a given magnitude of negative U, without changing the number of atoms. This means that the photons in the system act as a new degree of freedom through which the transition between different regimes can be manipulated. The significant effect the photons can have, can be seen from Fig. (4.7), which compares the ground states for $|\alpha|^2 = 0$, $|\alpha|^2 = 1$ and $|\alpha|^2 = 25$ for the same interaction strength U. The ground state of the system when $|\alpha|^2 = 25$ shows the "cat-like" state much sooner because the assisted tunneling $\tilde{J}$ becomes much smaller for the same value of U.

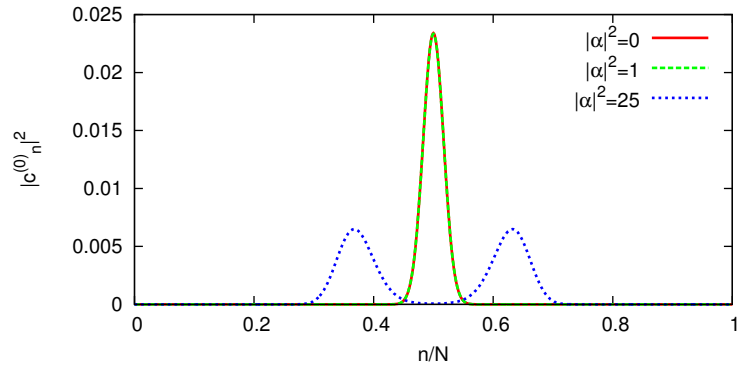

Figure 4.7: Coefficients $|c_n^{(0)}|^2$ as a function of n/N for $|\alpha|^2 = 0$, $|\alpha|^2 = 1$ and $|\alpha|^2 = 25$ and $U = -0.00052J$, for $W_{12} = 0.03J$ and $N = 1000$. When $|\alpha|^2 = 0$ and $|\alpha|^2 = 1$ the ground states do not differ for such a small interaction strength and are very similar to the atomic coherent state. On the other hand, the ground state of the system with $|\alpha|^2 = 25$ clearly shows the transition to the "cat state" regime. The coefficients $c_n^{(0)}$ are normalized so that $\sum_{n=0}^{N} |c_n^{(0)}|^2 = 1$.

4.5.3 $\tilde{J}/J < 0$

The change of the sign of $\tilde{J}$ is significant when analyzing the Hamiltonian of the system. In the case of the bare Josephson junction J can always be taken to be positive. However, by numerically calculating the ground state of the system we found out that the sign of $\tilde{J}$ bears no relevance to the coefficients $|c_n^{(0)}|^2$ and to the value of the quantum indicators. Therefore, choosing values of $|\alpha^2|$ such that the values of the assisted tunneling amplitude $\tilde{J}$ is the same as the ones we have just studied, but with opposite signs, leads to the same plots. Therefore, for $|\alpha|^2 = 65.666$, the assisted tunneling is $\tilde{J} = -0.97J$, and it is described by the same plots we used for $\tilde{J} = 0.97J$, that is Fig. (4.5) and Fig. (4.6). For $|\alpha|^2 = 67.666$, the assisted tunneling is $\tilde{J} = -1.03J$, and it is described by the same plots we used for $\tilde{J} = 1.03J$, that is Fig. (4.3) and Fig. (4.4).

It is very interesting to notice this analogy between the case with positive $\tilde{J}$ and negative $\tilde{J}$. One would at first think that, since the relevant parameter in the analysis is the ratio $U/\tilde{J}$, when $\tilde{J}$ is negative, the same results could be obtained by changing the sign of U as well. However this is not the case, and we can justify it by comparing the results we have achieved for the half-semiclassical system with the ones form the semiclassical analysis.

4.6 Analogies between the half-semiclassical and the semiclassical study of the system

In the half-semiclassical analysis of the problem we have studied how the ground state of the system is influenced by the cavity photons. In order to

compare the results we have achieved in this chapter with the ones in the semiclassical approximation of the previous chapter, we need to concentrate our attention on the equilibria of the assisted Josephson junction equations.

In fact, we can think of the ground state in which the distribution of the coefficients $|c_n^{(0)}|^2$ has a single maximum centered on $|c_{N/2}^{(0)}|^2$ as the quantum analogue of the zero-imbalance equilibria of the semiclassical system. In both cases the we have the same number of bosons in either well. When the distribution of the coefficients $|c_n^{(0)}|^2$ of the ground state shows two maxima, symmetrically placed on the sides of $|c_{N/2}^{(0)}|^2$,we can think that this state is the quantum analogue of the finite-imbalance equilibria of the semiclassical system, where there is a actual imbalance in the populations of the wells.

Since the system (3.13) has several equilibria we assume that the one with the lowest energy is the one that describes the ground state of the system, because it is the most energetically favourable.

At this point we can see the first analogy between the analysis of the system performed in the two approximations. From the study of the ground states we have seen how the presence of a negative $\tilde{J}$ did not influence the coefficients of the ground states. In particular this means that the transition to the cat state regime can occur only when the in-site interaction U is negative, independently of the sign of $\tilde{J}$. However, this is the same conclusion we reached when studying the equilibria of Eqs. (3.13), where we found that the finite imbalance equilibria are the most energetically favourable only when the interaction is negative, assuming that these equilibria do exist.

This leads to the second analogy. The finite imbalance equilibria exist only if the parameters of the system satisfy the condition:

$$(UN/2\tilde{J})^2 > 1. \tag{4.30}$$

We can try to compare the values of U for which we saw the appearance of the valley in the plots of the coefficients $|c_n^{(0)}|^2$ of the ground state with the ones given by the condition for the existence of the equilibria. When $W_{12} = 0.03J$ and $|\alpha|^2 = 1$, Eq. (4.30) gives $U < -0.00194J$, and from the numerical calculation of the coefficients $|c_n^{(0)}|^2$ we find that the valley appears when $U \simeq -0.00196J$. When $W_{12} = -0.03J$ and $|\alpha|^2 = 1$, Eq. (4.30) gives $U < -0.00206J$, and from the plot of the coefficients we get that the valley appears when $U \simeq -0.00209J$. When $|\alpha|^2 = 0$, Eq.(4.30) gives $U < -0.002J$, and from the plot of the coefficients we get that the valley appears when $U \simeq -0.00203J$. The critical values of U we got from both models are quite similar and therefore Eq. (4.30) describes quite well the transition between the two relevant regimes also in the half semiclassical case.

Chapter 5

Conclusions

In this thesis we have studied some features of the dynamics and of the statics of a Bosonic Josephson junction inside of an optical cavity. The Bosonic Josephson junction is made of an atomic Bose-Einstein condensate trapped in a symmetric double well potential in one direction and by a tightly harmonic potential in the two orthogonal directions. This makes the system quasi one-dimensional. In order for the atoms to interact with the light field, they have two electronic states, a ground state and an excited state with a transition frequency ω_A. The cavity has a characteristic frequency ω_C close to the atomic transition frequency ω_A, and it is pumped by a coherent laser light with frequency ω_L.

We have first derived the Hamiltonian that describes the system and we have introduced a simplified version of it using the two-mode approximation, that describes the condensate wave function as a sum of the condensate in the right and left well of the double well potential.

After introducing the "semiclassical approximation" that describes the condensate in both wells and the light field with a coherent state, we have written a set of four coupled differential equations that describe the dynamics of the system. Then we have calculated the equilibria of this system and analytically computed the small oscillation frequencies for the zero imbalance fixed points. In particular we have noticed how, close to these fixed points, the dynamics of the atomic and photon variables were no longer coupled.

We have then written a set of equations that approximate the complete system when, the photon variables can be considered as constant. This has allowed us to study the dynamics of the system, and in particular show that the system can be found in two different regimes, one were the average population imbalance is zero and one where it is different than zero. This last regime is called the self trapping regime. We have shown how the presence of photons can induce self trapping solutions, that would not occur in the bare Bosonic Josephson junction. After studying the system in the semiclassical

approximation, we have studied its static properties by treating the photon field as a coherent state, but describing the atoms in the wells with Fock states. By numerically diagonalizing the Hamiltonian of the system we have managed to see how the ground states of the system are modified by the presence of photons. In the bare Josephson junction, we have seen a transition between different kinds of ground states by changing the in-site interaction strength U between the atoms. When U is positive, by increasing its magnitude the ground state changes from a atomic coherent state to a separable Fock state. When U is negative, by increasing its magnitude the ground state changes form the atomic coherent state to the "macroscopic cat state". In our system, the cavity photons can be used as a new parameter that allows to change regime. In particular we have shown how the transition to the "cat state" regime can occur in the complete system for a given negative U, by appropriately changing the number of photons in the system. Lastly we have pointed out some analogies between the study of the static properties of the system when describing the condensate with a coherent state or in a purely quantum manner, using Fock states.

Bibliography

[1] A. Einstein, Slitzungsberichte der Preussischen Akademie der Wissenschaften **22**, 261 (1925).

[2] A. Einstein, Sitzungsberichte der Preussischen Akademie der Wiessenschaften **23**, 18 (1925).

[3] Anderson, M. H., Ensher, J. R., Matthews, M. R., Wieman, C. E., and Cornell, E. A., Science **269**, 5221 (2005).

[4] B. D. Josephson. Phys. Lett. **1**, 251 (1962).

[5] P.L. Anderson, and J.W. Rowell, Phys.Rev.Lett. **10**, 230 (1963).

[6] Michael Albiez, Rudolf Gati, Jonas Folling, Stefan Hunsmann, Matteo Cristiani, and Markus K. Oberthaler, Phys.Rev.Lett. **95**, 010402 (2005).

[7] E. L. Raab, M. Prentiss, Alex Cable, Steven Chu, and D. E. Pritchard, Phys. Rev. Lett. **59**, 2631 (1987).

[8] R. Gati, M. Albiez, J. Folling, B. Hemmerling, M.K. Oberthaler, App. Phys. B **82**, 207 (2005).

[9] L. Mandel, E. Wolf, Optical Coherence and Quantum Optics, Cambridge University Press (1995).

[10] S. Raghavan, A. Smerzi, S. Fantoni, and S.R. Shenoy, Phys. Rev. A **59**, 620 (1999).

[11] G. Szirmai, G. Mazzarella, and L. Salasnich, Phys. Rev. A **91**, 023601, 2015

[12] R. Grimm et al., Adv. At. Mol. Opt. Phys. **42**, 95-170 (2000).

[13] G. Mazzarella, L. Salasnich, A. Parola, and F. Toigo, Phys. Rev. A **83**, 053607 (2011).

[14] H. Ritsch, P. Domokos, F. Brennecke, and T. Esslinger, Rev. Mod. Phys. **85**, 553 (2013).

[15] C. Maschler and H. Ritsch, Phys. Rev. Lett. **95**, 260401 (2005).

[16] C. Maschler, I. B. Mekhov, and H. Ritsch, Eur. Phys. J. D **46**, 545 (2008).

[17] J. F. Corney, and G. J. Milburn, Phys. Rev. A **58**, 2399 (1998).

[18] A. Vukics, C. Maschler, and H. Ritsch, New J. Phys. **9**, 255 (2007).

[19] J. M. Zhang, W. M. Liu, and D. L. Zhou, Phys. Rev. A **77**, 033620 (2008).

[20] J. M. Zhang, W. M. Liu, and D. L. Zhou, Phys. Rev. A **78**, 043618 (2008).

[21] M. Zuppardo, J. P. Santos, G. De Chiara, M. Paternostro, F. L. Semiao, and G. M. Palma, Phys. Rev. A **91**, 033631 (2015).

[22] W.P. Schleich, Quantum Optics in Phase Space (Wiley, Berlin, 2001).

[23] F.T. Arecchi, E. Courtens, R. Gilmore, H. Thomas, Phys. Rev. A **6**, 2211 (1972); G. J. Milburn, J. Corney, E. M. Wright, D. F. Walls, Phys. Rev. A **55**, 4318 (1997).

[24] B. Julia-Diaz, D. Dagnino, M. Lewenstein, J. Martorell, and A. Polls, Phys. Rev. A **81**, 023615 (2010).

[25] L. Pitaevskii and S. Stringari, Phys. Rev. Lett. **83**, 4237 (1999); L. Pitaevskii and S. Stringari, Phys. Rev. Lett. **87**, 180402 (2001).

[26] J.R. Anglin, P. Drummond, and A. Smerzi, Phys. Rev. A **64**, 063605 (2001).

[27] K.W. Mahmud, H. Perry, and W.P. Reinhardt, J. Phys. B: At. Mol. Opt. Phys. **36**, L265 (2003); K.W. Mahmud, H. Perry, and W.P. Reinhardt, Phys. Rev. A **71**, 023615 (2005).

[28] G. Ferrini, A. Minguzzi, F. W. Hekking, Phys. Rev. A **78**, 023606(R) (2008).

[29] J.I. Cirac, M. Lewenstein, K. Molmer, and P. Zoller, Phys. Rev. A **57**, 1208 (1998).

[30] D.A.R. Dalvit, J. Dziarmaga, and W.H. Zurek, Phys. Rev. A **62**, 013607 (2000).

[31] Y.P. Huang and M.G. Moore, Phys. Rev. A **73**, 023606 (2006).

[32] L.D. Carr, D.R. Dounas-Frazer, and M.A. Garcia-March, EPL **90**, 10005 (2010).

[33] D.W. Hallwood, T. Ernst, and J. Brand, e-preprint arXiv:1007.4038.

[34] L. Pezzè and A. Smerzi, Phys. Rev. Lett. **102**, 100401 (2009).

[35] C.H. Bennett, H.J. Bernstein, S. Popescu, B. Schumacher, Phys. Rev. A **53**, 2046 (1996); S. Hill and W. Wootters, Phys. Rev. Lett. **78**, 5022 (1997); L. Amico, R. Fazio, A. Osterloh, V. Vedral, Rev. Mod. Phys. **80**, 517 (2008); J. Eisert, M. Cramer, M. B. Plenio, Rev. Mod. Phys. **82**, 277 (2010).

[36] W.K. Wootters, Phys. Rev. D. **23**, 357 (1981); C. W. Helstrom, *Quantum Detection and Estimation Theory* (Academic Press, New York, 1976), Chap. VIII; A. S. Holevo, *Probalistic and Statistical Aspect of Quantum Theory* (North-Holland, Amsterdam, 1982); S.L. Braunstein and C. M. Caves, Phys. Rev. Lett. **72**, 3439 (1994).

[37] B. Gertjerenken, S. Arlinghaus, N. Teichmann, C.Weiss Phys. Rev. A **82**, 023620 (2010).